HITRAP

Technical Design Report

Editors: Th. Beier, L. Dahl, H.-J. Kluge, Chr. Kozhuharov, and W. Quint.

GSI Darmstadt
October 2003

Table of Contents

Contributions to this Technical Design Report were received from:
Joseba Alonso Otamendi (Univ. Mainz), Norbert Angert (GSI), Winfried Barth (GSI), Alexander Bechtold (Univ. Frankfurt/Main), Bruno Becker-de Mos (GSI), Thomas Beier (GSI), Heinrich Beyer (GSI), Klaus Blaum (CERN), Michael Block (GSI), Georg Bollen (NSCL/MSU, East Lansing), Stefan Borneis (GSI), Fritz Bosch (GSI), Angela Bräuning-Demian (GSI), Gerhard Breitenberger (GSI), Ludwig Dahl (GSI), Slobodan Djekic (Univ. Mainz), Georg Fehrenbacher (GSI), Achim Fischer (GSI), Peter Forck (GSI), Bernhard Franczak (GSI), Bernhard Franzke (GSI), Bernhard Froitzheim (GSI), Erhard Gaul (GSI), Georg Gruber (GSI), Siegbert Hagmann (Univ. Frankfurt/Main), Frank Herfurth (CERN), Gerald Hutter (GSI), Charles Kitegi (Univ. Frankfurt/Main), H.-Jürgen Kluge (GSI), Christophor Kozhuharov (GSI), Andreas Krämer (GSI), Thomas Kühl (GSI), Dieter Liesen (GSI), Rido Mann (GSI), Sergei Minaev (Univ. Frankfurt/Main and ITEP, Moskva), Robert B. Moore (McGill Univ., Montreal), Wilfried Nörtershäuser (Univ. Tübingen), Andreas Peters (GSI), Dorothea Plazura-Olszowski (GSI), Wolfgang Quint (GSI), Ulrich Ratzinger (Univ. Frankfurt/Main), Hartmut Reich-Sprenger (GSI), Daniel Rodríguez Rubiales (GSI), Alwin Schempp (Univ. Frankfurt/Main), Stefan Schwarz (NSCL/MSU, East Lansing), Stefan Stahl (Univ. Mainz), Markus Steck (GSI), Rudolf Steiner (GSI), Thomas Stöhlker (GSI), Tao Sun (NSCL/MSU, East Lansing), Tristán Valenzuela Salazar (Univ. Mainz), Wolfgang Vinzenz (GSI), Manuel Vogel (Univ. Mainz), Christine Weber (GSI), Günther Werth (Univ. Mainz).

Editors: Th. Beier, L. Dahl, H.-J. Kluge, Chr. Kozhuharov, and W. Quint.

i. Institutions and Collaborations

Authors from these institutions contributed to this Technical Design Report:

CERN	Centre Européenne pour la Recherche Nucléaire, Geneve
GSI	Gesellschaft für Schwerionenforschung, Darmstadt
ITEP	Institute for Experimental and Theoretical Physics, Moskva
McGill Univ., Montreal	Mc Gill University, Montreal, Quebec
NSCL/MSU, East Lansing	National Superconducting Cyclotron Laboratory, Michigan State University, East Lansing, Michigan
Univ. Frankfurt/Main	Institut für Angewandte Physik, Universität Frankfurt/Main
Univ. Mainz	Institut für Physik, Universität Mainz
Univ. Tübingen	Physikalisches Institut der Universität Tübingen

Experiments to be performed at HITRAP are prepared within the EU-RTD Network HITRAP (HPRI-CT-2001-50036), consisting of teams from GSI, GANIL Caen, KVI Groningen MPI-K Heidelberg, UJ Kraków, Imperial College London, Universität Mainz, MSI Stockholm, Technische Universität Wien,

and are partly based on techniques developed within the EU Research Network EUROTRAPS (TMR Network CT-97-0144) and the EU RTD Network EXOTRAPS (ERBFMGE-CT-98-0099).

ii. Abstract

The design of the HITRAP facility at the Experimental Storage Ring (ESR) at GSI is presented. The facility will employ deceleration of heavy highly-charged ions from 4 MeV/u down to cryogenic temperatures. Ions up to U^{92+} at 4 MeV/u will be provided by the ESR. The possibility to decelerate ions to such low energies and extract them from the ESR forms an essential part of this proposal. Deceleration down to 3 MeV/u has been successfully performed in the ESR. Extraction at this energy and the pointing stability of the extracted beam are under current investigation. The further deceleration in the HITRAP facility itself is provided by a single Interdigital-H (IH) structure operated at 108.408 MHz, which reduces the energy down to 500 keV/u, followed by a Radio-Frequency-Quadrupole (RFQ) structure operated at the same frequency for further deceleration to 6 keV/u. In order to increase the efficiency, a buncher will be placed before the IH structure, and another one between the IH and the RFQ structure.

After the RFQ structure, the ions will be trapped and cooled down to cryogenic temperatures by means of electron and resistive cooling. From this trap, they can be extracted again and used for experiments. Extraction is possible both in DC mode and bunched mode at a total rate of 10^5 ions / 10sec. Transfer takes place in bakeable transfer lines at ultra-high vacuum ($10^{-11.}$ mbar). Typical extraction voltages will be around 10 kV.

Existing 200-kW RF-tube amplifiers can supply both decelerator structures. This considerably reduces the costs for the set-up. Bunchers, IH, RFQ, and cooler trap will be located in the re-injection channel that leads from the Experimental Storage Ring, ESR, to the Heavy-Ion Synchrotron, SIS, along the existing beam line. The experiments behind the cooler trap will be located on top of the re-injection channel where the cold ions are guided by an ultra-high vacuum beam line. The necessary supplies and the control rooms for the experiments will be put on a platform above the existing power supplies for the magnets in the re-injection-channel. Requirements for the additional electrical power and for cooling water are met at the planned location.

The total calculated costs of the facility amount to 2.86 MEuro. Design and construction of the HITRAP facility will take two years.

iii. Editor's preamble

This Technical Design Report, TDR, describes the HITRAP facility as it shall be built. The form of the report is close to that for the CERN Heavy-Ion Facility [CERN 93-01], which was written in 1993 under participation of some of the authors of the current report.

The contributions to the present TDR reflect the variety of groups involved in the project, ranging from pure fundamental scientists to accelerator experts and to extremely capable providers for all infrastructural services required to run an accelerator facility like GSI smoothly. The final editing was performed in a way still to reflect this variety. In particular, the tables of required components and their costs reflect the traditions present in the different departments.

Cross-checking quality controls assured that the different technical sections form a comprehensive whole, i.e. - a machine that would work if being built along the given outline. Each chapter represents the work of leading experts in the field and/or at GSI. These people have numerous publications on the subject, not cited here. In the few cases where information was taken from external sources, this is clearly stated.

The wide range of components implicated in the project implies a large set of abbreviations and acronyms, which for ease and completeness is collected in two comprehensive lists at the beginning of the report: One comprises the general abbreviations of accelerators and institutions, the second one the components of accelerators in use, technical abbreviations etc.

iv. Glossary, Acronyms, and Abbreviations

Acronyms and Abbreviations for Accelerators, Institutes, and Collaborations

ASACUSA	Atomic Spectroscopy And Collisions Using Slow Antiprotons, one of the three low-energy antiproton collaborations at CERN
ATHENA	AnTiHydrogEN Apparatus, one of the three low–energy antiproton collaborations at CERN
ATRAP	Antihydrogen TRAP, one of the three low-energy antiproton collaborations at CERN
CERN	Centre Européenne pour la Recherche Nucléaire, European Centre for Nuclear Research, Geneva, Switzerland
ESR	Experimental Storage Ring, the accelerator at GSI behind the SIS, which allows for electron cooling and in-beam experiments
EU	European Union
FLAIR	Facility for Low-energy Antiproton and Ion Research at the future GSI facility, to be located at the NESR of the GSI Future Facility, common project of the current low-energy antiproton collaborations and the Atomic physics at GSI and related experimental groups.
GANIL	Grand Accelerateur des Ions Lourds, Large Accelerator for Heavy Ions, a National Accelerator located in Caen, France
GSI	Gesellschaft für Schwerionenforschung mbH, Darmstadt, the facility where HITRAP is planned to be set up
HITRAP	Heavy-Ion Trap, the name of an EU RTD network and of the planned set-up at GSI
IAP Frankfurt	Institut für Angewandte Physik, Institute for Applied Physics, at the University of Frankfurt/Main
ISOLDE	Isotope-Separation-On-Line Device at CERN
ISOLTRAP	Trap facility at ISOLDE
KVI	Kernfysisch Versneller Institut, Nuclear Physics Accelerator Institute, Groningen, Netherlands
MPI-K	Max-Planck Institut für Kernphysik, Max-Planck Institute for Nuclear Physics, Heidelberg, a Research institution of the German National Max-Planck society.
MSL	Manne-Siegbahn Laboratoriet, Stockholm, Sweden, one of the four Swedish national research institutions
MSU	Michigan State University, East Lansing, Michigan, USA
NESR	New Experimental Storage Ring, the successor of the ESR at the GSI Future Facility
NSCL	National Superconducting Cyclotron Laboratory, located at MSU
RTD	Research and Technical Development, a class of network-funding within the fourth and fifth framework programmes of EU research funding
SIS	SchwerIonenSynchrotron (Heavy-Ion Synchrotron), the synchrotron at GSI where the highest energy per nucleon is gained
UJ	Uniwersytet Jagielloński, Jagiellonian University, Kraków, Poland
VDE	Verband Der Elektrotechnik Elektronik Informationstechnik, Association for Electrical, Electronic, and Information Technologies, German technical association which *inter alia* controls the standards for installation and safety related to their fields

Conventional and GSI Names and Abbreviations for Elements of Accelerators and Decelerators, Methods, and Other Abbreviations Used Throughout the Text

BW	Band Width
CCD camera	Charge-Coupled Device camera (standard type of camera for experiments)
CDR	Conceptual Design Report, first elaborate proposal for the GSI Future Facility
CVD	Chemical Vapour Deposition, a way to create *inter alia* diamonds
DTL	Drift-Tube Linear accelerator
EBIS	Electron-Beam Ion Source
EBIT	Electron-Beam Ion Trap
FEP	Field-Emission Point
FFT	Fast Fourier Transformation
FT-ICR	Fourier-Transform-Ion-Cyclotron-Resonance, method to investigate ions in a trap
GA	Gebäude- und Anlagentechnik (Technics of buildings and installation), GSI department responsible for *inter alia* construction and media supply
HCI	Highly Charged Ion(s)
HD	Heidelberg, this refers to the currently being built accelerator for ion therapy at the German Centre for Cancer Research
HLI	'Hoch-Ladungs-Injektor' (High-Charge Injector), an accelerator structure established at GSI for the first acceleration stage of highly charged particles
HV	High Voltage
IH	Interdigital-H, radio frequency structure for accelerators
IP	Ion Pump
LEBT	Low-Energy Beam Transport
LORASR	Computer code to calculate the DTL beam dynamics
MCP	Multi-Channel Plate
μP	Microprocessor
NEG material	Non-Evaporable Getter material
OFHC copper	Oxygen-Free High-Conductivity copper
PLC	Programmable Logic Control
PP	Pre Pump, fore pump
PSU	Power-Supply Unit
QP	Quadruple
RF, rf	Radio frequency
RFQ	Radio Frequency Quadrupole, structure used for accelerators
rms	Root Mean Square
SE	Steuer-Einheit (Control unit), specific part of the GSI controls structure
SEM	Secondary-Electron emission
SIMION	Computer code to simulate ion trajectories
SVE	StromVersorgungsEinheit, cf. PSU, Power-Supply Unit
T	Kinetic Energy
TE	A transfer section between SIS and ESR at GSI
TIF	TIming Interface
TOF	Time Of Flight
TP	Turbo Pump
UHV	Ultra-High Vacuum, better (less) than 10^{-8} mbar
ZKS	Zugangs-Kontrollsystem (System for Access Control), the GSI-internal system for control along the beam lines and experiments with radiation

1. Introduction

1.1. History of the Present Project

The world-unique possibility of providing hydrogen-like or even bare ions up to uranium for atomic-physics experiments at GSI also suggests to perform dedicated experiments, which require these highly charged ions being at rest or as beams with extremely low energies.

In 1990, the late Helmut Poth organized a first workshop at GSI on the topic of decelerating heavy highly charged ions and storing them in a trap. In order to demonstrate single-ion efficiency of highly-charged ions and the ultimate precision achievable, a precision trap for g-factor investigations of highly charged ions created by electron bombardment was developed by GSI in close collaboration with the group of G. Werth at the University of Mainz, starting in 1994. With that set-up, the g factor of hydrogen-like carbon ($^{12}C^{5+}$) was determined to 10 digits, a precision, which in combination with theory led to the to-date most accurate determination of the electron's mass in August 2001. It was clearly demonstrated that the concept of storing and cooling of highly charged ions in a Penning trap at cryogenic temperatures is sound and that experiment and theory together would allow for a more accurate determination also of nuclear parameters of heavy highly charged ions stored in a trap.

In parallel to that experiment, the original idea of a decelerator prior to the trap was further developed and the first proposal for the HITRAP facility at GSI was submitted in November 1998. The GSI directorate approved it in January 1999. On this basis, a European RTD network 'HITRAP' was initiated and started in November 2001 with the purpose of developing set-ups and experiments for the HITRAP facility. The role of GSI within this network is the construction of the decelerator. In October 2002, a new layout of HITRAP with an outline of a new unique type of decelerator, suitable both for heavy highly charged ions and also antiprotons, was submitted at GSI. A decelerator is planned in the re-injection channel behind the ESR. The construction will be performed in such a way that the whole decelerator and the subsequent elements can be moved to the GSI Future Facility which was approved by the German Federal Ministry for Research and Education in February 2003. In the CDR for the GSI Future Facility, HITRAP forms an essential part of the future atomic-physics programme at GSI. On a workshop on December 11th, 2002, the proposal and the desired experiments were presented in order to be evaluated by an international advisory committee. As the next step of bringing our plans to reality, we now present a technical-design report about the detailed planning and estimated requirements of the HITRAP facility.

1.2. Organization of the Project

Since 1999, the HITRAP project is an approved mid-term project at GSI, carried out by the Atomic Physics Group. After the approval, a number of external collaborators interested in the design of the HITRAP facility and experiments to be performed there formed an EU-RTD network coordinated by H.-J. Kluge from the Atomic Physics at GSI, in order to ensure ongoing collaboration in particular for experimental set-ups for the new facility. In parallel, teams from the Institute of Physics from the University of Mainz, lead by G. Werth, the Institute for Applied Physics at the University of Frankfurt (groups of U. Ratzinger and A. Schempp), and the Michigan State University (group of G. Bollen, East Lansing, Michigan) work on the technical realization of the decelerator itself. H.-J. Kluge coordinates this realization stage together with Th. Beier, Chr. Kozhuharov and W. Quint. From the GSI-accelerator department, W. Barth and L. Dahl coordinate the related activities. Agreements about contributions and deliverables from the different participants in particular for the experiments are

fixed by the EU contract HPRI-CT-2001-50036 'HITRAP'. As far as the realization of the decelerator itself is concerned, obligations were only orally fixed so far. The deceleration within the ESR is part of the responsibility of the ESR operating team (M. Steck). Ion-optical calculations up to the IH structure are also performed by GSI. U. Ratzinger (Univ. Frankfurt, IAP) is responsible for the IH decelerator structure and A. Schempp (Univ. Frankfurt) has designed and plans to build the RFQ decelerator structure. The adjacent beam line into the cooler trap will be organized by GSI. The Cooler Trap itself lies within the responsibility of the group of G. Werth at Mainz. This responsibility is already fixed by the EU contract HITRAP (see above). Experiments behind the cooler trap have to be supplied by beam lines, which fall in the responsibility of the HITRAP collaboration.

The operation of the decelerator is planned to be carried out together with the ESR operation. The experimental operation will start only from the injection of particles into the cooler trap. Only this second part of the set-up will be controlled locally.

The present TDR provides a suitable and cost-effective design for the complete decelerator structure, starting form the ESR and comprising all elements up to the beam line towards the experiments behind the Cooler Trap. The experiments themselves are tasks of the external collaborators (both in design and costs) and are therefore not comprised here. The presented material has already been checked by the accelerator specialists among the editors (W. Barth and L. Dahl) for soundness, thoroughness, and completeness, and also for soundness of the specified costs.

1.3. General features and layout

Up to now, GSI is the world's only facility, which provides heavy highly charged ions up to U^{92+} for atomic-physics experiments. The high charge states are obtained by a first acceleration stage to 11.4 MeV/u in the UNILAC and consecutive stripping up to typically U^{73+}, a second acceleration stage up to about 400 MeV/u in the SIS and stripping up to bare nuclei during the transfer from the SIS to the ESR. The ESR is equipped with instrumentation for stochastic cooling and electron cooling which allows for the preparation of high-quality beams (small emittance). Precision experiments on the highly charged ions are performed directly on the moving particles in the ring, e.g., measurements of the $1s_{1/2}$ Lamb shift, investigations of the hyperfine-structure splitting in heavy highly charged ions by laser spectroscopy, etc.

Compared to EBIS/EBIT set-ups, the new HITRAP facility will be the first ever set-up to abundantly provide ions of selected charge-states up to U^{92+} *at cryogenic temperatures* in the laboratory frame, thus allowing for investigating them in a trap or for slow-collision experiments with surfaces or other atoms, ions, and molecules. Experiments of these kinds have been *impossible* up to now.

One of the main features of the HITRAP facility will be the ability to decelerate heavy highly charged ions up to U^{92+} from 4 MeV/u down to rest. A deceleration down to energy of 3 MeV/u in the existing ESR was already successfully demonstrated. The subsequent steps are ejection from the ESR, re-bunching and a first stage of deceleration by an IH structure operated at 108.408 MHz. This reduces the energy to about 500 keV/u. An RFQ structure is used for further reduction down to 6 keV/u, an energy at which the highly charged ions can be trapped in a cylindrical Penning trap and be cooled further by electron and resistive cooling. From this trap, the cold ions can be extracted and transported to the final experiments. The finally planned rate of decelerating and cooling is about 0.1 Hz (1 cycle per 10 sec., including the manipulation in the ESR). A total of about 10^5 ions per cycle are expected to be available for experiments after final electron cooling. Figure 1-1 gives an overview of the deceleration process at HITRAP.

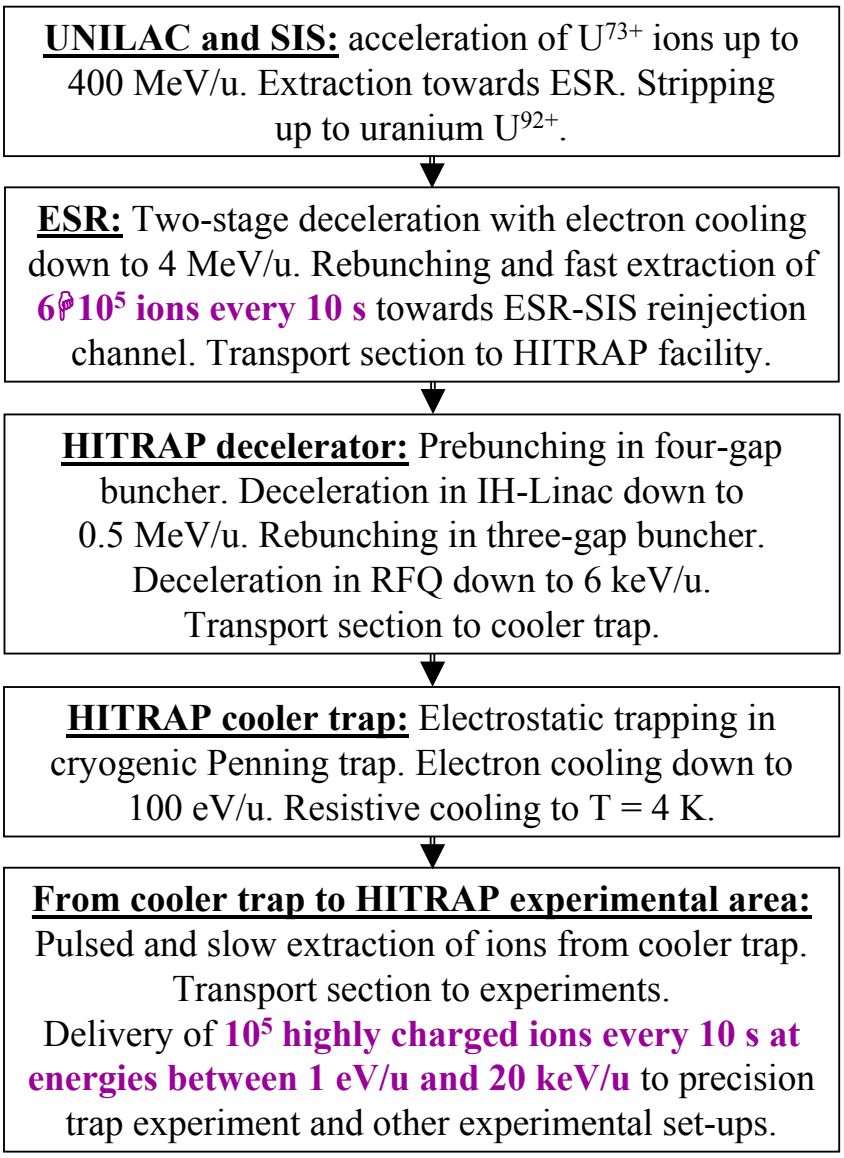

Fig 1-1. Overview of the HITRAP process with the design ion U^{92+} as an example.

A number of unique experiments are planned at the HITRAP facility. One is the investigation of a single ion stored in a Penning trap, similar to the ongoing g-factor measurements on carbon- and oxygen ions at Mainz, but employing ions of much higher charges, up to hydrogen-like uranium. These measurements will provide a test of strong-field quantum electrodynamics to a new order of magnitude. Other experiments are laser and x-ray spectroscopy of clouds of trapped ions in order to circumvent the difficulties of such measurements on ions of higher energy in the ESR. It is expected that due to missing needs for Doppler correction etc, the precision of transition energies can be performed much more precisely, thus allowing for more accurate determinations of energy levels and hyperfine structure splitting in highly

charged ions. In addition, HITRAP will also allow for the investigation of the energy levels of highly charged radioactive ions, which up to are not investigated at any existing facility.

Heavy highly charged ions at low kinetic energies planned to be used for collision studies with the reaction microscope developed at GSI (J. Ullrich). For the first time it will be possible to study collisions of single atoms, ions, or molecules with high charges at low kinetic energies. Similar studies are also planned for collisions of highly charged ions with surfaces and with guidance of highly charged ions through microcapillaries. For these experiments, a cooled beam of highly charged ions at a well-defined energy up to several kV is essential.

The planned location and set-up of the HITRAP decelerator are shown in Figs. 1-2 – 1-7. The ejection of the beam from the ESR takes place into the existing re-injection channel beam line. After passing the wall, which separates the ESR and the re-injection channel, pre-bunching for HITRAP takes place in order to allow for a sufficient fraction of the ejected beam to be decelerated by the following IH and RFQ structures. Including sections for drifting after re-bunching and for differential pumping between the RF cavities and the UHV of the ESR on one side and the traps on the other, the total length of the decelerator section before the cooler trap is planned to be not longer than 16 m. Thus it well fits into a transport section of the existing re-injection channel from where it is planned to be removed in case of re-injection operation. The adjacent experiments will be located outside of the re-injection tunnel on top of it.

The effort to remove the decelerator structures from the beam line and reinstall it after re-injection operation is small and can be handled within the usual breaks between beam times at the accelerator. They do not require major shut-downs. Taking into account that only three cases occurred where the re-injection channel was used since the start of the ESR operation in 1991, plus a fourth request for 2004, these reconstruction events can be estimated to occur only infrequently. In addition, adjacent to the HITRAP experiment, also a part of the PHELIX set-up is planned to be located (Figs. 1-3 and 1-6). For x-ray PHELIX experiments with highly-charged ions delivered by the ESR, the PHELIX laser beam passing over the re-injection channel at a height of 7.5 m above floor level (Fig 1-7) is going to be guided into a beam compressor located in the re-injection channel. The compressed laser beam then is directed into the re-injection-channel beam line in direction opposite to the incoming ion beam from the ESR. Experiments will take place in an interaction zone of the laser beam and the particle beam. In the region planned for this, only the first differential-pumping stage and the first buncher of the HITRAP facility are located which can easily be removed from and reinstalled at the beam line in case of PHELIX experiments with ions from the ESR. It has been carefully checked that neither a change to re-injection operation nor to PHELIX operation is essentially hindered by the location of the HITRAP set-up in the re-injection tunnel as it is presented here.

To provide sufficient space for electronics, controls, and the supply for the RF, a platform will be constructed in a height of 4.2 m close to the re-injection channel in the north-western corner of the existing ESR hall. Under it, the existing power supplies for the magnets in the re-injection channel are located. The location of the platform is also indicated by Figure 1-7.

Both HITRAP decelerator and experiments are intended to being moved to the low-energy atomic physics region at the GSI future facility where they are already part of the corresponding CDR. The expertise currently existing at GSI and within the RTD network strongly suggests to perform any possible investigations at the present ESR facility before the GSI future facility is ready for operation. The remaining time of operation at the existing facility allows for cost-efficient solutions.

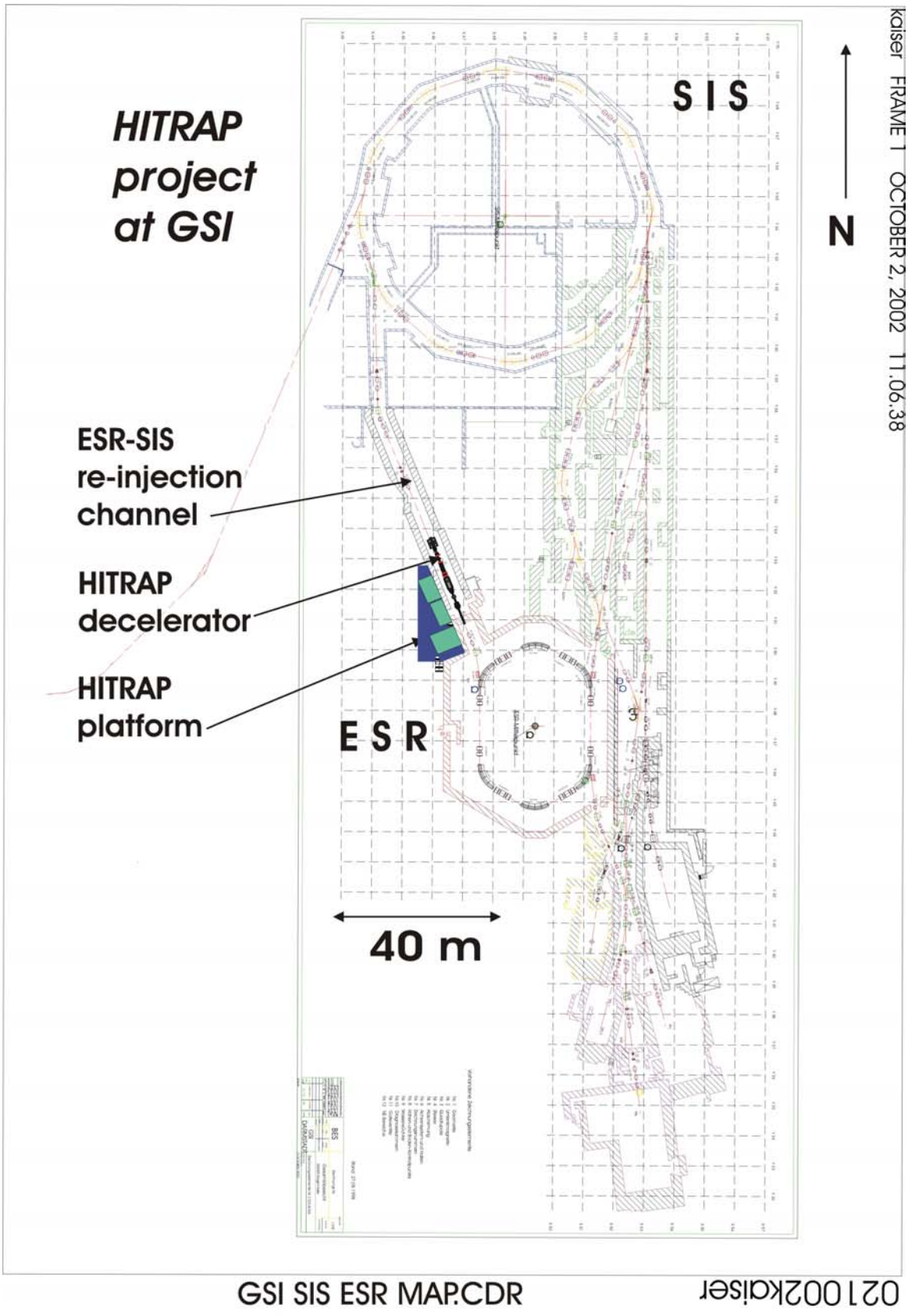

Figure 1-2. Location of HITRAP within the existing system of GSI accelerators. Top: SIS, middle: ESR, left: re-injection channel from ESR to SIS. The HITRAP decelerator will be located in the first half of this re-injection channel, the experiments on the ceiling of the channel, and the supplies on the HITRAP platform close to it at a height of 4.2 m above floor level.

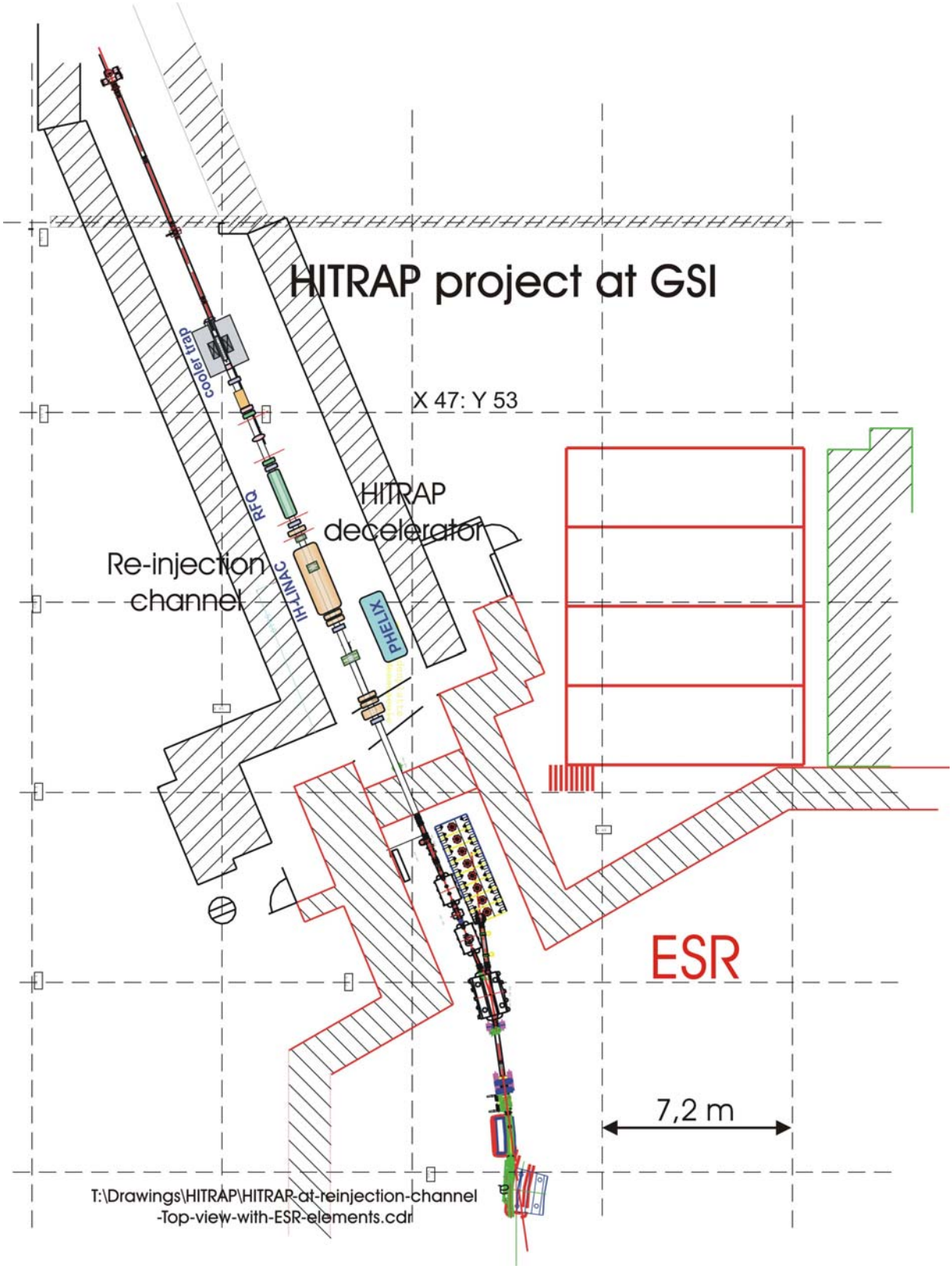

Figure 1-3. Location of the HITRAP decelerator within the re-injection channel with respect to the ESR and the re-injection beam line. The planned location of the PHELIX laser-beam compressor is also shown.

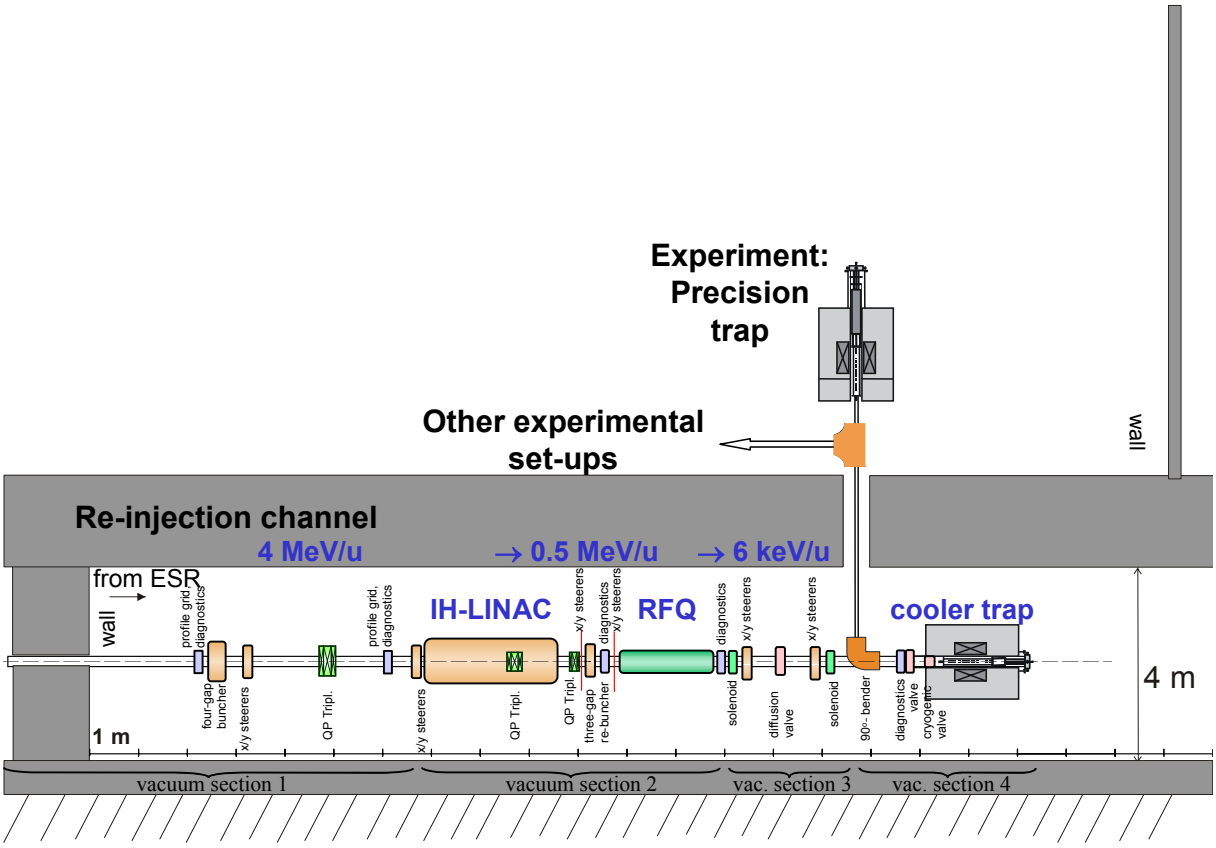

Figure 1-4. Outline of HITRAP in the re-injection channel (longitudinal cut along the beam line). In this view, the ESR is located to the left and the continuation of the re-injection channel towards SIS is on the right. The vacuum sections refer to the sections of Chapter 11. All other components are listed at Figure 1-5. The wall to the right indicates the northern end of the ESR hall.

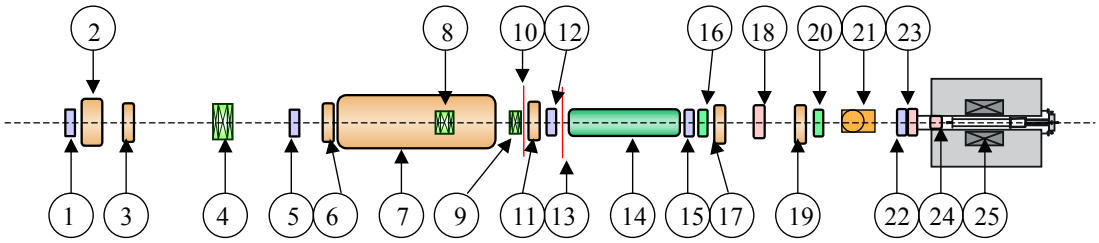

Figure 1-5. HITRAP-decelerator beam line seen from the top with all ion-optical and beam-diagnostics components. These components are the major issues of the following chapters.

1	Diagnostics box	Chapter 9
2	4-gap pre-buncher	Chapter 3
3	1st pair of x/y steerers before the IH cavity	Section 2.6.1., Chapter 8
4	Quadrupole triplet before the IH cavity	Section 2.6.1., Chapters 3 and 8
5	Diagnostics box	Chapter 9
6	2nd pair of x/y steerers before the IH cavity	Section 2.6.1., Chapter 8
7	IH cavity, first decelerator stage	Chapter 3
8	Quadrupole triplet inside the IH cavity	Chapters 3 and 8
9	Quadrupole triplet in the inner-tank section	Chapters 3 and 8
10	1st pair of x/y steerers in the inner-tank section	Chapter 8
11	3-gap re-buncher before the RFQ cavity	Chapter 3
12	Diagnostics box in the inter-tank section	Chapter 9
13	2nd pair of steerers in the inter-tank section	Chapter 8
14	RFQ cavity, second decelerator structure	Chapter 4
15	Diagnostics box after the RFQ cavity	Chapter 9
16	1st solenoid magnet of the LEBT section	Chapters 6 and 8
17	1st pair of steerers in the LEBT section	Chapter 8
18	Fast shutter	Section 7.7.1.
19	2nd pair of steerers in the LEBT section	Chapter 8
20	2nd solenoid magnet in the LEBT section	Chapters 6 and 8
21	90° bender for extraction from the trap to experiments	Section 7.8.
22	Diagnostics box ahead of the cooler trap	Chapter 9
23	UHV valve to separate the trap from the beam line	Section 7.7.2.
24	Ball valve to close the trap in the 4 K region	Section 7.7.3.
25	Cooler Trap	Chapter 7

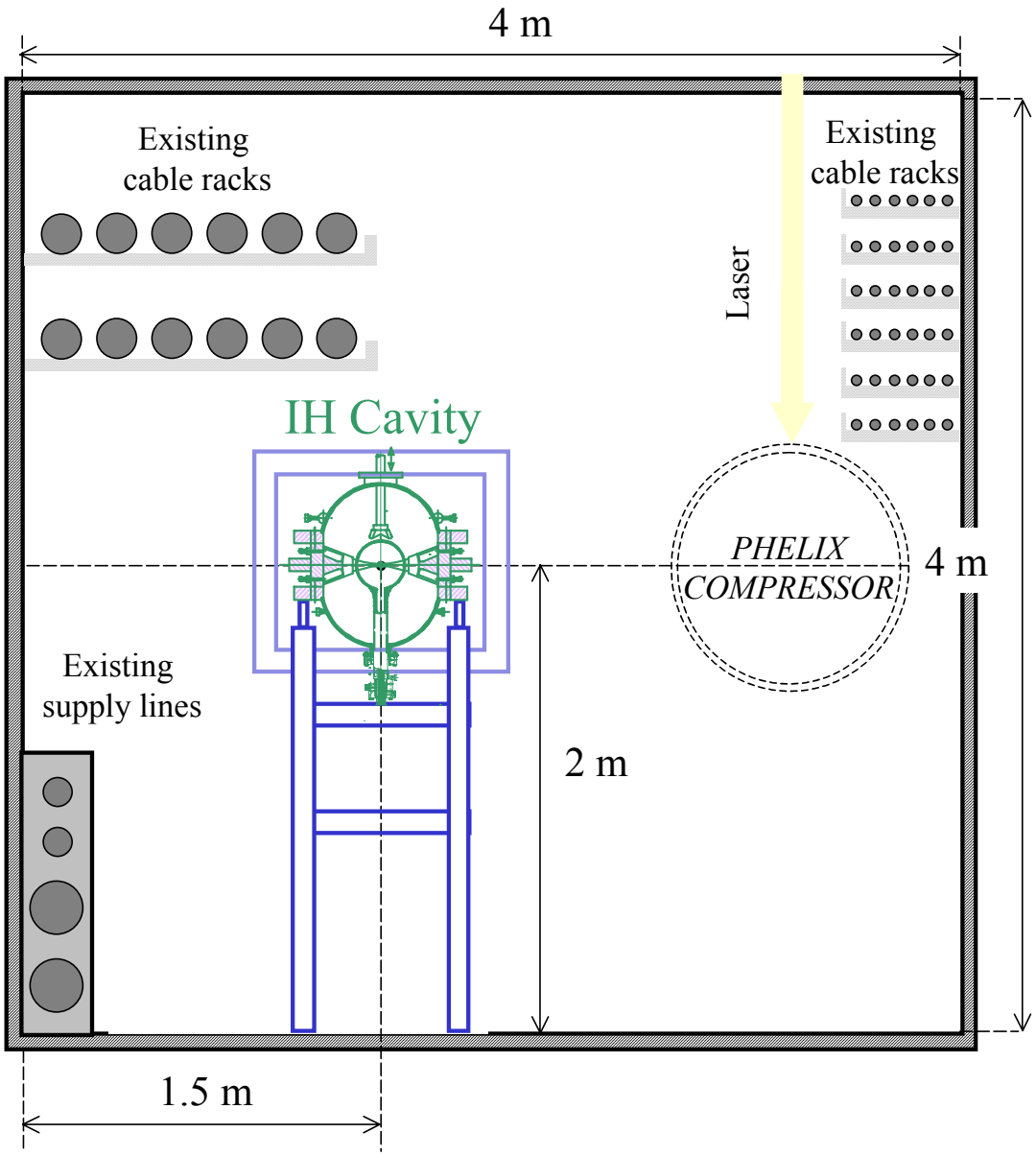

Figure 1-6. Location of the decelerator in the re-injection channel. Transversal cut across the location of the IH cavity, view to the north (in direction of the beam). To the right, the approximate size and location of the planned PHELIX laser-beam compressor are shown. Both installations fit well together in the re-injection channel.

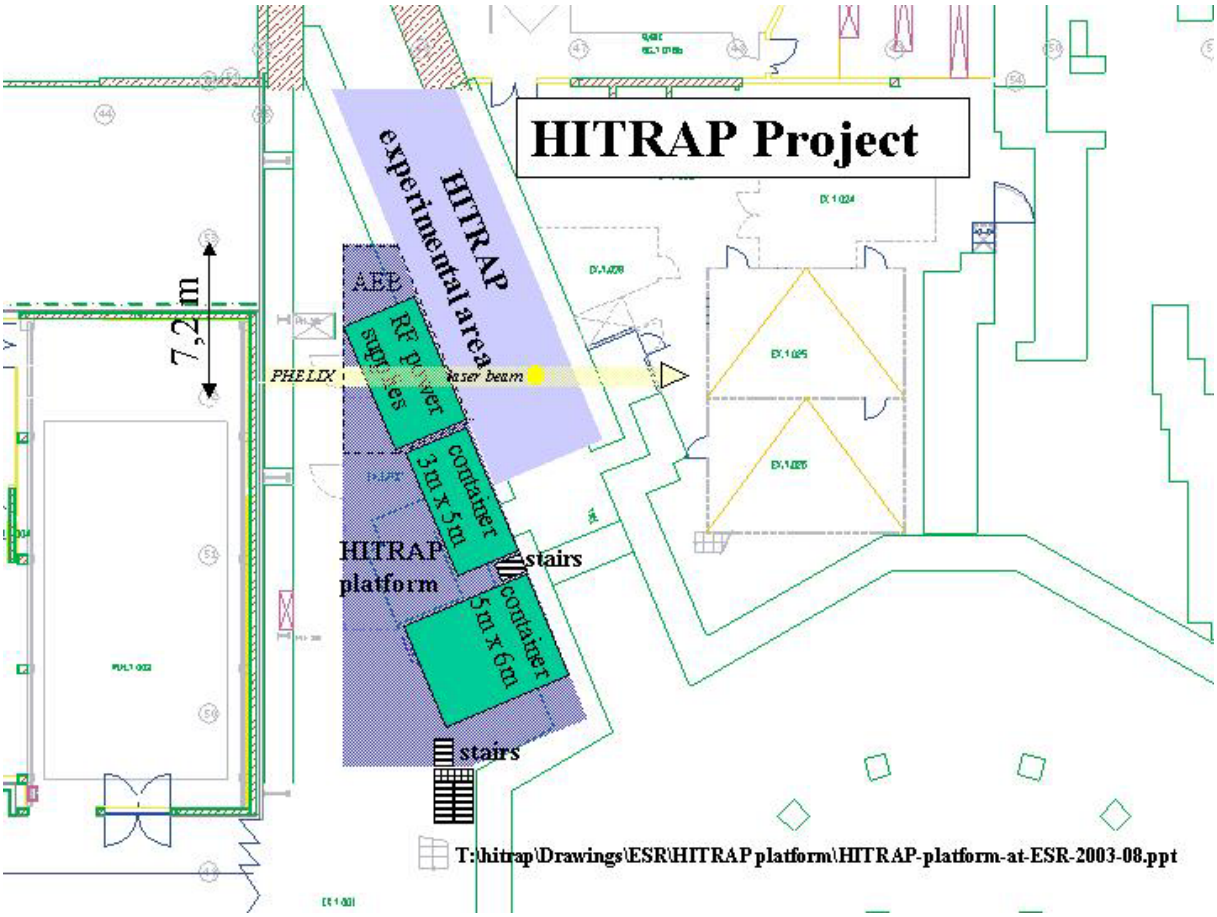

Figure 1-7. HITRAP experimental area outside the re-injection channel in the northwestern corner of the ESR hall. The platform is designed to deliver a floor 4.2 m above ground level. On this platform, containers for measurement electronics are located, and also the RF power supplies. The height of the passing PHELIX beam is at 7.5 m above floor level, which leaves enough space to place all RF power supplies at the foreseen location. From this laser beam line, a beam can be directed to the part of the PHELIX set-up planned to be located in the re-injection tunnel (cf. Fig. 1-6). The stairs which give access to the HITRAP platform already exist. Only short connections from these stairs to the platform and from the platform onto the roof of the re-injection channel have to be constructed. 'AEB' indicates the 'enclosed electrical area' around the RF supplies for reasons of safety (cf. Section 12.3.). The roof of the re-injection channel will house the experiments connected to the beam line from the cooler trap.

2. Deceleration down to 3 MeV/u in the ESR storage ring

2.1. The ESR storage ring

The experimental storage ring ESR has a magnetic bending power of 10 Tm and allows storage of heavy-ion beams at energies of more than 500 MeV/u. High beam quality can be provided by the cooling systems installed in the ESR. Stochastic cooling is used for fast pre-cooling of hot radioactive beams and electron cooling provides final beam quality over the whole range of beam energies. High yields even of bare heavy ions can be achieved by stripping the ions after acceleration in the heavy-ion synchrotron SIS. For experiments with highly charged ions at low velocity, all magnetic components and the RF frequency can be ramped at a maximum rate which corresponds to a change of the bending field of 1 T/s. The minimum velocity of the decelerated ions is determined by the lowest frequency of the RF system and the lowest magnetic-field level which provides sufficient field quality over the large acceptance of the storage ring. The ESR was designed for deceleration of ions to a minimum energy of 3 MeV/u. Machine experiments during spring 2003 have successfully demonstrated the feasibility of beam deceleration to this design minimum energy of 3 MeV/u. Future experiments will also demonstrate a stable ejection of the beam from the ESR into the re-injection beam line. As the 12-year operation of the ESR over almost the whole design range of energies never was hampered by instabilities of the magnets. The number of high-precision mass measurements that were carried out at the ESR allow for the conclusion that the magnets and their power supplies operate stable far beyond their original specifications. Therefore, difficulties are not expected. However, a stable extraction yet has to be demonstrated.

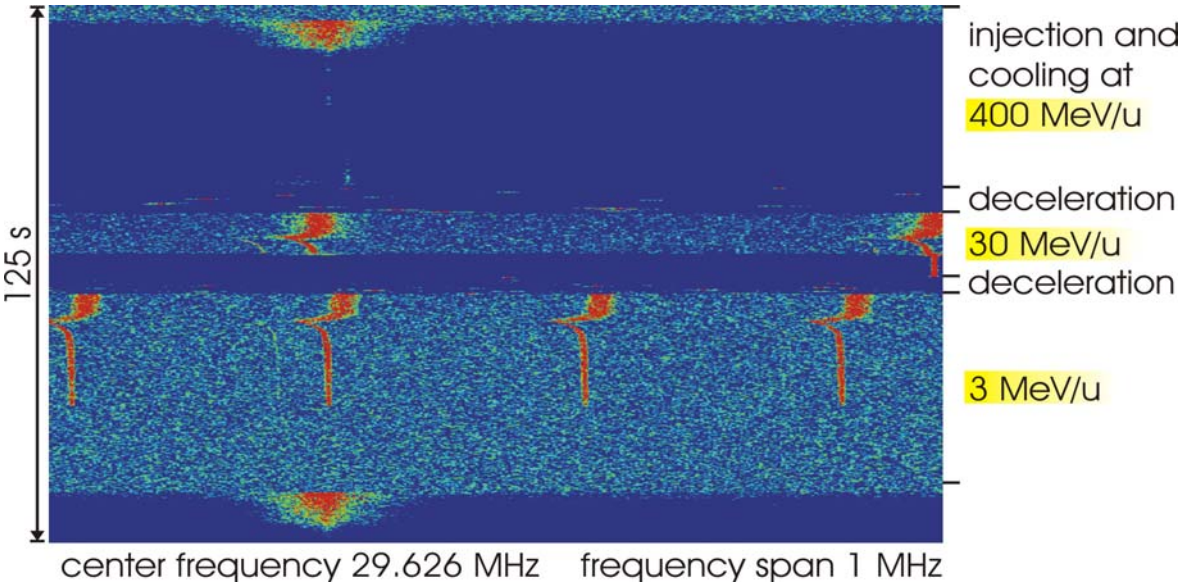

Figure 2-1. Signal of the Schottky pick-ups during the deceleration procedure. At the bottom, the next deceleration cycle already starts.

After several years of improvements of the deceleration mode, which resulted in ever decreasing minimum beam energies, in the most recent machine development at the ESR, deceleration of bare uranium from 400 MeV/u to 3 MeV/u could be achieved (Fig 2-1). The main reason for the progress was the ability to ramp the magnetic field of the electron cooler. The constant magnetic field in the electron cooler in previous tests resulted in a closed orbit distortion in the vicinity of the electron cooler, which grew inversely proportional to the ion-

beam momentum. Thus, with decreasing energy, the beam was lost at the places with largest beam excursions. This can be avoided, if the magnetic field of the electron cooler is ramped to lower values during beam deceleration.

As deceleration to 3 MeV/u really requires operation at the very low end of the equipment, an energy of 4 MeV/u was chosen as the end energy of the beam in the ESR in a scenario which employs further deceleration by a subsequent RF decelerator structures. The designed extraction energy of 4 MeV/u allows for safe operation of the ESR for A/q ratios in the range of 1 to 3. On the other hand, this extraction energy still allows for a simple RF linac decelerator structure consisting of only one IH structure and a subsequent RFQ structure (cf. Chapter 3).

2.2. Details of beam deceleration in the ESR

2.2.1. Injection

The present injection energy of 400 MeV/u is close to the maximum energy at which the electron cooling system can be operated reliably. It provides satisfactory yield of bare or highly charged heavy ions from the TE-line-stripper foil (the stripper foil between SIS and ESR). The stochastic-cooling hardware is adjusted to the corresponding beam velocity and is available for pre-cooling, e.g., if the electron-cooling time is too long because of large emittance of the injected beam.

2.2.2. Cooling after injection

Cooling the injected beam before deceleration is indispensable for high efficiency of deceleration. With electron cooling, the cooling time for the beam after injection was about 10 s. This was caused by the momentum spread and emittance which was provided from SIS and which is degraded by the interaction with the stripper foil. A significant reduction of the cooling time by electron cooling cannot be expected as the electron current cannot be increased by more than a factor of two. Stochastic cooling after injection is an option, but would make the machine cycle even more complex. Stochastic cooling has been demonstrated successfully, but it has not yet been integrated into a deceleration cycle.

2.2.3. Displacement to a central orbit

By deceleration with the RF system (by about 1% in momentum), the ion beam after cooling on the injection orbit was moved to a central orbit which allowed more space for closed-orbit distortions and beam motion due to mismatch between RF frequency and magnetic field strength during deceleration. Usually the displaced beam was re-cooled for a few seconds before deceleration.

2.2.4. First section of deceleration to an intermediate energy of 30 MeV/u

The deceleration from 400 MeV/u to 30 MeV/u was performed with a ramp rate of 0.15 T/s. It required about 7s. For higher ramp rates, increased losses were observed during the course of ramping. An improvement of the ramping procedure by optimising the ramps for the various ring elements will require extensive machine development. Another limitation came from the high-voltage system of the electron cooler, which needs major technical modifications to allow for faster ramping down. The efficiency of deceleration was dependent on the initial beam intensity, the maximum intensity after deceleration to 30 MeV/u amounted to about 5×10^7 ions, even if much larger particle numbers were injected. An increase of the

number of decelerated ions might be achieved after careful optimisation of the ramps for the ring elements.

2.2.5. Intermediate-energy cooling

The growth of the phase-space volume of the beam during deceleration resulted in the necessity of intermediate cooling. Deceleration to 30 MeV/u allowed for good efficiency for deceleration, deceleration to lower energy without cooling caused increased beam losses. The intermediate cooling restored the beam quality and allowed further deceleration with good efficiency. As electron cooling is faster at low energy and as the decelerated beam had been cooled at injection energy, the cooling time at intermediate energy was less than 5 s. The intermediate plateau in the magnetic-field ramp could also be utilized to change the RF frequency from harmonic h = 2 to h = 4 by de-bunching and re-bunching at the higher harmonic of the revolution frequency. This procedure was necessary because of the lower frequency limit of the rf system which limits the energy for h = 2 to about 11 MeV/u. With h = 4, the beam could be decelerated to 3 MeV/u.

2.2.6. Second section of deceleration

For the second part of deceleration, the ramping rate had to be further reduced to 0.05 T/s in order to avoid significant beam losses. Thus, the second part of deceleration took about 5 s. For this second section of deceleration, it was of high importance that the magnetic field of the electron cooler was ramped to a value below 0.05 T. Otherwise the beam did not reach energies below 9 MeV/u. Previous machine experiments showed a clear limitation of the minimum ion beam energy for fixed magnetic field in the electron-cooling system. During the current deceleration procedure, the magnetic field of the electron cooler was reduced from 0.078 T at the injection energy to 0.015 T at 3 MeV/u.

2.2.7. Electron cooling at the final energy

After completion of deceleration, electron cooling again was applied. In order to reduce losses during the cooling of an ion beam decelerated to lowest energy, the electron current had to be reduced to 5-10 mA and therefore it took on the order of 10 s to cool the decelerated beam. By further improvements, it should be possible to find a setting where higher electron currents and consequently faster cooling can be achieved. At present it is not clear, whether the small magnetic guiding field of 0.015 T applied at the lowest energies affected the cooling rate.

2.3. Results of deceleration tests

As the main objective of the machine development in spring 2003 was a demonstration of the minimum energy of the decelerated bare uranium beam, the first deceleration section from 400 to 30 MeV/u was not fully optimised. For low beam intensity, the efficiency for this first section was about 50 %. The maximum particle number after deceleration to 30 MeV/u was 2×10^7. In previous tests, about a factor of two higher intensities could be decelerated to 30 MeV/u. In the second deceleration section, a maximum of 6×10^6 uranium ions could be decelerated to 5 MeV/u. The beam current of the ions after deceleration to 3 MeV/u was just above the detection limit of the current transformer (1 μA), which corresponds to about 2×10^5 ions.

At both energies (5 and 3 MeV/u) the beam quality of the cooled beam could be measured by Schottky diagnostics (longitudinal momentum spread) and with the residual-gas-

ionisation beam profile monitor (horizontal emittance). No information on the vertical emittance was available, but for a cooled beam horizontal and vertical emittance should be of similar value. The current of the electron cooler at the lowest energies was reduced to 5 mA, as the decelerated ion current was rapidly lost when higher electron currents were applied. Therefore it took several seconds to cool the beam after deceleration. With 5 mA electron current at 5 MeV/u, the parameters (2σ) for about 10^6 stored ions were for the momentum spread $\delta p/p = 2.4\times10^{-4}$ and for the horizontal normalized emittance $\varepsilon_{x,\,n} = 0.093\ \pi$ mm mrad ($\varepsilon_{x,\,abs.} = 0.9\ \pi$ mm mrad). At 3 MeV/u, the beam parameters for roughly 10^5 bare uranium ions cooled with 5 mA electron current were measured to $\delta p/p = 1\times10^{-4}$ (Fig. 2-2) and $\varepsilon_{x,\,n} = 0.056\ \pi$ mm mrad ($\varepsilon_{x,\,abs} = 0.7\ \pi$ mm mrad, Fig. 2-3).

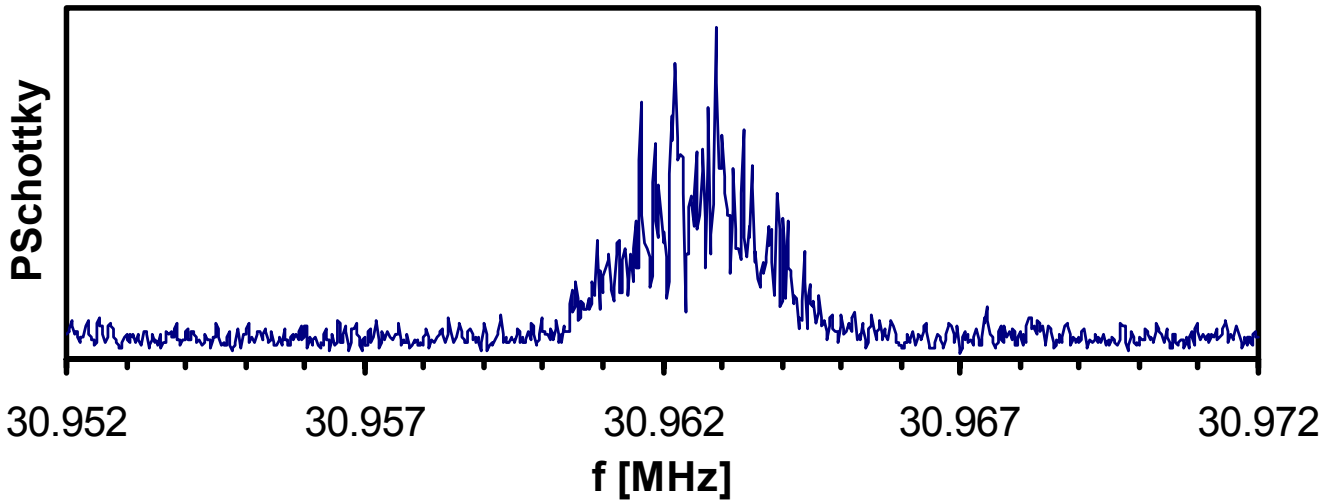

Figure 2-2. Schottky spectrum of the cooled and decelerated U^{92+} beam at 3 MeV/u, $\delta p/p = 10^{-4}$.

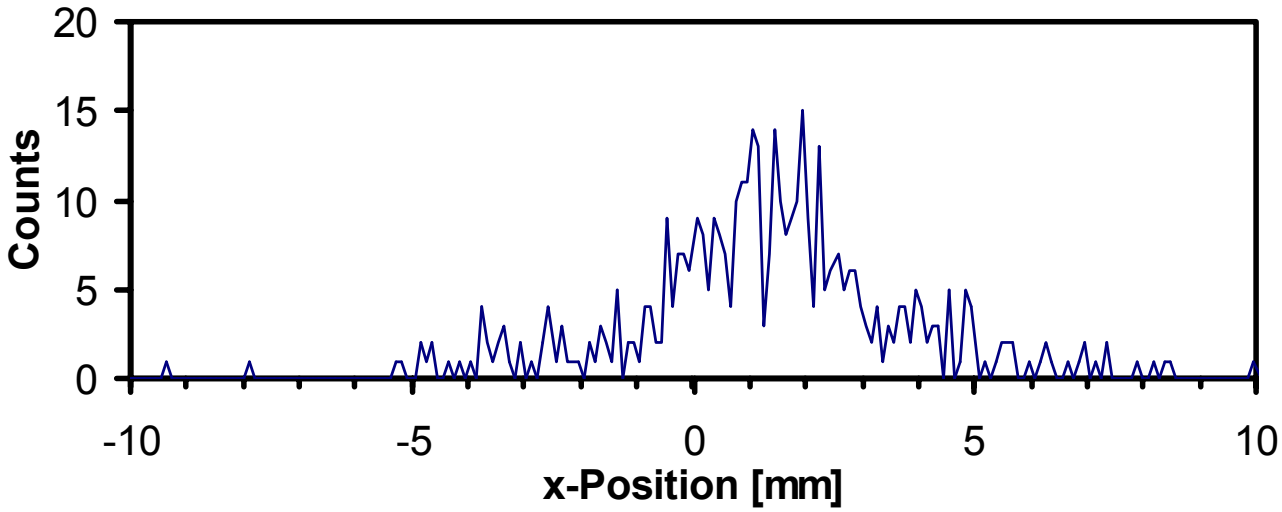

Figure 2-3. Transverse width of the decelerated and cooled U^{92+} beam in x-direction at 3 MeV/u. An emittance of $\varepsilon_{x,\,n} = 0.056\ \pi$ mm mrad ($\varepsilon_{x,\,abs}$=0.7 π mm mrad) was determined by the residual-gas ionisation beam-profile monitor.

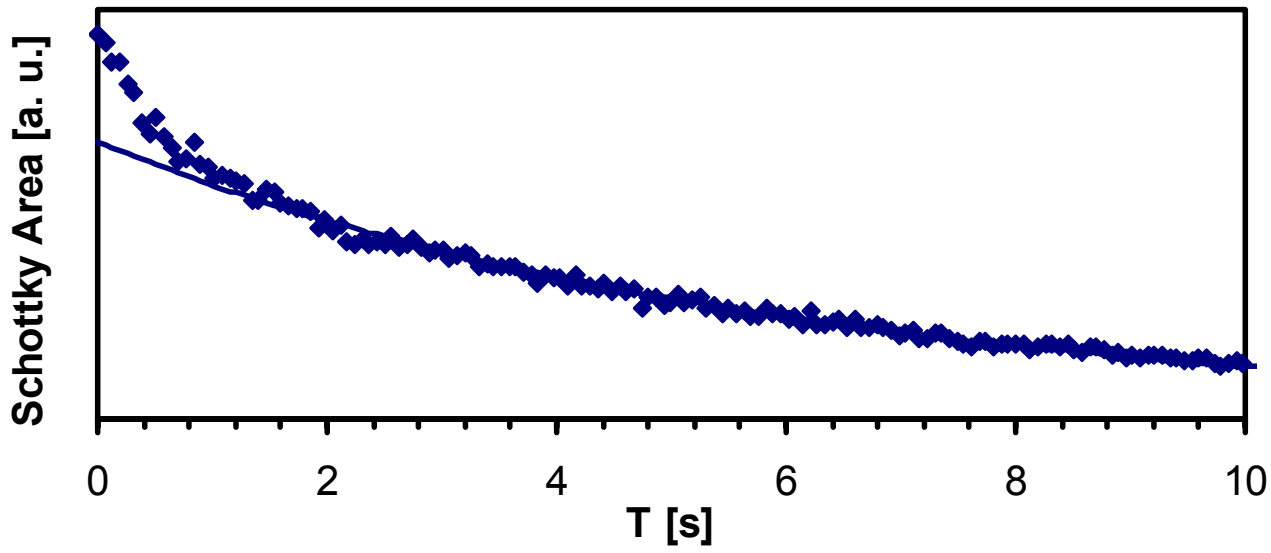

Figure 2-4. Lifetime of the U^{92+} ion beam stored at 3 MeV/u and at a pressure of 3×10^{-11} mbar, determined from the Schottky signal.

The lifetime of the ion beam stored at 3 MeV/u was determined from the integrated Schottky noise power. The residual gas limited the lifetime. No contribution from recombination in the electron cooler could be found. The lifetime at 3 MeV/u was about 6 s for an average ring vacuum of $p = 3 \times 10^{-11}$ mbar (Fig. 2-4). According to later measurements at a total pressure of $p = 2 \times 10^{-11}$ mbar with a residual gas analyser the composition was as follows: 23% H_2, 1% He, 23% H_2O, 40% N_2/CO, 4% O_2, 5% CO_2, 3% Ar, 1% C_xH_y.

2.4. Fast extraction from the ESR

Fast extraction of the decelerated beam with the ESR injection kicker towards the re-injection channel is supported by the existing hardware, but it has not been performed at the time of writing the present TDR. A maximum pulse length of the extraction kicker of 3 μs is about a factor of two longer than the pulse length accepted by the cooler trap. The possibility either to compress the beam into a shorter bunch or to transfer the beam in smaller portions by a suitable bunching scheme still needs to be investigated.

Diagnostics in the re-injection line must be tested for the low-energy beam after fast extraction. Increase of the intensity of the decelerated beam would be useful with respect to the sensitivity of beam-diagnostic devices. The stability of the extracted beam is affected both by the elements in the storage ring and by the components in the extraction lime. The reproducibility of the parameters and the pointing stability of the extracted beam will be examined by suitable diagnostics in the near future. The extraction energy is planned to be 4 MeV/u in order to have some safety margin towards the lowest energy now possible in the ring. Although the pointing stability still has to be tested, major problems that would limit or prevent a successful operation of HITRAP are not expected due to the extreme reliability the ESR set-up has shown so far.

2.5. Future machine development at the ESR

Improvements of the efficiency of deceleration can be expected after implementation of online measurements of beam position and tune during the ramp and development of an algorithm to correct the magnet values according to the measured beam behaviour. Electron cooling after deceleration with higher electron currents will allow faster cooling and better quality of the extracted beam.

Faster cooling at injection energy can be achieved if stochastic cooling is used. It is not clear whether the stochastically cooled beam can be decelerated with the same efficiency as the electron cooled beam. The use of stochastic cooling will allow a faster ramping-down as the ramping rate of the electron energy is presently the main limitation for faster deceleration. By special RF techniques the decelerated beam could be compressed longitudinally in the ESR in a way, which will allow the extraction of the entire decelerated beam. These techniques are not yet available and have to be developed. It is expected that the total deceleration time in the ESR can be reduced to about 10 seconds.

2.6. Beam transport to the IH structure

This section and the following Chapters 3, 4, and 6 deal with the beam transport from the ESR to the cooler trap and with its deceleration. The characteristic beam parameters of each transport section are subsumed in the Tables in Section 6.3.

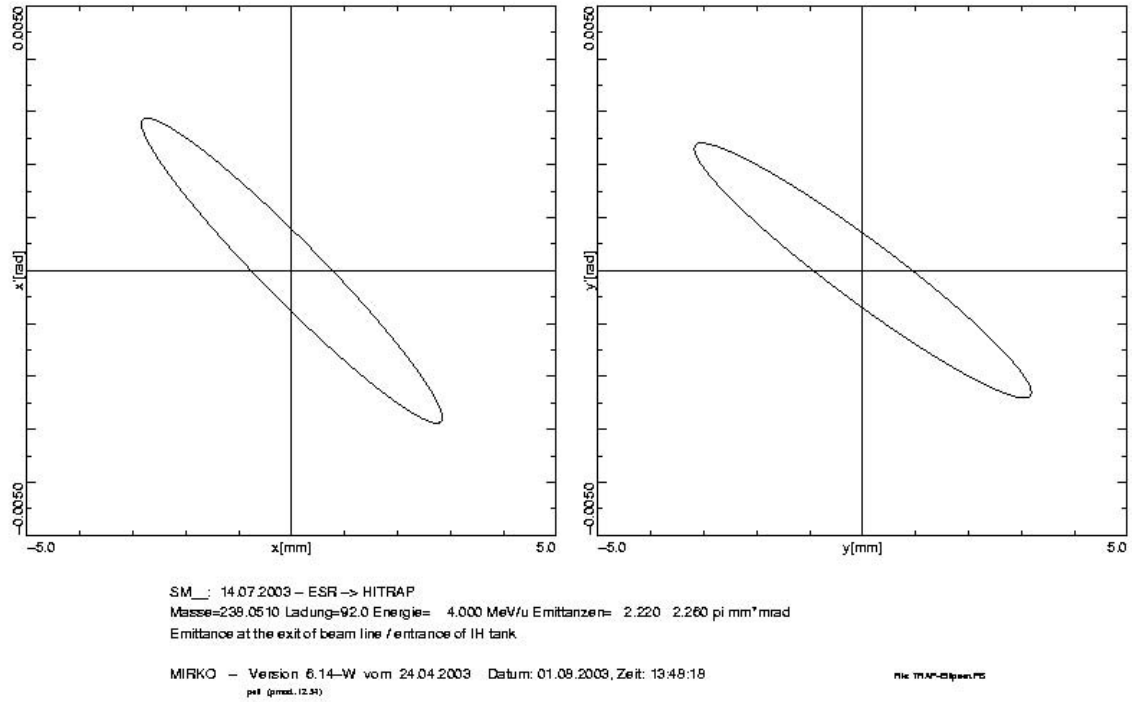

Figure 2-5.Transversal phase-space ellipses of the beam at the entrance of the IH tank. Normalized emittances are $\varepsilon_{x,n} = \varepsilon_{y,n} = 0.21\ \pi$ mm mrad.

2.6.1. Ion optics for HITRAP operation

For the matching of the beam coming from the ESR to the entrance of the IH tank, a quadrupole triplet located half way between the buncher and the tank and two pairs of steerers

are planned. The steerer positions are close to the buncher and at the entrance of the IH. In addition, two profile grids should be used, one in the pumping section and the other one near the steerers close to the IH.

Basis for the ion-optical calculation was the beam coming from the ESR. The first two dipole magnets and the first quadrupole doublet as currenty installed in the re-injection line directly after the ESR (cf. Fig. 1-3) are considered in these calculations. For the matching conditions, the acceptance of the IH (2.2 and 2.3 π mm mrad) was used although the emittance of the ESR is expected to be smaller by a factor of at least two. Figure 2-5 shows the phase-space ellipses at the entrance to the IH. With the proposed position of the triplet, the beam size in the buncher region can be kept reasonably small, and so are the required magnetic-field gradients. Shifting the triplet towards the IH, the beam in the buncher could be made even smaller, but the necessary field gradients would increase. For the present solution, three lenses of 100 mm length and 40 mm aperture diameter are planned. For safety margins, this aperture is about a factor of two larger than the expected beam size. The magnetic-field gradients are 15 T/m at maximum. Figure 2-6 shows the beam envelopes, starting at the exit from the ESR. It is worth mentioning that the distance between the wall and the entrance to the IH cavity can be enlarged by a few metres without requiring more or different components than those mentioned here. This would also allow for extensions of the part of the PHELIX set-up planned in the re-injection channel.

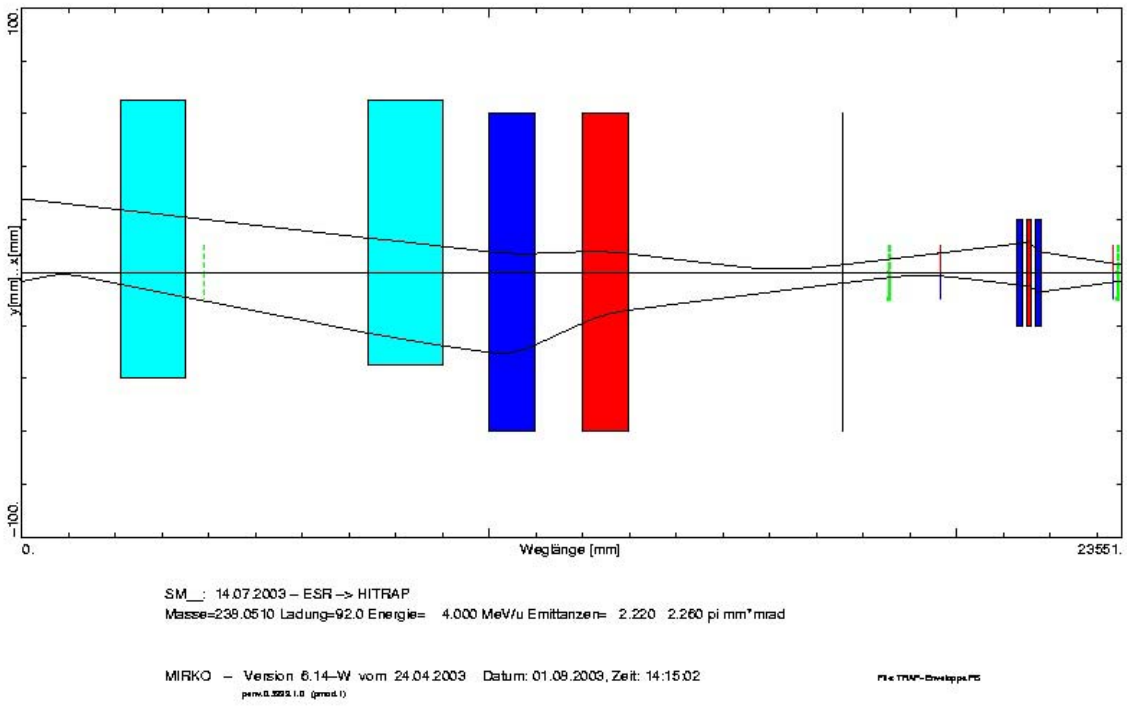

Figure 2-6. Beam envelopes between ESR (left) and IH-tank (right). The cyan-coloured boxes to the left are the existing dipole magnets after the ESR, blue and red boxes are horizontally defocusing and focusing quadrupoles, respectively. The large ones already exist (Fig. 1-3); the small ones form the new matching triplet. Green dotted lines indicate beam diagnosis elements and blue and red lines vertical and horizontal steerers. Above the axis the horizontal beam half size and below it the vertical half size is shown. The vertical black line marks the border between the ESR area and the HITRAP beam line, i.e., the existing wall between the ESR and the re-injection channel.

For steering, the two existing dipole magnets of the ESR beam line could be used. But since the magnetic rigidity for HITRAP is only about 5 % of the design value for this beam line, the achievable resolution is only in the order of some 0.1 mrad. With the required transverse optics, the slope and position error at the IH entrance due to this inaccuracy would be 0.3 mrad and 0.4 mm. Therefore, two pairs of steerers dedicated for the low magnetic rigidity should be used. The necessary strength will not exceed 3 mrad horizontally and 8 mrad vertically assuming that the uncorrected beam just fits into the aperture.

2.6.2. Ion optics for the re-injection into SIS

In case of re-injection operation, completely different requirements apply to the beam line. In particular, the apertures of the HITRAP beam line are not sufficient for even a cooled high-energy beam, which has to be focused through the re-injection channel. In order to keep the general solution as simple as possible, the original re-injection beam line will be employed for the rare cases of re-injection operation. The HITRAP components with narrow apertures will be mechanically removed from the beam line for re-injection operation. Due to this, new ion-optical calculations for re-injection operation are not required.

2.7. Required components

The steerers and magnets listed above, including their power supplies, will form the subject of Chapter 8 where all ion-optical elements are subsumed. Therefore, here no compilation and cost estimate is given. All required components are listed in Chapter 8.

3. IH-Linac

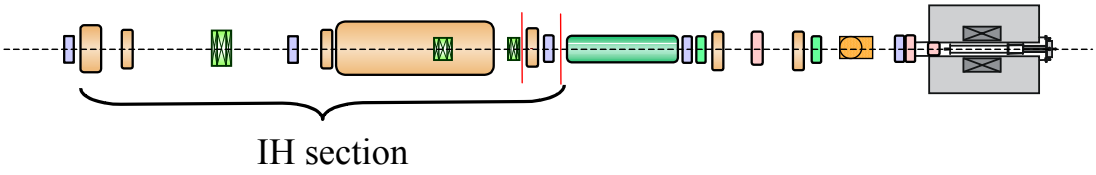

3.1. Principle

3.1.1. General

The beam-ejection energy for $^{238}U^{92+}$ ions from the ESR is planned to be at 4 MeV/u. If only an RFQ structure is used for further deceleration, as it has been done at the CERN-AD ring, the linear decelerator becomes too long and expensive and consumes too much RF power. The alternative proposed here is a two-stage decelerating set-up consisting of one IH-DTL structure and one RFQ structure, both operating at 108.408 MHz with a repetition time of approximately 10 seconds. The single IH-DTL section decelerates the ions to an intermediate energy of 0.5 MeV/u. The final energy of 6 keV/u is then obtained by the RFQ section. Such a combination of IH-DTL and RFQ structures became conventional for ion accelerators, e.g., at the accelerator currently being built for ion therapy at the DKFZ in Heidelberg. It is thought to be efficient for deceleration, too.

3.1.2. Details

This chapter describes the intermediate deceleration based on an IH-DTL cavity and the matching of the beam to the final RFQ section. It also comprises a buncher before the IH structure, the corresponding drift length towards the IH structure, and a re-buncher between the IH-tank and the RFQ-tank. It also includes a complete ion-optical calculation from the first buncher via the IH and the re-buncher up to the entry of the RFQ. This includes a second ion-optical calculation from the first buncher to the IH with the quadrupole triplet mentioned in Section 2.6.1. placed closer to the IH tank. This has been done for comparison and to get an estimate for the parameter range imposed by different locations of this triplet. The solution of Section 2.6.1 does well match the one presented here in this chapter. In the light of cost reduction and easiness of construction, that of Section 2.6.1. is finally be preferred up to the IH tank although the whole calculation in the present chapter assumes the first triplet being placed close to the IH-cavity.

3.2. General lay-out of the IH-type decelerator

The beam of highly stripped heavy ions with a charge-to-mass ratio up to 1/3, covering $^{238}U^{92+}$ ions, has to be decelerated in the IH-DTL from 4 MeV/u down to 0.5 MeV/u. The main features of the beam delivered by ESR, after deceleration down to 4 MeV/u and cooling, are a small transverse emittance, a low energy spread and negligible space charge effects. The intermediate decelerating array has been designed as simple as possible with a minimum of necessary units. It includes the main IH tank with one internal quadrupole-triplet lens, a four-

gap bunching cavity in front of the tank, a three-gap re-buncher behind the IH tank and two external triplet lenses which match the beam to the IH and RFQ sections, respectively. The last lens at the IH tank exit provides both a convergent beam for RFQ input and a short drift section for possible beam diagnostics (Fig. 3-1).

Effective RF voltages of 54 kV and 60 kV, respectively, have to be applied to the gaps at the first and second bunching cavity. The distances between the gap centres in these cavities are 124.6 mm and 45.2 mm, respectively. The distance between the centres of the first and the last gap of the IH structure is 2468.4 mm. Two decelerating sections separated by an internal lens contain 15 gaps and 10 gaps within lengths between gap centres of 1542.4 mm and 587.6 mm, respectively. The expected effective voltage distribution along the main IH tank is shown by Figure 3-2.

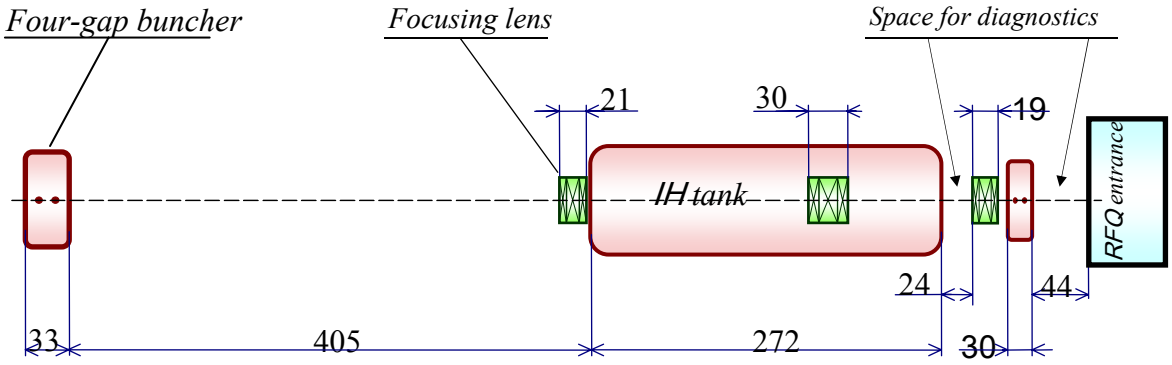

Figure 3-1. Intermediate decelerating array based on the IH DTL structure. Scale in cm. At the right there are the second buncher and the entrance to the RFQ. The first quadrupole triplet ('Focusing lens') at the entrance to the IH tank is located further to the left (beam up) in the final design (cf. Section 3.1.2).

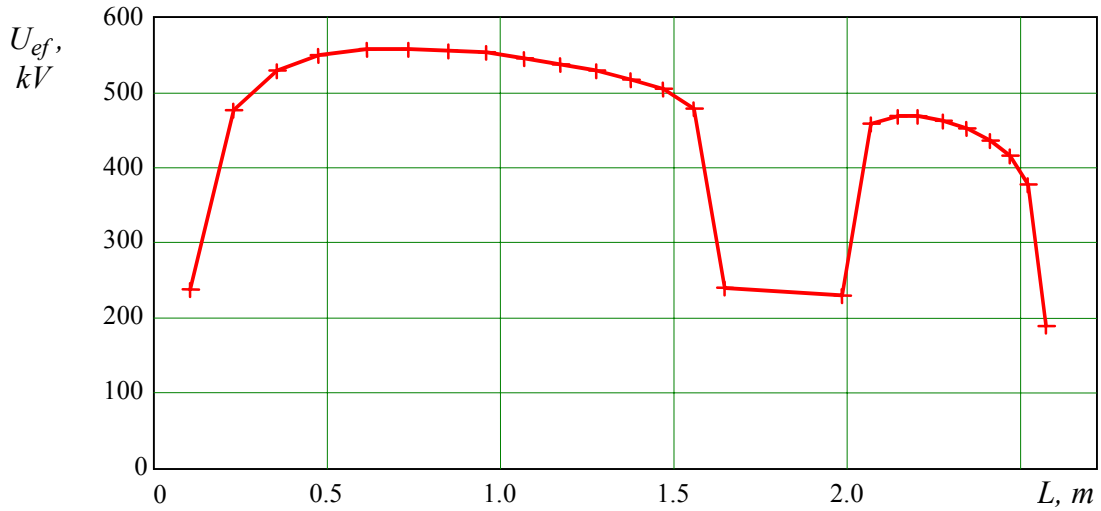

Figure 3-2. Effective voltage distribution along the main IH tank. The gap in the middle corresponds to the location of the inner-tank quadrupole triplet.

According to estimations, an RF power of about 180 kW is necessary to drive the IH cavity. Although this value fits to the output power of the existing RF generators (200 kW), great care has to be taken to reduce the RF power losses as much as possible.

The parameters of the focusing triplet lenses are given in Table 3-1. The small aperture and modest magnetic gradient of the first and second lenses make their design quite comfortable. The numbers for the first triplet can be reduced if it is placed further beam-up as

mentioned in Section 2.6.1. In that case, existing quadrupoles might be employed. The third lens needs twice the aperture in order to provide a relatively long drift towards the RFQ section. Nevertheless, the magnetic induction at the pole tips does not exceed the value of 0.8 T, which is close to the limit for the existing production technology, involving Vacoflux (a cobalt alloy). An additional magnetic field analysis will be performed at the final design stage.

Table 3-1. Parameters of the focusing magnetic quadrupole lenses. The values for triplet No. 1 were used in the ion-optical calculations of this chapter and do not represent the final solution (cf. Section 3.1.2.). The design values for all three triplets are given in Table 8-1.

Triplet No	Effective pole length (mm)	Magnetic gradient (T/m)	Aperture radius (mm)	Eff. longitud. distance between poles (mm)
1	40	45.0	8.0	25
	80	44.0		
	40	45.0		
2	70	53.3	8.0	20
	120	52.0		
	70	53.3		
3	40	53.1	15.0	20
	72	52.0		
	40	53.1		

3.3. Beam dynamics

Beam dynamics simulations have been done with the LORASR code, developed and suited especially for IH structures. The simulations were performed for q/A=1/3 ions at zero beam current. Figure 3-3 shows the 98%-beam-transverse envelopes for a normalized transverse beam emittance of 0.2 π mm mrad.

Within the decelerating sections, the beam is very close to axial symmetry. This provides minimum transverse size and maximum transmission. The beam radius in the drift-tube sections does not exceed 2 mm besides the very few gaps at tank injection. Designed aperture radii of 6 mm at the first section (before the internal quadrupole triplet) and 5 mm at the second section (after the triplet) provide enough safety for such a beam taking into account possible misalignments and even a larger emittance as will be discussed below.

Being decelerated down to 0.5 MeV/u, the beam has to be matched to the RFQ section where a convergent beam with a radius of less than 2 mm is required. Also, free space along the axis is necessary for diagnostics and steering. In order to avoid any second lens between the IH- and RFQ-sections, the output triplet is installed at a distance of 240 mm behind the IH tank, allowing the beam to expand up to 8 mm in radius. Then it is focused again to the RFQ entrance so that the independently driven re-buncher and a diagnostic box can be installed in front of the RFQ section.

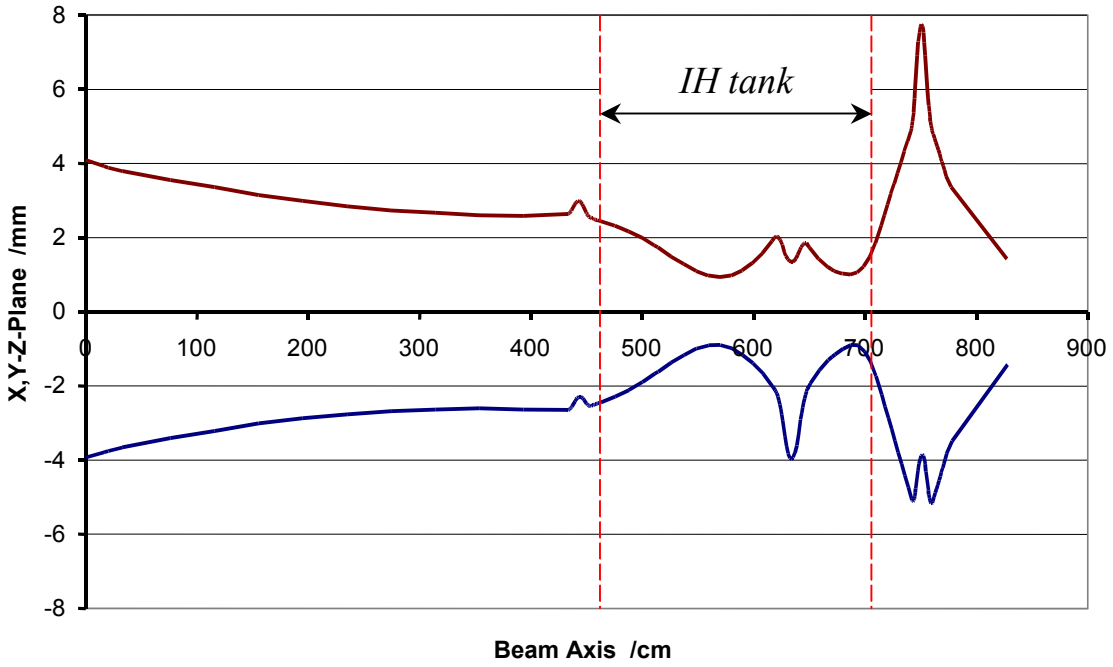

Figure 3-3. Transverse 98%-beam envelopes along the IH deceleration array. Red: X, Blue: Y. The location of the IH cavity is indicated. The Z-axis is the beam axis.

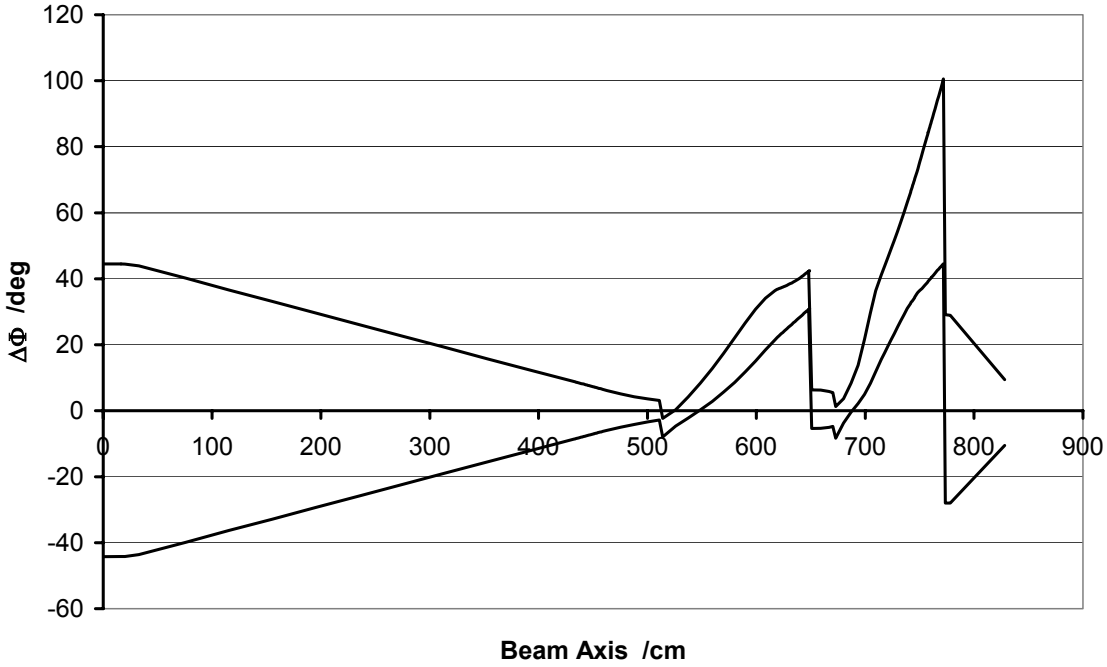

Figure 3-4. Longitudinal 98% -bunch envelope along the IH deceleration array. The deviation from the reference axis is given for beginning and end of the bunch. The phase width at a given position is the difference between both curves.

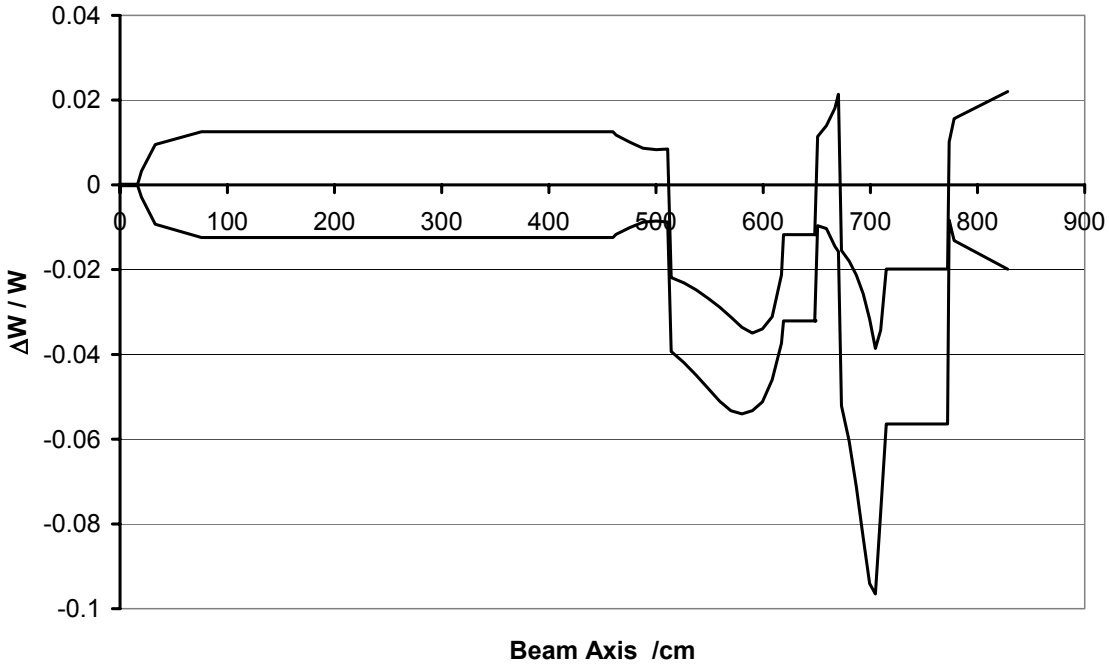

Figure 3-5. Bunch-energy spread along the IH deceleration array. The deviation from the reference axis is given. The lines denote the particles with highest and lowest energy, respectively. The energy width at a given position is the difference between both curves.

Figure 3-4 shows the longitudinal 98%-bunch envelope. The beam energy spread along the decelerating array is shown by Figure 3-5. The phase and energy widths are given by the difference between both lines while the absolute deviations $\Delta\phi$ and ΔW correspond to the virtual parameters used for the design of the drift-tube array.

The four-gap buncher cavity in front of the decelerator is operated at a frequency of 108.408 MHz. After this buncher, a short drift range of 4 m length has been chosen in order to relax the stability requirements for the bunching RF voltage amplitude and the RF phase. Since the bunch is too much convergent in the longitudinal direction after 4 m drift, the IH tank starts with four de-bunching gaps. After the exit from the IH tank, the bunch expands up to nearly $\pm 30°$ while drifting to the second re-bunching cavity, which then provides the required phase length of around $\pm 10°$ at the RFQ entrance.

The first buncher accepts 100° out of 360° injected by the ESR into the end bucket, corresponding to 28% of the particles from the ESR. A second, second-harmonic bunching cavity may be additionally installed in order to focus up to 75 % of the particles into the IH structure. In this case, the drift length has to be optimised.

The flexibility of the proposed system has to be underlined: The parameters of the output beam can be easily varied by the pre-bunching voltage and by the output lens gradient. Additionally, the beam energy may be tuned in some limits by the pre-buncher RF-phase variation.

Figure 3-6 shows the projections of the beam emittance at the entrance to the first buncher and at the exit from the section under discussion here, i.e., the entrance to the RFQ structure. The beam is axially symmetric both at the input and at the output of the section. The configuration of the output projections satisfies the RFQ requirements in terms of emittance (cf. Chapter 4).

Beam input to the first buncher

ε_x=0.19 π mm mrad ε_y=0.19 π mm mrad ε_z=0.96 π keV/u ns

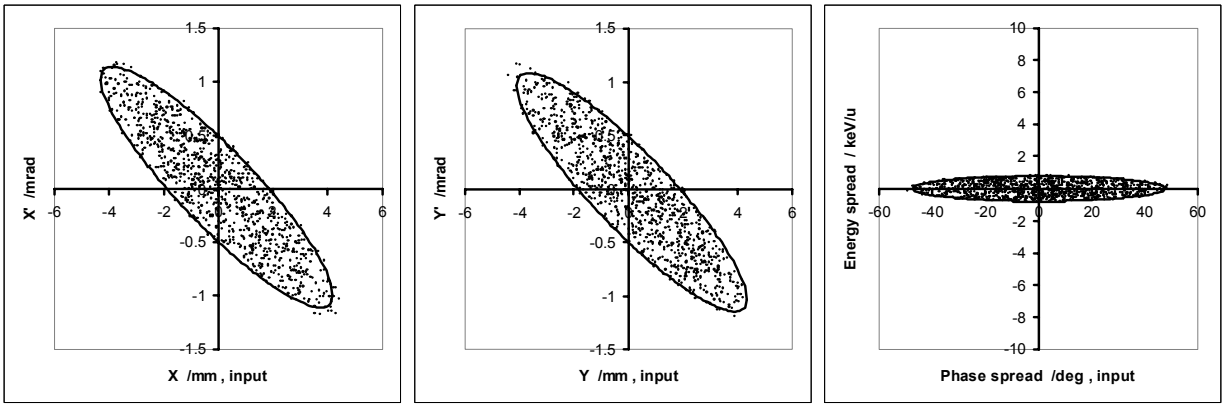

Beam output after the IH = Beam input to the RFQ

ε_x=0.24 π mm mrad ε_y=0.24 π mm mrad ε_z=4.22 π keV/u ns

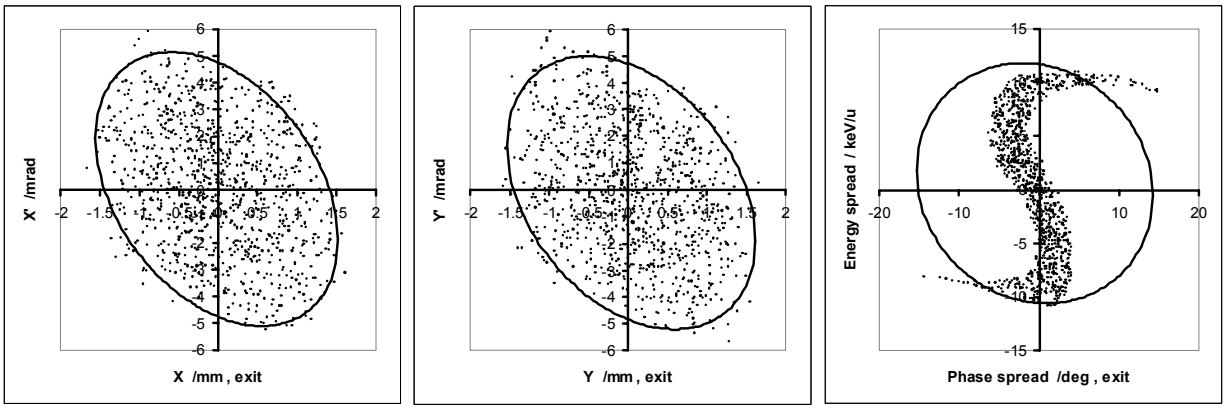

Figure 3-6. Projections of the beam emittance at the input to the first buncher and at the entrance to the RFQ-structure. All given emittance values are normalized emittances.

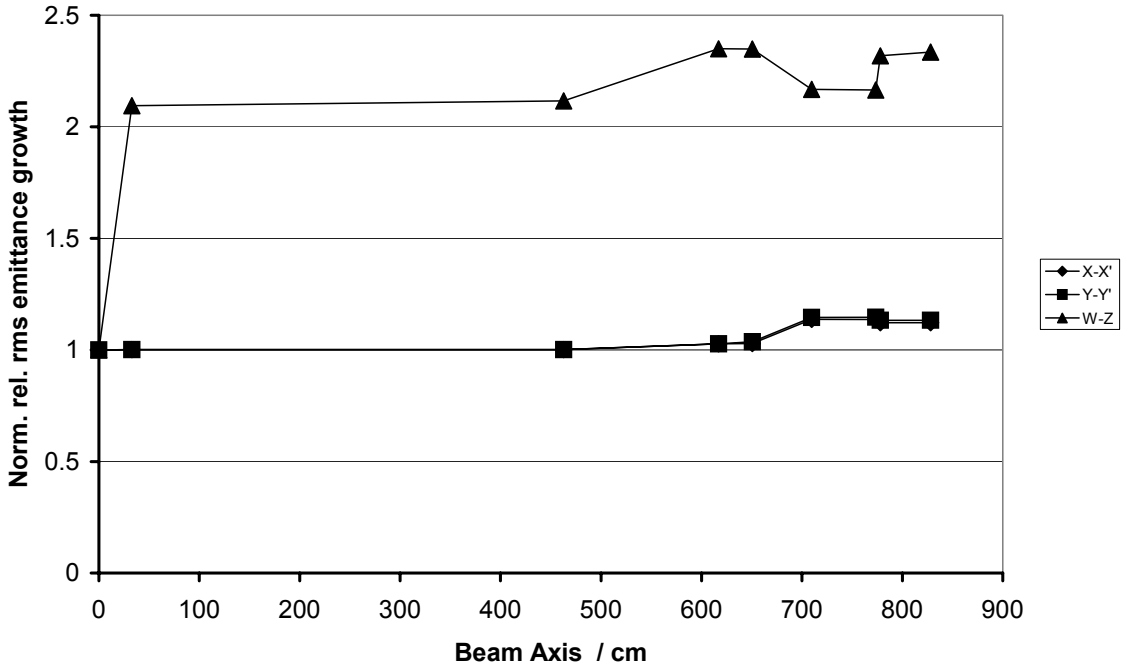

Figure 3-7. Normalized rms emittance growth along the decelerating structure. The values for X-X' and Y-Y' almost coincide at any given point. W-Z denotes the growth in energy spread along the structure.

In Figure 3-7, the normalized rms-transverse-emittance growths during the deceleration are displayed. The normalized transverse rms-emittance growth is only 15%, while the increase in longitudinal rms-emittance increase is about a factor of 2.3. In practise, the final longitudinal emittance does not depend on the initial energy spread, but is determined by the non-linearity of the RF decelerating field, mainly at the first buncher. A remarkable improvement of the longitudinal beam emittance for the given input-bunch length can be achieved only by a second buncher before the IH structure.

3.4. Structure ability for larger emittance and beam displacement

It is clear that a structure, designed for small beam emittance and with small aperture, may be sensitive to the input-emittance increase and beam displacements, especially when including the long drift range from the ESR to the IH-DTL. Figure 3-8 shows the transverse beam envelopes for two values of the normalized transverse emittance, 0.2 π mm mrad and 0.45 π mm mrad, respectively. For the increased emittance, the envelopes for both x and y become larger by a factor of 1.5. Nevertheless, this is still quite safe within a drift-tube aperture of 5-6 mm radius. In the last lens, with an aperture radius as large as 15 mm, the beam with the increased emittance can be accepted and focused into the RFQ at x,y< 2 mm.

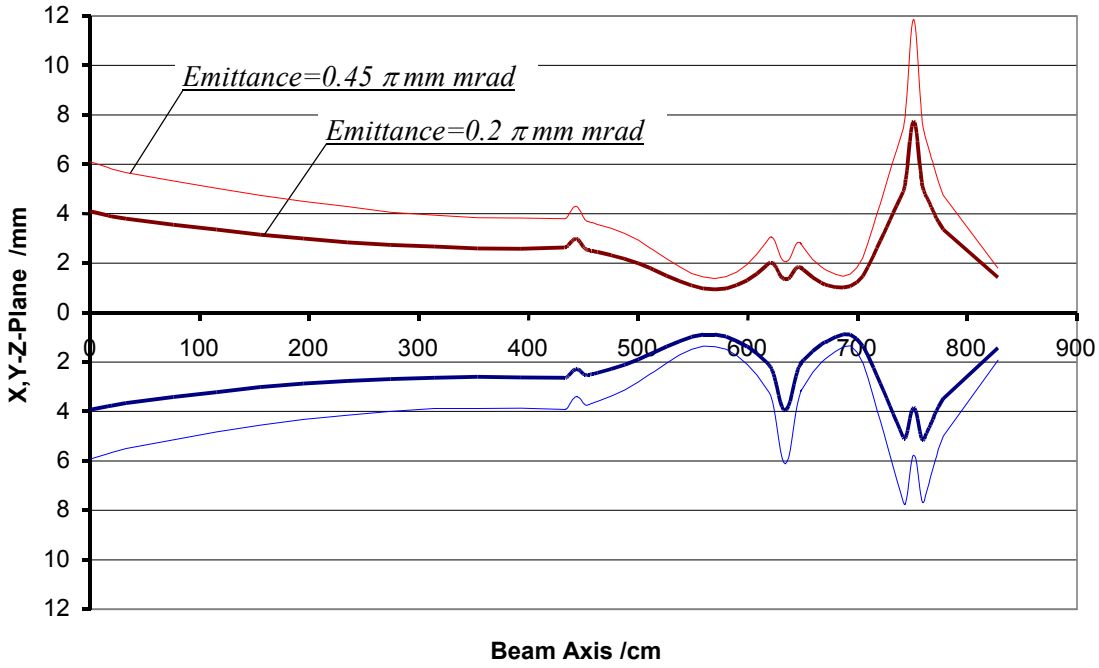

Figure 3-8. Transverse 98%-beam envelopes for two different values of normalized transverse emittance. The larger of the two emittances (0.45 π mm mrad) shows the acceptance of the IH structure. The design value for the normalized transversal emittance is 0.2 π mm mrad which already includes a safety margin of a factor of 2 compared to the output value from the ESR.

In order to investigate effects of an off-axis beam, Figure 3-9 and Figure 3-10 show the transverse envelopes of the beam displaced by 1.5 mm in x and y directions, respectively, at the location of the first buncher. Such a displacement does not lead to particle losses in the IH structure. Efficient beam transport is still safe within the aperture. In front of the RFQ entrance, corrections can take place by steering.

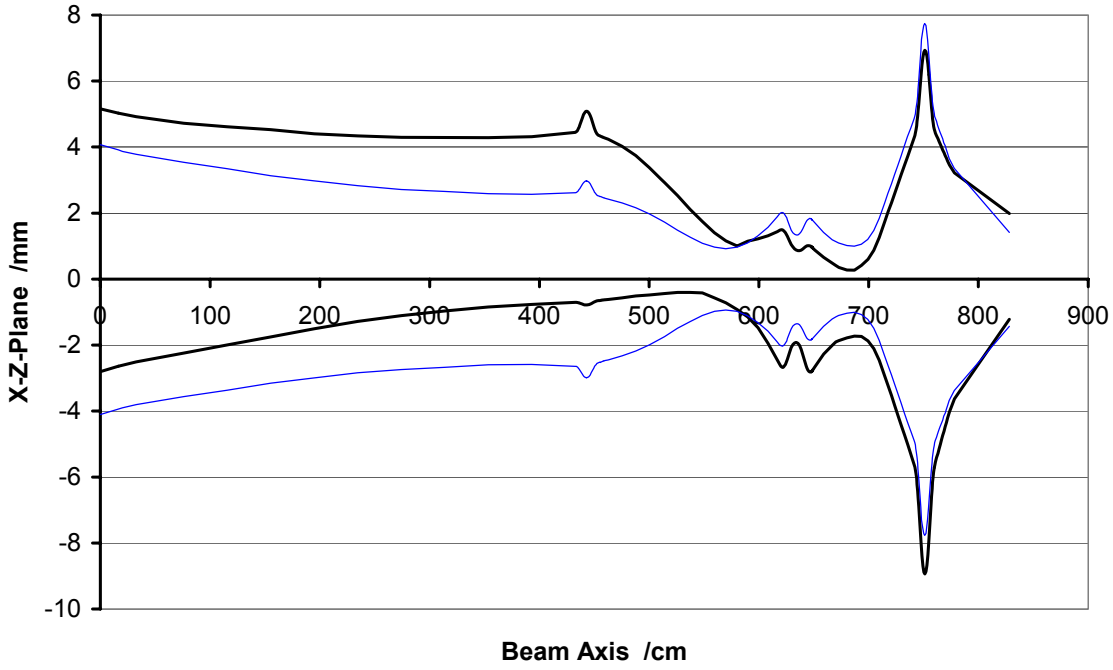

Figure3-9. Transverse 98%-beam envelope for a beam displaced by 1.5 mm in positive x direction. The blue curve indicates the envelope of the on-axis beam.

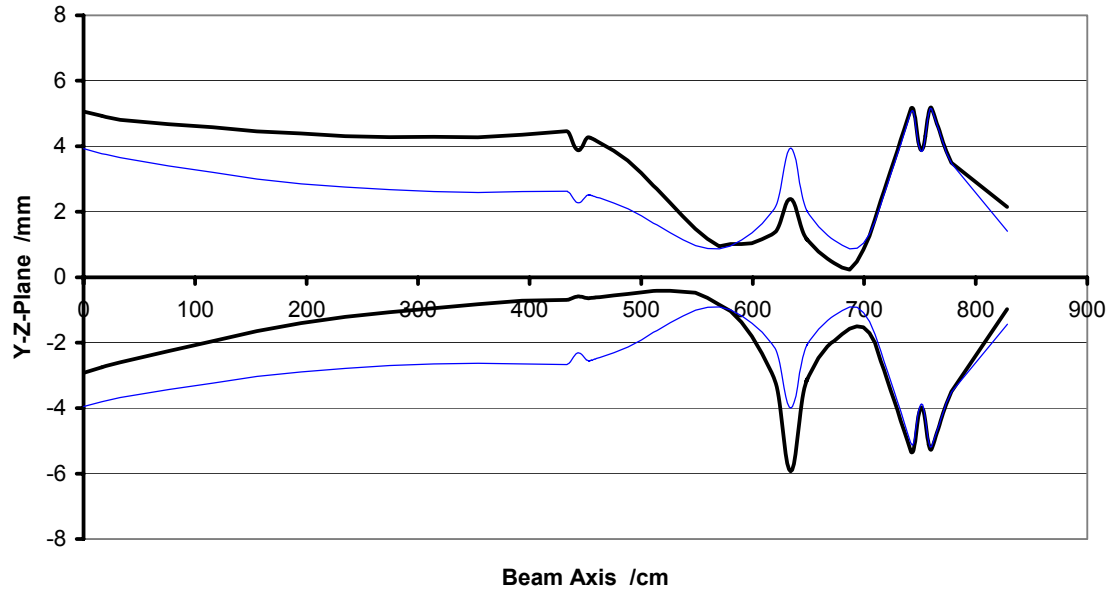

Figure 3-10. Transverse 98%-beam envelope for a beam displaced by 1.5 mm in y direction. The blue curve indicates the envelope of the on-axis beam

3.5. Summary of the simulation

An IH-DTL cavity efficiently decelerates the ions with charge-to-mass ratio of 1/3 from 4 MeV/u to 0.5 MeV/u and matches the beam to the RFQ entrance. The total length and power consumption are much lower than compared to the case of an RFQ-only decelerator. On the other hand, an IH-DTL solution without any RFQ structure would need considerably more design efforts and would imply the bunching at a lower RF frequency (36 MHz) with the consequence of longer drift ranges at the high-energy side of the beam line. The suggested

IH – RFQ combination provides an optimal solution with respect to cost minimization at an adequate performance. The relatively short 4 m drift range does not require extremely high stability of the bunching RF voltage and phase. The main parameters of the IH tank are given in Table 3-2. Great care has to be taken to keep the RF power consumption within the limit of 200 kW, determined by existing RF amplifiers.

Table 3-2. Parameters of decelerating IH-DTL tank and the bunchers

Simulated charge-to-mass ratio	q/A	1/3
Operating frequency	MHz	108.408
Tank length	m	2.72
Input / output energy	MeV/u	4.0 / 0.5
Aperture diameter	mm	12 – 10
Number of the internal triplet lenses		1
Number of accelerating gaps		25
Normalized transverse emittance (ellipse area)	π mm mrad	0.2
Transverse rms emittance growth	%	20
Normalized longitudinal emittance (ellipse area)	π keV/u ns	0.96 (input) – 4.2 (output)
Total effective RF voltage	MV	11.35
Average accelerating rate	MV/m	4.2
Maximum electric field on axis	MV/m	12
Estimated RF power consumption	kW	180
Total effective RF voltage at the first buncher	kV	216
Drift length	m	4
Total effective RF voltage at the second buncher	kV	120

3.6. Detailed Design of the buncher cavities and the IH-DTL

The HITRAP decelerator will profit enormously form the tradition of designing, building, and operating IH cavities at GSI. In this section, the key engineering is described.

3.6.1. Four-gap buncher before the IH structure

The proposed buncher cavity is a quarter-wave coaxial line with two different inner diameters at the inductive and the capacitive side of the resonator. The number of accelerating gaps is four. The drift tube geometry is the same as that for any IH cavity. The original beam-transport simulation above was carried out using a two-gap buncher ahead of the IH. The four-gap cavity presented here has the same effects as a two-gap cavity if the total voltage in both gaps is the same. The simulation therefore is still according to the specified components. The reason to finally choose a four-gap buncher is a smaller need for RF power of only 2 kW. In the case of a two-gap buncher, about 5 kW would have been required, with the need for a considerably more expensive power supply. The 2-kW solution allows for the use of UNILAC spare parts in case of power-supply failure.

Three of such cavities are already in use at the UNILAC High-Charge-State Ion Injector HLI (Figure 3-11). Therefore, designing and operating this kind of cavity is well-known at GSI. During operation, these cavities have shown a high efficiency at room temperature for different energies.

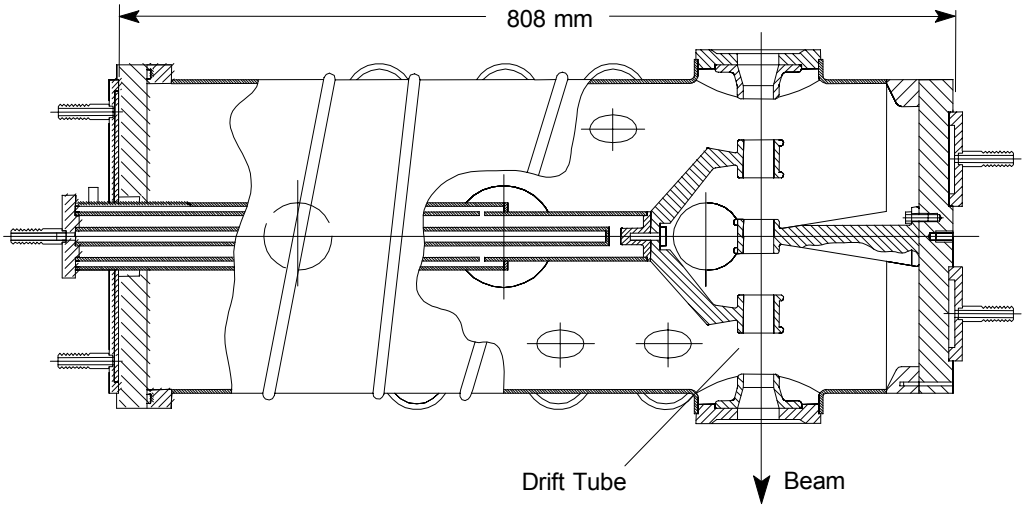

Figure 3-11. Longitudinal cut of the four-gap buncher at the High Charge State injector at GSI.

The technical parameters of the 4-gap buncher are specified in Table 3-3.

Table 3-3: Parameters of the 4-gap buncher cavity

Resonance frequency	108.408 MHz
Beam energy	4 MeV/u
Length	675 mm
Outer diameter	511 mm
Inner diameter	110 mm / 57 mm
Estimated Q value	9500
Effective shunt impedance	80 MΩ / m
Effective voltage	216 kV
RF power	≤ 2 kW

3.6.2. IH-cavity engineering: Mechanical design

The IH cavity consists of three major parts:

- one central rectangular frame which carries the small drift-tube bodies
- two semi-spherical shells above and below the rectangular part which form an enclosed structure together with the rectangular part.

These three separate parts allow for easier machining, copper plating, handling, and mounting. The lower semi-spherical shell is connected to the support frame.

The drift tube containing the quadrupole triplet is directly connected to the support frame by a stem. The stem passes through the lower shell via bellows. This drift tube therefore is completely independent from the tank

Each piece of the tank cavity is to be manufactured by external companies. For a tank of the specified size, the choice of the shell material, mild steel or stainless steel, will hardly change the cost of manufacturing.

All inner surfaces are not machined and grounded, in order to prepare for the copper plating process. The mounting surfaces on the centre frame have to be machined very precisely because no transverse adjustments are foreseen to align the small inner drift tubes. However, it will be possible to adjust drift tubes longitudinally. Stem and drift-tube bodies are made from stainless steel and are copper plated. The copper plating will be carried out at GSI where the required specific knowledge is present.

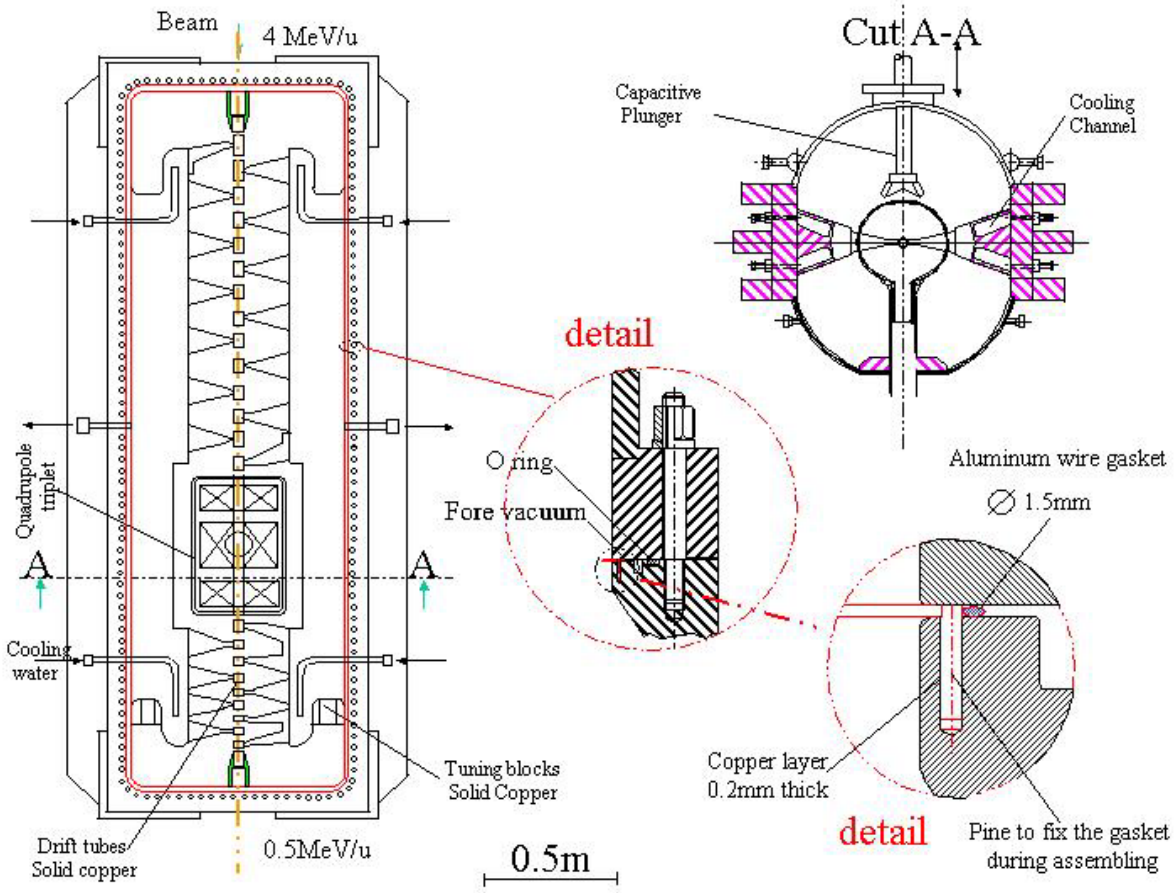

Figure 3-12. Longitudinal and transversal cut through the IH cavity.

3.6.3. IH-cavity engineering: Alignment

The standard tolerance for mechanical misalignment at the GSI accelerator complex does not exceed 0.2 mm. This is well in the acceptable range specified in Sections 3.2 – 3.5. Deviations of the beam from the axis can easily be corrected by the steerers.

The alignment of the cavity will be done in the same way as for the HLI: Three screws under the lower shell assure alignment. Off-axis targets which are directly connected to the tank could be used to measure alignment (Figure 3-13). This method will also be employed at the GSI future facility where HITRAP is going to be located (cf. Chapter 16).

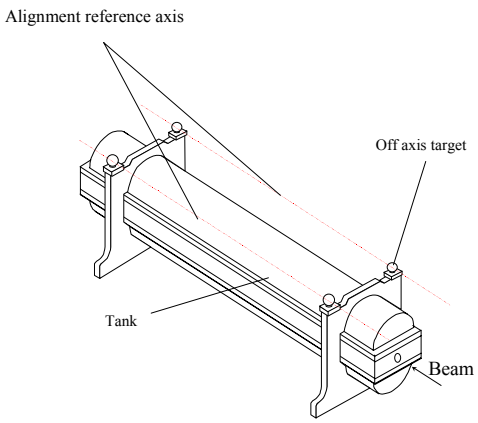

Figure 3-13. Alignment of the IH cavity by external axes.

3.6.4. IH-cavity engineering: Vacuum

In order to obtain good vacuum, the complete tank will be aluminium sealed as shown in Figure 3-12, detail. To obtain a good vacuum tightness and good RF contact, this 1.5 mm of aluminium has to be compressed to half of its diameter. About 130 screws are necessary to assure this compression. The cavity will be equipped with a turbo pump and three ion pumps. The detailed presentation of the vacuum installations is the subject of Chapter 11.

3.6.5. Re-buncher between the IH structure and the RFQ structure

The re-buncher between the IH structure and the RFQ has to provide a longitudinal focus at the RFQ entrance at 500keV/u. An existing spiral-loaded cavity will be employed, which has been in use at the UNILAC.

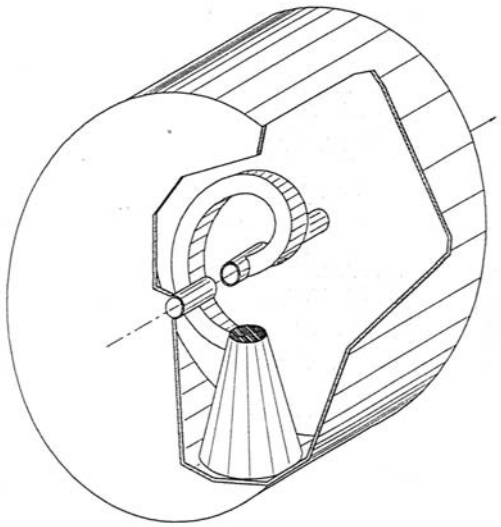

Fig 3-14. Sketch of a spiral resonator.

Spirals are λ/2-transmission-line resonators and can be treated as coaxial resonators in which the inner conductor has been wound up to reduce its size (Figure 3-14). This makes the frequency of the resonator indepedent of the outer cavity and allows for modifications and

tuning in a wide range. These resonators are generally used as post-accelerator structures and as beam-matching devices.

In the decelerator, the resonator works at a fixed value of energy/nucleon. In order to reduce the power consumption, a three-gap electrode structure with a total length of 5 βλ/2 will be employed, which fits into the present re-buncher cavity.

Table 3-4: Parameters of the 3-gap re-buncher

Length / Diameter	300 /500 mm
Length per cell ($\beta\lambda$)	9 cm
No. of cells	3
Frequency	108.408 MHz
Cavity voltage U_{eff}	120 kV
R_p-value	9 MΩ
RF power	1.8 kW

3.7. Requirements for space and cooling water

The diameter of the IH tank is about 0.8 m. It forms the widest part of the decelerator, and care has to be taken whether it can be placed without conflict by existing cable racks in the re-injection channel and also PHELIX equipment to be installed. Figures 1-3 and 1-6 indicate sufficient space even in the case the design values are slightly exceeded.

Cooling water is required for the quadrupole lenses and the IH tank. For the lenses, the water circuits available in the section for the existing quadrupoles of the re-injection channel can be employed. Due to the very low duty cycle (~ 0.15%, cf. the RF-supply, Chapter 5), the cooling of the IH cavity is not a critical task. The energy to be dissipated in the tank is very low, only 300 J/s. The energy to be dissipated in the pulsed inner quadrupole triplet is comparable. The water flow to assure a constant temperature of 28° C (±1° C) should be approximately 4.5 litres per minute in the tank and the triplet. The cavity has to be cooled by 'black water', a very high quality water (<16µS/cm), if the tank is made from mild steel with its good heat conductivity. In this case, two different water-cooling systems are required, to avoid corrosion of the parts made from stainless steel, copper and plastic. Nevertheless, the low cooling requirement in total allows for manufacturing the tank in stainless steel and so using only one cooling system for the complete cavity. The cost estimates below already consider the manufacturing of the tank cavity from stainless steel. The thin drift tubes are not cooled directly but just via the contact surface by heat conduction which will be sufficient at the low duty cycles of the HITRAP set-up. The power supplies for the magnets are specified in Chapter 8.

3.8. Costs of the IH-DTL structure and the bunchers

The estimated costs of the following subsections comprise all costs of RF structures to be purchased or manufactured, including supports. They do not comprise the required vacuum equipment, which is the subject of Chapter 11 and also not any external RF facilities such as transmitters. These are the subject of Chapter 5. The quadrupole lenses mentioned in this chapter are specified in detail in Chapter 8. The cost estimates for the IH cavity allow for a manufacturing from stainless steel as mentioned in Section 3.7.

3.8.1. 4-gap buncher before the IH structure

Table 3-5. Cost details of the 4-gap buncher

	estimated acquisition value (k€)
Cavity	60
Drift tubes	2
Tuner	15
RF in-coupler	5
Vacuum and pumps	*cf. Chapter 11*
Mechanical support	4
Other components	5
Design costs	35
Total:	**126**

3.8.2. IH cavity

Table 3-6. Cost details for the IH cavity

	estimated acquisition value (k€)
Vacuum tank	200
Internal quadrupole lenses (1 triplet)	60
Drift tubes	18
Tuner	15
RF in-coupler	10
Vacuum and pumps	*cf. Chapter 11*
Mechanical support and alignment	8
Other components	5
Design costs	35
Total:	**351**

3.8.3. Re-buncher between IH structure and RFQ

This buncher is going to be a 3-gap spiral-resonator cavity, which is available from GSI stock. The actual costs therefore reduce to some modifications of the existing cavity for the new purpose and a support structure. Comparing with the costs for the 4-gap buncher ahead of the IH structure, thus **savings** of about **100,000 Euro** are achieved by using a cavity available at GSI (Table 3-7).

Table 3-7. Cost details for the 3-gap re-buncher

	estimated acquisition value (k€)
Modifications of the existing cavity	5
Mechanical support	4
Total:	**9**

3.8.4. Additional beam-line elements up to the RFQ

In the inter-tank section between the IH cavity and the RFQ cavity, both a quadrupole triplet and steerers have to be placed which due to the length restrictions have to be of special geometry. These components will be listed in Chapter 8.

3.8.5. Total costs for IH structure and bunchers

According to the three Tables 3-5 – 3-7 presented here, the **total costs** for the IH-DTL cavity and the two bunchers are estimated to be **486 k€**.

4. Radio-Frequency Quadrupole decelerator structure (RFQ)

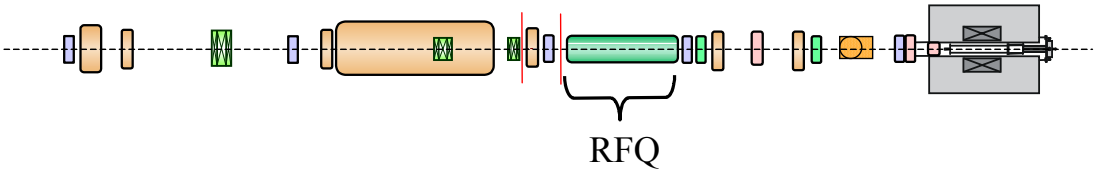

The RFQ is the second stage of the decelerators. It can decelerate and focus the beam from the first IH-decelerator stage to low energies. It is planned to inject the beam from the IH-decelerator at 500 keV/u into the RFQ and decelerate down to 6 keV/u within this structure. The RFQ is designed to keep the radial-emittance growth small, (i.e., the normalized emittance approximately constant). In addition, it will yield a high transmission rate.

4.1. Specification and choice of parameters

The RFQ is designed to be a 4-rod RFQ operating at 108.408 MHz at modest peak fields and low power consumption (cf. Table 4-1). It is modelled along the lines of the GSI-HLI RFQ, which serves as injector for moderate charge states (q/A > 1/9) and accelerates heavy ions from 2.5 keV/u to 300 keV/u. The HITRAP decelerator is designed for high charge states of q/A> 1/3, which eases the rf-power problems and allows for a compact short structure.

Table 4-1 Parameters of the RFQ decelerator. Values for two different spreads of the input energy are given. For the longitudinal output emittance, the values for 80 % and 100 % of the particles are indicated separately.

Input phase width / energy spread	± 9° / ± 10 keV/u	± 9° / ± 5 keV
Injection energy / output energy	500 keV/u / 6 keV/u	
Charge-to-mass ratio q/A	> 1/3	
Operation frequency	108.408 MHz	
Electrode voltage	70 kV	
Modulation	2.44	
Phase range	–18° – –70°	
RFQ length	1.9 m	
Aperture	4 mm radius	
Input emittance (normalized)	0.24 π mm mrad	
Output energy spread	± 0.5 keV/u (8.3 %)	± 0.38 keV/u (6.3%)
Longitudinal input emittance	23 nsec .keV/u	11.5 nsec keV/u
Longitudinal output emittance (80 %)	10 nsec keV/u	5.6 nsec keV/u
Longitudinal output emittance (100 %)	23 nsec keV/u	9.0 nsec keV/u
Radial output emittance (normalized)	0.37 π mm mrad	0.25 π mm mrad
Transmission	93%	100%
Power consumption	80 kW	

4.2. Beam-dynamics simulations

The crucial RFQ-design parameters are the longitudinal emittance, the energy spread, and the phase width of the beam. A value of an energy spread of $\Delta T/T=1\%$ at the RFQ-high-energy input translates to 66% at the low energy end.

A design scheme has been developed which reduces the output-energy spread to approximately ± 6%. With an input-phase width of $\Delta\phi < 20^{o}$ and asynchronous deceleration, the beam pulse can be kept compact with reduced phase oscillations. The required output emittance restricts the possible input phase width and energy spread. A $\Delta T/T$ of 2% is the upper useful limit. For the radial emittance, a value of 0.24 π mm mrad has been used for input.

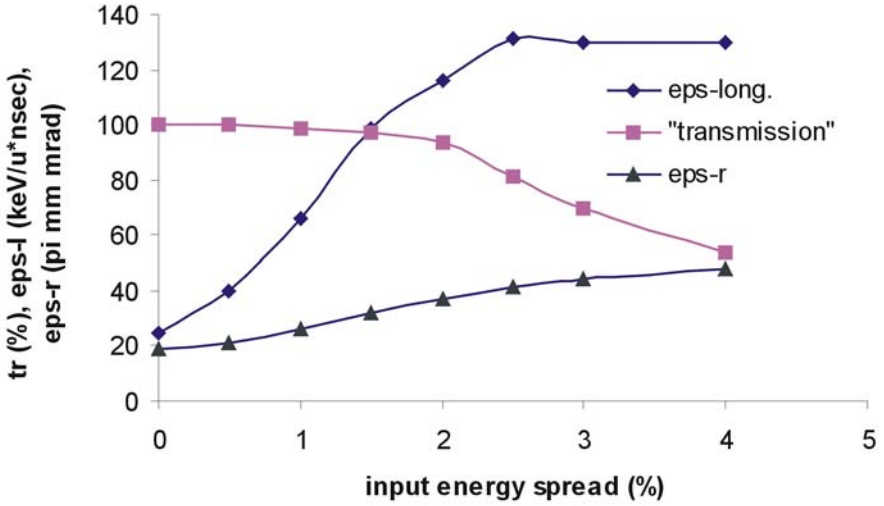

Figure 4-1. Influence of the spread of the input energy on transmission (in %), $\varepsilon_{longitudinal}$, and $\varepsilon_{transversal}$.

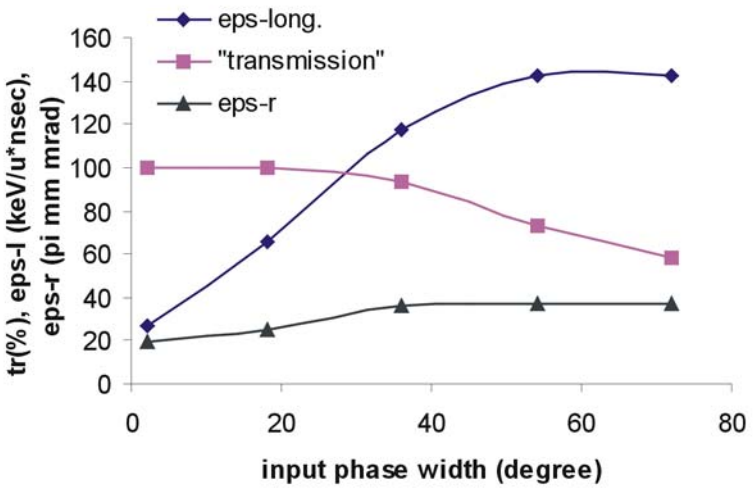

Figure 4-2. Influence of the spread of the input-phase width on transmission (in %), $\varepsilon_{longitudinal}$, and $\varepsilon_{transversal}$.

The design is a compromise between acceptance, output emittance, transmission, length, and power consumption. Small input-beam emittance is favourable for output beam quality. Figures 4-1 and 4-2 illustrate the strong influence of the input parameters bunch phase, width, and energy spread. Figures 4-3 and 4-4 show beam parameters for input and output of the decelerator RFQ.

From Figure 4-4, a beam symmetrical in X and Y can be concluded at the output of the RFQ structure. This allows for the use of solenoid magnets as ion-optical components in the section between RFQ and cooler trap, as described in Chapter 6.

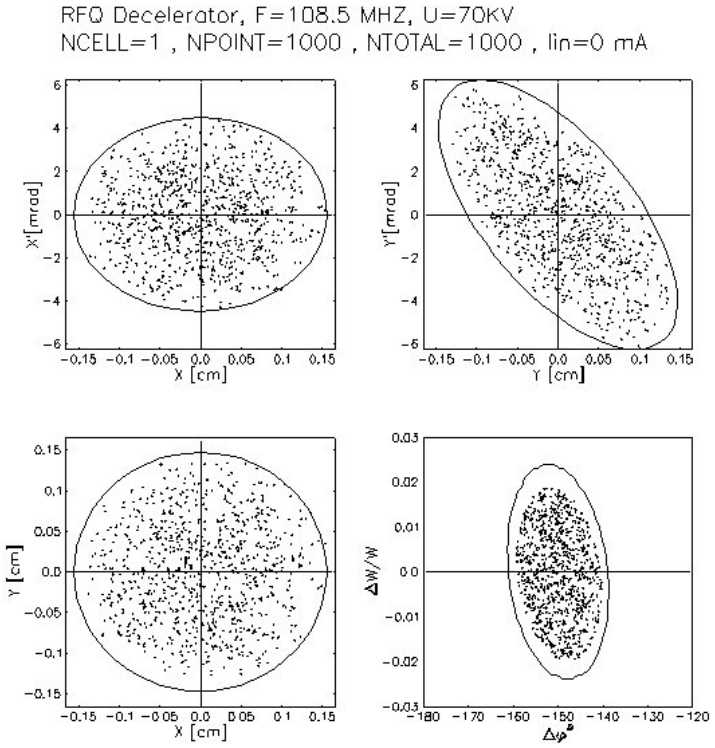

Figure 4-3. Input-beam parameters for the transport calculations through the RFQ. ΔT/T = ±2 % is assumed.

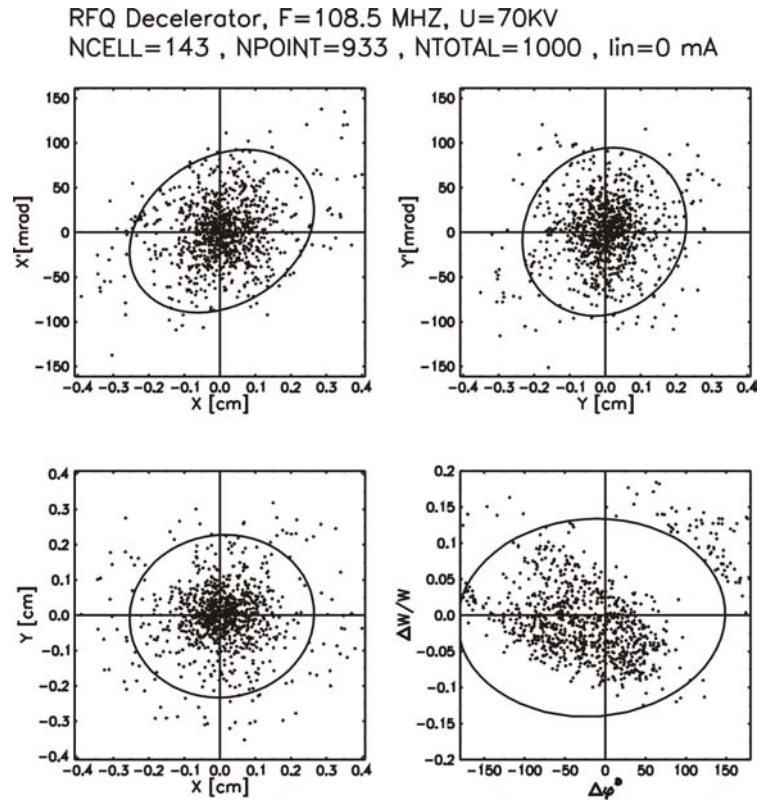

Figure 4-4. Output from the RFQ for the input from Figure 4-3.

4.3. Instrumentation and costs

The decelerator-RFQ is planned to be 1.9 m long with an inner cavity diameter of 35 cm (cf. Fig. 4-5). The cavity will be equipped with a turbo pump and two ion pumps. Details of the vacuum considerations are given in Chapter 11. Power requirements and costs can be extrapolated from the experience with the HLI-RFQ and similar projects.

Maximum support is anticipated from the University of Frankfurt (IAP) for the design, assembly, tuning and installation of the RFQ decelerator.

Table 4-2. Costs of the RFQ decelerator. Design and construction will be provided by the IAP, Frankfurt.

No.	Type of instrument	(k€)
1	RFQ tank with resonant insert	125
2	Couplers, tuners, pick ups	14
3	Vacuum pumps, valves	35
4	RF control	23
	Total costs:	**197**

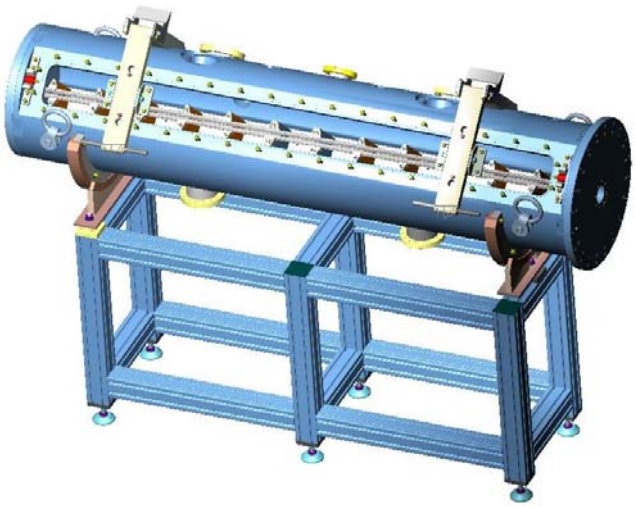

Figure 4-5. Schematic drawing of the planned decelerator-RFQ. The inner diameter of the structure is 35 cm, the length 1.9 m.

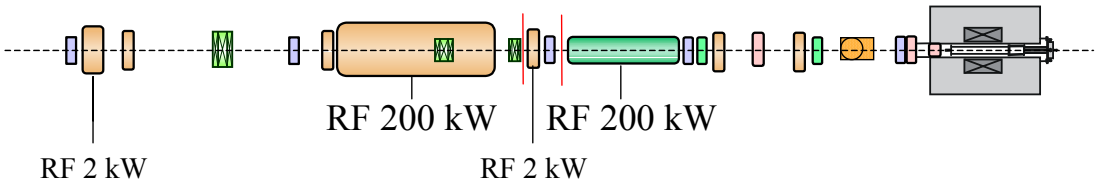

5. Radio-frequency supply

In the HITRAP linac, four RF amplifier chains are required for the operation of the RFQ and IH sections and for the two buncher cavities. It is proposed to use two of the 30-years-old amplifier chains, which are no longer required for the operation of the UNILAC single-gap resonators. These 200-kW tube amplifiers are well suited to feed the RFQ and IH sections. They need a general inspection and control of all functions. In addition, an upgrade with programmable controller (SPS) and new RF-amplitude and phase controls is required to match the present state of the art. Power lines including directional couplers are on stock. One of the available power supplies can be used to supply both amplifier chains. The necessary modifications are included in the cost estimate.

To feed the two bunchers, two 2-kW solid-state amplifiers have to be purchased.

5.1. Low-Level RF

Due to the resonant frequency of 108.408 MHz for the HITRAP Linac, the UNILAC low-level-drive signal should be used. A stable and noise-free RF signal has to be delivered over a distance of approximately 300 - 400 m. To compensate mainly the losses of the RF cable (FLEXWELL HF ⅜" CuH) which were calculated to be 2,9 dB/100 m, a modified loop with an output power of 25 W cw is required (Fig. 5-1). This passive solution is not expensive and very safe.

Needs for RF control-loop cables can be supplied by the UNILAC stock. For the inter-connection between UNILAC and HITRAP, up to 400 meters of FLEXWELL HF ⅜" CuH have to be ordered. An external company will do cable laying and connector assembly.

5.2. Amplifiers

5.2.1. Radio-tube amplifiers

After some modifications, two of the 200 kW tube amplifiers can be used to supply the IH (approx. 180 kW pulse power) and the RFQ (approx. 80 kW pulse power) with a maximum pulse length of 1.5 ms and a repetition rate of 1s (duty cycle ~ 0.15%).

This modification includes:

→ complete new wiring
→ mechanical modification
→ integration of the following new devices:
Programmable control (SIMATIC S5),
RF-control unit, and computer interface
→ inspection and service of the RF circuits

→ RF commissioning at the test bench
→ amplifiers will be equipped with new tubes (RS 1084 and RS 2024)

For tube heating, solid-state amplifiers, control electronics etc., both amplifiers are supplied by 400 V three-phase current. The connected power is approximately 6 kVA, the fuse protection should be 3 × 25 A for each. Because of the very short duty cycle, heat development occurs basically by tube heating. Heat emission per 200-kW amplifier is estimated to be 4.0 kW at maximum.

The final stages of these amplifiers are equipped with water-cooled electron tubes. Cooling water requirements are 15 l / min per amplifier. For quality of the cooling water cf. 5.5.1.

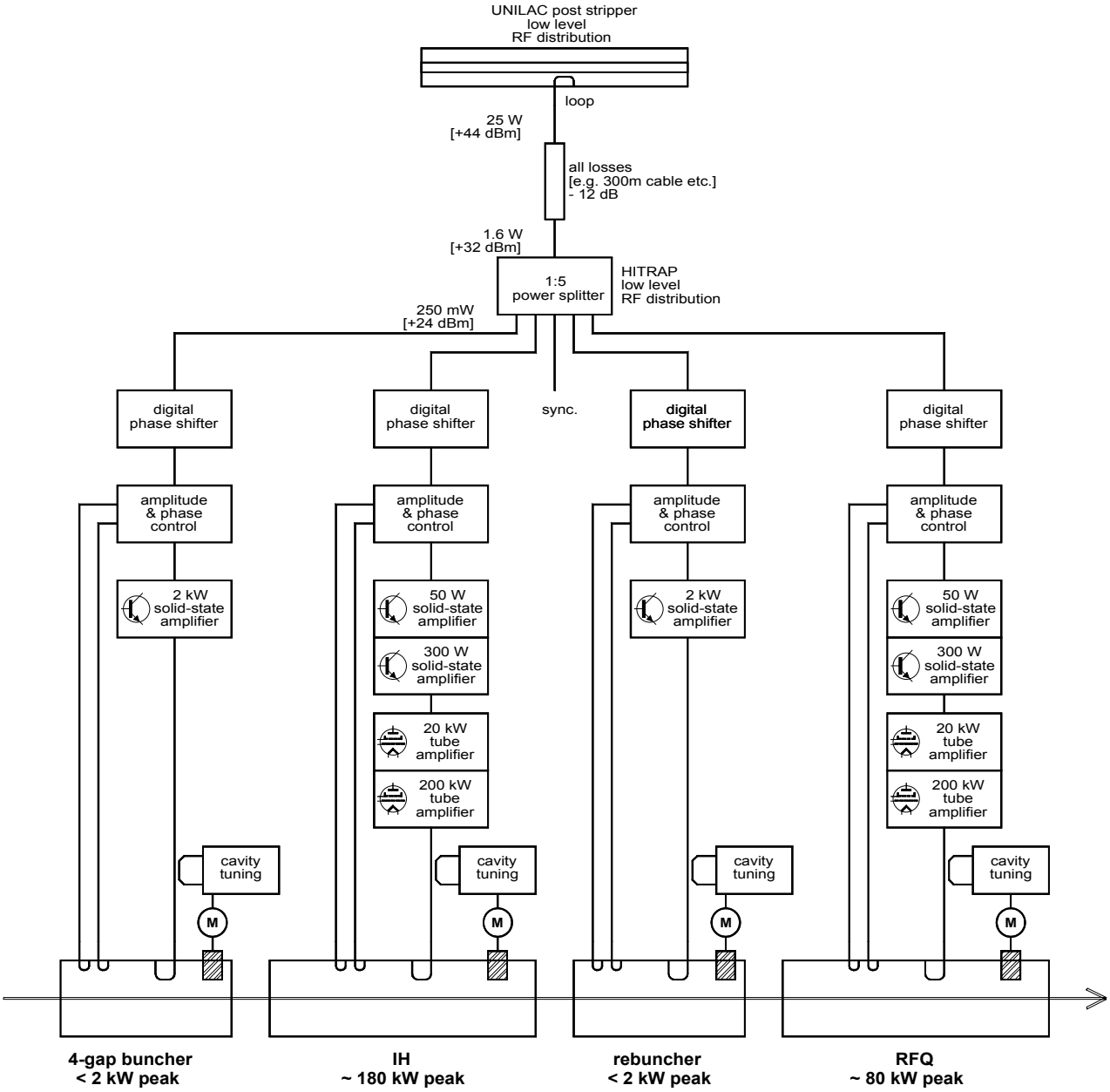

Figure 5-1. HITRAP RF system with cavity tuning.

5.2.2. Solid-state amplifiers

To supply the four-gap buncher in front of the decelerator as well as the three-gap buncher in-between the IH and the RFQ, two 2-kW solid-state amplifiers have to be purchased. All additional equipment like the programmable control, the RF controls, the computer interface and the plunger electronics are included in the cost estimate.

5.3. RF specific controls

5.3.1. Amplitude and phase control

All amplifiers are equipped with the same type of control unit.
Some important data:

For each cavity, the phase can be set from 0 to 360° in steps of 1 degree.
The phase-control loop has a bandwidth of 1 MHz and an accuracy of ± 0.1 degree.
The bandwidth of the amplitude control is set to $f_{cut\text{-}off}$ = 500 kHz while the accuracy is up to ± 0.1%.

Separate control loops are used for amplitude and phase control. So, each cavity has to be equipped with at least two inductive probes.

5.3.2. Cavity tuning

To adjust the cavity to the resonant frequency and assure the stay at this frequency, all cavities, also the smallest, need at least one tuning element. The tuning procedure starts after RF is switched on. The system tunes automatically in the right direction and locks to the resonant frequency. It can also be operated manually. The standard mode of operation at GSI is to detect the phase difference between the forward and the reflected voltage by a separate directional coupler (RF power line). A stepping-motor unit drives the plunger.
This equipment is not on stock and has to be designed and bought.

5.3.3. Computer interface and software

To operate the devices by the main-control-room staff, the same computer interfaces as used by the UNILAC RF will be installed. This technology is established since many years. All units have to be reordered. Furthermore, the HITRAP RF has to be integrated into the UNILAC operating software. This needs an extension of the RF device model as well as the operating software.

5.3.4. Timing

The timing information for rf-pulse width, pulse space and sampling time, transmitted via a GSI two-wire bus, is decoded in a special timing interface (part of the computer interface). Therefore a separate timing central and a bus system have to be installed, which are part of the general control system. The start signal for operation will be given from the ESR (cf. Chapter 10).

5.3.5. Stand-by mode

The extremely low duty cycle of the HITRAP facility (one deceleration event per 10 seconds) requires particular care for the stabilization of the RF components. In order to keep

them at operation temperature, intermediate 'keep-warm' pulses will be employed between the operational pulses. It has already been proven at the UNILAC that this is a successful, reasonable, and simple way to thermally stabilize the accelerator structures. It is sufficient to generate RF pulses with about 25 % of the 'normal-operation' power. By introducing a separate virtual accelerator within the existing virtual-accelerator framework at GSI, the required sequence of pulses is very easy to generate. A repetition rate in the region from 5 Hz to 10 Hz is sufficient. The total energy balance is only slightly altered by this (about 1.2 kW in total), and the below stated cooling requirements already consider this stand-by mode operation.

5.4. Power supplies

5.4.1. 200 kW anode and grid-2 power supplies

One existing 100-kVA power supply is used to supply the IH and RFQ 200-kW final stages in a shared mode. For this special type of combined operation, some electrical and mechanical modifications have to be done.
Note: This mode of operation means that the 200-kW stages must be operated always at the same time.

The connected power is 100 kVA. Because of the start-up peak, the fuse protection should be 3 × 200 A. The amount of heat to be dissipated (transformers and rectifiers) is about 1.5 kW.

5.4.2. 20 kW anode and grid-2 power supplies

One 20-kVA power supply is used to supply the IH and RFQ 200-kW driver stages in a shared mode, cf. 200 kW supplies. The connected wattage is 20 kVA. Because of the start-up peak, the fuse protection should be 3 × 50 A. The amount of heat to be dissipated from the transformers and rectifiers is about 1.0 kW.

5.5. Infrastructure requirements

5.5.1. Cooling water

The cooling-water requirement for two final stages is 1.8 m^3/h. The primary pressure is at approx. 6.5 bar at a pressure difference of 4.5 bar. The electrical conductivity should be below 1µS/cm and the flow temperature should be 24° C.

5.5.2. Air cooling

The required cooling air for two 200 kW amplifiers (including the air-cooled drivers) has to be calculated with 30 m^3/min at a velocity of 7.5 m/s.

The 'driver' power supply needs 3 m^3/min at a velocity of 6 m/s and the 'final' power supply has to be assessed to 7 m^3/min at a velocity of 4 m/s.

In all cases the flow temperature should be near 20° C. The air temperature in the ESR hall will be sufficient for cooling.

5.5.3. Required space

For operation and maintenance, the required space is shown in Figure 5-2. This space will be provided by the operating platform, cf. Chapter 12. It is worth mentioning that a laser-beam line from the PHELIX experiment is crossing the planned location at a centre height of 7.5 m above ground-floor level. Taking into account a platform height of 4.23 m (cf. Chapter 12), and a beam-line diameter of about 1m for the PHELIX line, this leaves still the height of 2.6 m which is the maximum required for most of the RF components. The final-stage power supply (height 2.8 m) can easily be placed in order not to collide with the PHELIX beam line.

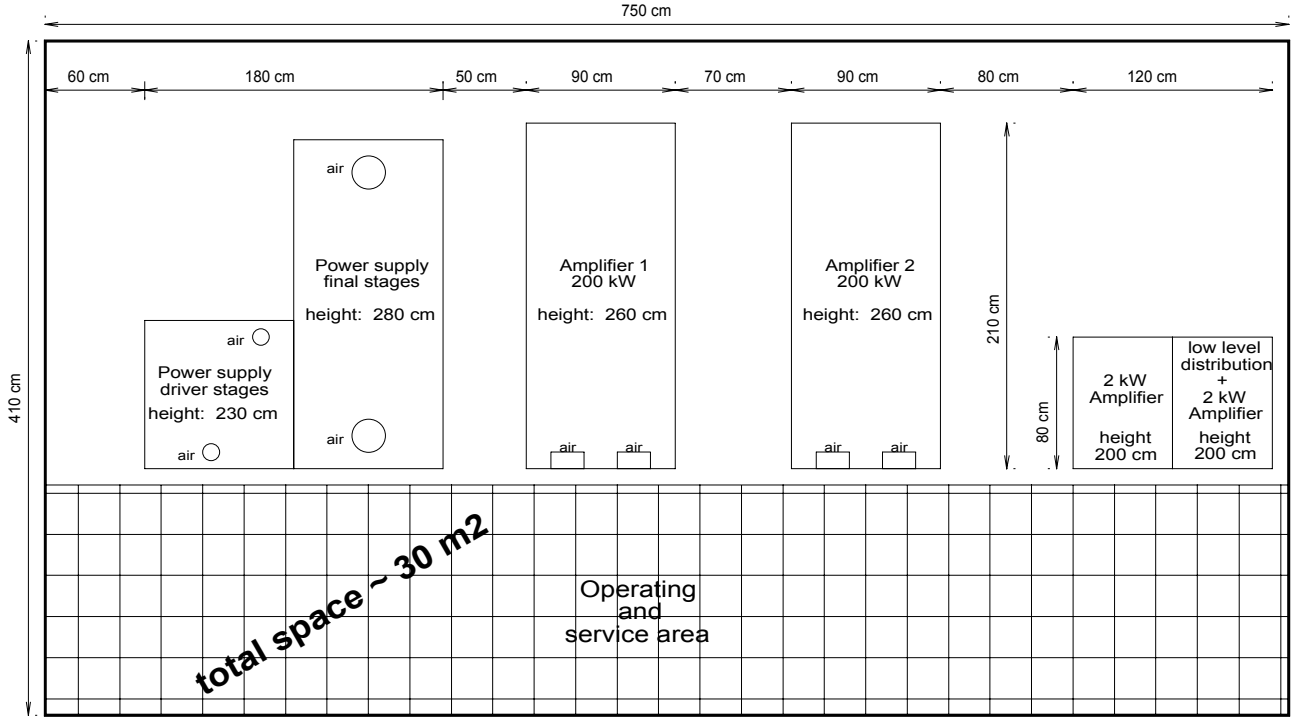

Figure 5-2. Required space for the RF supplies (top view)

5.6. Cost estimation for the HITRAP RF system

As shown in Tab. 5-1, the most expensive parts of the RF system for HITRAP are already available at GSI. Compared to these values, the amount to be invested in order to ensure RF equipment nearly as good as new amounts to about 20 % of the total costs of the RF equipment.

Table 5-1. Expected total costs for the HITRAP RF supplies.

Explanation: acqu. value = acquisition value, the costs if to reorder
abs. value = number x cost/unit
The green figures indicate material available for use at HITRAP.

number	component		acqu. value	cost/unit	abs. value
2	RF Amplifier	RFQ and IH			
	108.408 MHz 200 kW peak power	GSI pool	1.200.000		
	Modification of PLC, rf controls, Interface	to order		30.000	60.000
	Electron tube final stage			16.000	32.000
	Electron tube driver stage			5.500	11.000
	Service RF circuits			10.000	20.000
2	RF Amplifier	2 + 4 gap buncher			
	108.408 MHz 2 kW peak power	to order		25.000	50.000
	PLC, rf controls, Interface	to order		30.000	60.000
1	Power supply				
	200 kW anode and grid 2	GSI pool	250.000		
	Expansion of the capacitor battery.	GSI pool	15.000		
	Modification of the PLC for 2 outputs.				
	Ext. manpower			25.000	25.000
1	Power supply				
	20 kW anode and grid 2	GSI pool	150.000		
	Modification of the PLC for 2 outputs.				
	Ext. manpower			10.000	10.000
6	Automatic resonator tuning				
	2 per IH and RFQ; 1 per buncher	to order		7.000	42.000
1	Low level RF				
		GSI pool	10.000		
	loops, splitter, RF line [400m]	to order		10.000	10.000
1	Complete device setup				
	RF low level and power lines	GSI pool	30.000		
	Ext. manpower			35.000	35.000
1	Internal costs				
				50.000	50.000
		Expected total costs [€]	**1.655.000**		**405.000**

6. Low Energy Beam Transport from the RFQ to the Cooler Trap

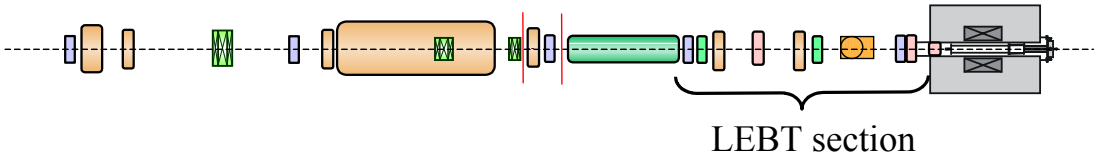

After the final deceleration in the RFQ, the ions have to be injected into the cooler trap for further reduction in energy. The cooler trap has to be at an extremely good vacuum and also the beam line ahead of it, which is also used to feed the experiments, should be kept at UHV. Therefore, a differential-pumping stage is planned directly after the RFQ structure. The ion-optical calculations along this line are the topic of this chapter. It will be shown that the required fields can be generated by solenoid magnets existing at GSI. Suitable power supplies also exist and therefore no additional costs for beam transport have to be considered here.

In addition, a study is included which shows that a beam with the properties at the end of the differential pumping section can be injected into the cooler trap with its strong solenoidal magnetic field. Therefore, this chapter is the last one in this TDR to demonstrate the ion-optical feasibility to bring the beam extracted from the ESR to rest in a trap with the ion-optical and decelerating elements described so far.

6.1. Ion optics in the differential pumping section after the RFQ

The low-energy beam transport system (LEBT) performs the imaging of the transversal beam parameters at the RFQ exit onto the required focus at the ion-trap entrance. The RFQ-output emittance is nearly symmetric in its horizontal and vertical planes. This allows the use of solenoid magnets and dedicated power supplies, which are available at GSI from the former EPOS and ORANGE experiments. Therefore equipping the LEBT beam line with ion optical elements will not contribute to the cost of the HITRAP project.

The transversal envelope of the proposed layout of the LEBT is shown in Figure 6-1. Between the two solenoids, there is space of more than two meters for a differential pumping section, beam diagnostics, and two steerer magnets, each acting in horizontal and vertical direction. Downstream behind the second solenoid, space is foreseen for the installation of a 90°-bending unit, to transport the cooled ions from the ion trap further to the experiments.

For the design ion $^{238}U^{92+}$ with beam energy of 6 keV/u, the calculated magnetic inductions of the two solenoids are B = 0.35 and 0.17 Tesla, respectively. The apertures are 60 and 80 mm. The expected beam-energy spread of $\Delta T/T = \pm 7\%$ causes a beam halo, which is partly considered by normalized emittance values of $\varepsilon_{x,y,\ norm} = 0.55\ \pi\cdot$mm·mrad which are 50% above the calculated RFQ-output emittance numbers of 0.37 $\pi\cdot$mm·mrad (cf. Chapter 4). Finally, a beam focus of a radius r = 6 mm at a fixed position inside the ion trap is performed (cf. Section 6.2.). Figure 6-2 shows the transversal RFQ-output emittance with the assumed high divergence (diagonal ellipses) and the phase space ellipses at the desired focus within the ion trap (horizontal ellipses).

The presented calculation shows the possibility of matching the beam out of the RFQ into the cooler trap with the required boundary conditions imposed by the field of the trap (cf. Section 6.2). The exclusive use of existing equipment for guiding the ion beam along the

LEBT section is a particularly welcome side effect in keeping the costs of the HITRAP set-up within reasonable limits.

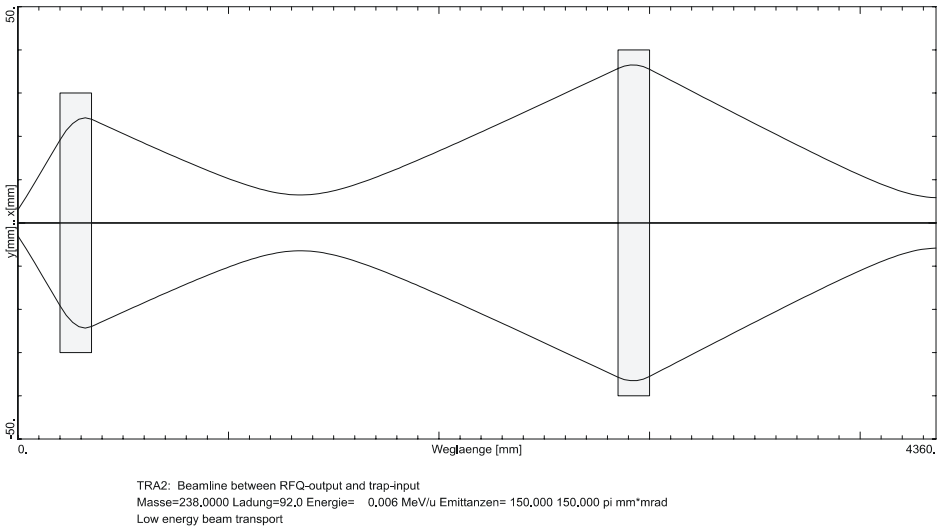

Figure 6-1. Envelope along the LEBT section from the exit from the RFQ (left) to the entrance into the cooler trap (right). The normalized emittances are $\varepsilon_{x,\,n} = \varepsilon_{y,\,n} = 0.55\ \pi\cdot$mm·mrad.

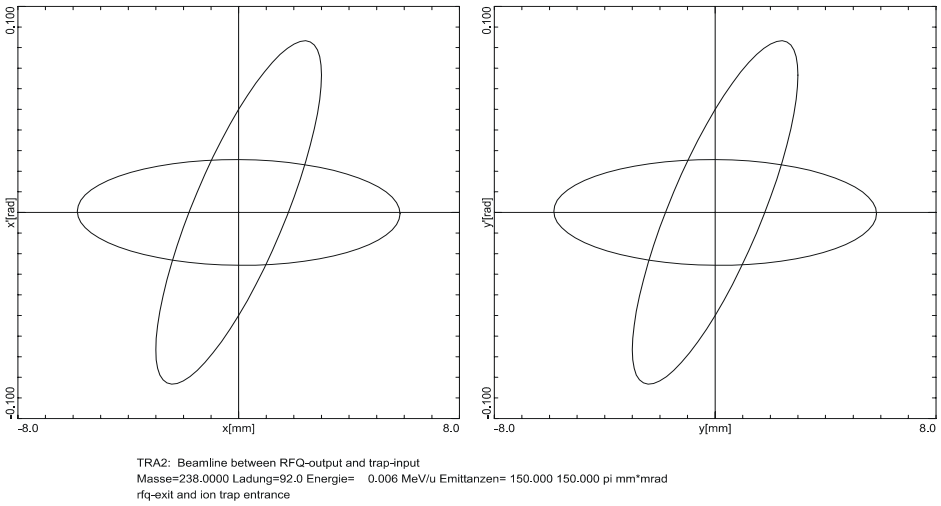

Figure 6-2. Transverse phase-space ellipses at the exit from the RFQ (diagonal) and at the entrance into the cooler trap (horizontal). The normalized emittances are $\varepsilon_{x,\,n} = \varepsilon_{y,\,n} = 0.55\ \pi\cdot$mm·mrad.

6.2. Injection into the cooler trap: a feasibility study

In the HITRAP project highly charged ions extracted from the ESR are decelerated by a RFQ decelerator and then injected into the cooler Penning trap. This ion-optical study investigates the injection of a beam of highly charged ions into the strong magnetic field of the cooler trap. The simulations are based on beam data shown in Table 6-1 and the magnetic field plot as displayed in Figure 6-3 which is similar to that provided by an iron-shielded superconducting magnet system at ASACUSA, CERN.

Table 6-1. Properties of the U^{92+} ion beam as used in the simulation 2 m ahead of the trap centre.

Ion mass	Charge state	Total energy	Total energy spread	Bunch length	Emittance (at initial energy of 1428 keV)
238	92	1428 keV (6 keV/u)	± 100 keV ΔE/E = ± 7 %	1 μs	100 π mm mrad (norm.: 0.37 π mm mrad)

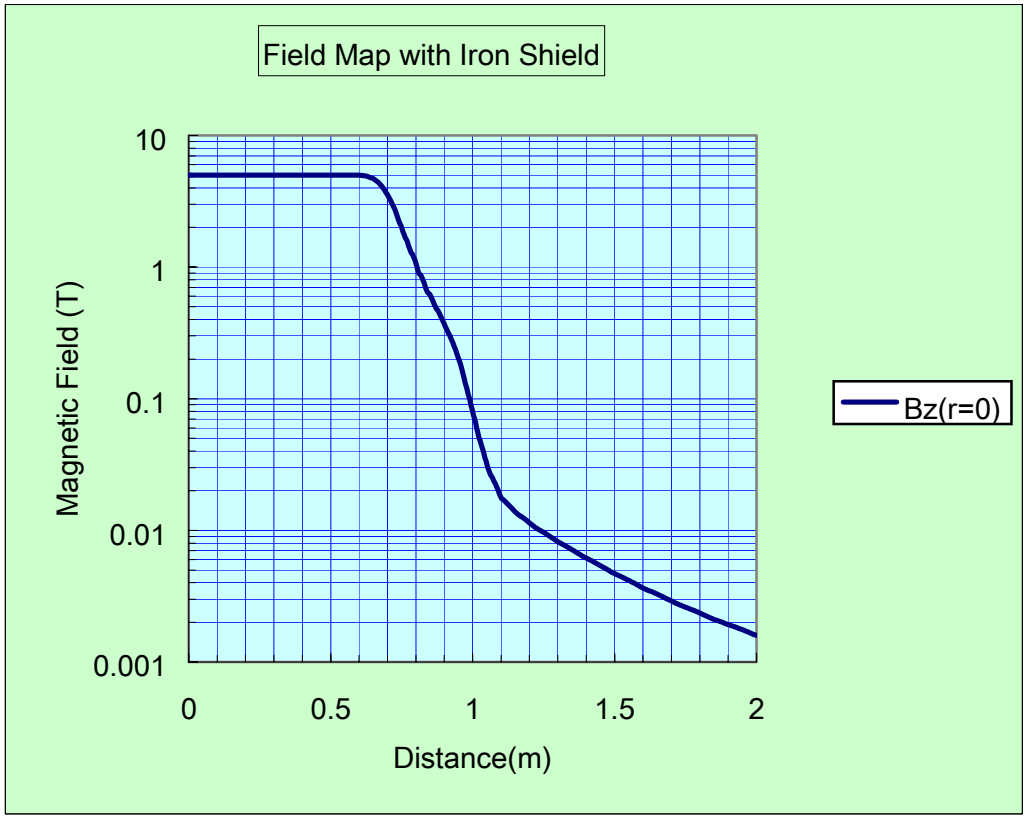

Figure 6-3. Magnetic field strength on the axis of the solenoid. The distance given is the distance from the center of the cooler trap.

6.2.1. Simulation goal

The basic idea of the simulations is to focus the injected ions into the strong magnetic field in such a way that their trajectories follow the magnetic field lines as closely as possible. This way, the reflection of the injected ions at the steep magnetic gradient ('magnetic-mirror effect') is completely avoided. The goal of the simulations is to find the optimum injection

parameters, in particular (*i)* the size r_{foc} of the focus and (*ii)* the position z_{foc} of the focus on the field axis.

With optimum injection parameters the radial-energy pickup, i.e. the conversion of axial energy into radial energy, is minimized. In this case, the time structure of the ion bunch is very little affected.

6.2.2. Simulation Procedure and Results

The simulations were carried out with SIMION 3D 7.0. The magnetic potential required by SIMION was calculated from the magnetic field data (Fig. 6-3). For the injection into the magnetic field, the ion trajectories are calculated from the starting position at z_0=2500 mm, with the field centre at z=0. In the simulation, the magnetic field is taken into account only over a distance of 2000 mm from the field centre. Beyond z=2000 mm, the magnetic field strength is negligibly small. The ions are focused to a point z_{foc} such that without magnetic field and for the given emittance a beam with radius r_{foc} would be obtained at the focus. The virtual focus parameters z_{foc} and r_{foc} are used to characterize the beam injection. The energy and time distributions of the ion bunch are taken into account in a Monte-Carlo type variation of the initial conditions for different ion trajectories. The ions are injected into the magnetic field and allowed to pass through it. Their radial energy and time-of-arrival distributions are 'measured' in the trap center.

According to Figure 6-3, the magnetic-field gradient reaches its maximum at a distance of about 1100 mm from the field center. Basically, it can be expected that the best injection conditions are achieved if the virtual focus z_{foc} is close to that point and between this point and the field center. The optimum value of the focus size r_{foc} is less obvious. The task of finding the global minimum for the radial energy pickup ΔE_r as a function of the focus position z_{foc} and the focus size r_{foc} is solved in the following iterative optimization procedure:

I. A virtual focus position z_{foc} is chosen, and the radial energy pickup ΔE_r is determined for different focus sizes r_{foc}.
II. The focus size r_{foc} is fixed to the value which gives the lowest radial energy pickup, and the focus position z_{foc} is varied. With the new focus position, step I is repeated.

In the beginning of the optimization procedure, a number of beams with different focus sizes r_{foc} and with a fixed focus position at z_{foc}=1100 mm are simulated. The focus size with the lowest radial energy pickup is r_{foc}=6 mm (see Figure 6-4). For this focus size the focus position z_{foc} is now varied with results shown in Figure 6-5. The best focus position is z_{foc}=800 mm. For this position the radius is varied once more (Fig. 6-6) and a better radius of r_{foc}=4 mm is found. A final iteration of z_{foc} verifies that an overall minimum has been found (Fig. 6-7).

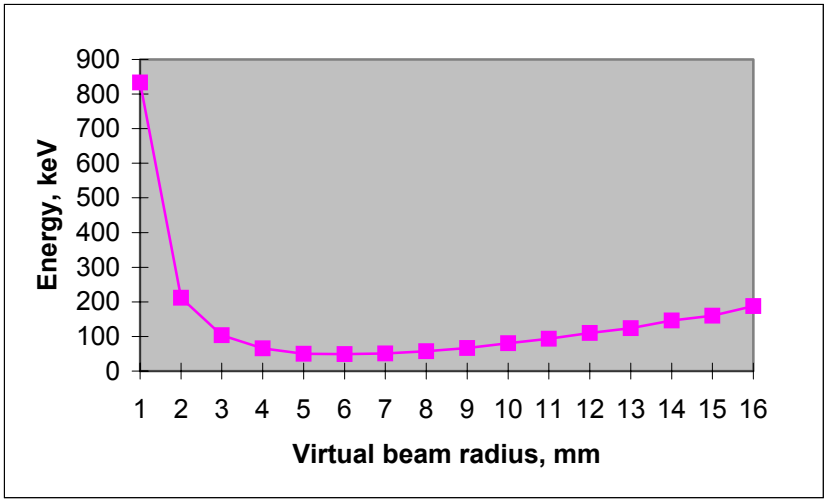

Figure 6-4. Iteration step 1: Radial energy as a function of the radius r_{foc} of the virtual beam focus for z_{foc} = 1100 mm.

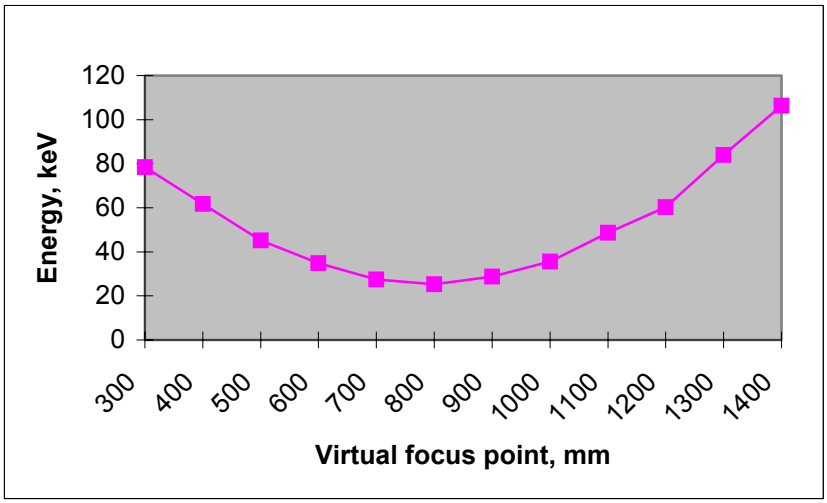

Figure 6-5. Iteration step 2: Radial energy as a function of the position of the virtual focus z_{foc} for r_{foc} = 6 mm.

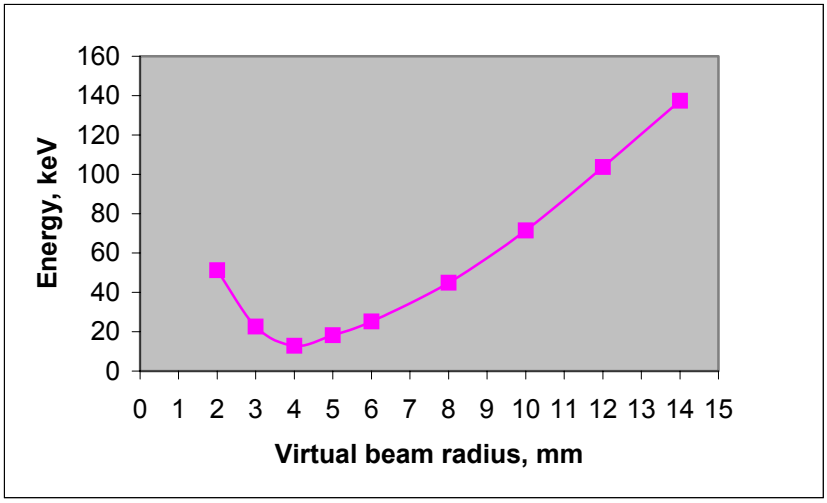

Figure 6-6. Iteration step 3: Radial energy as a function of the radius r' of the virtual beam focus for z' = 800 mm.

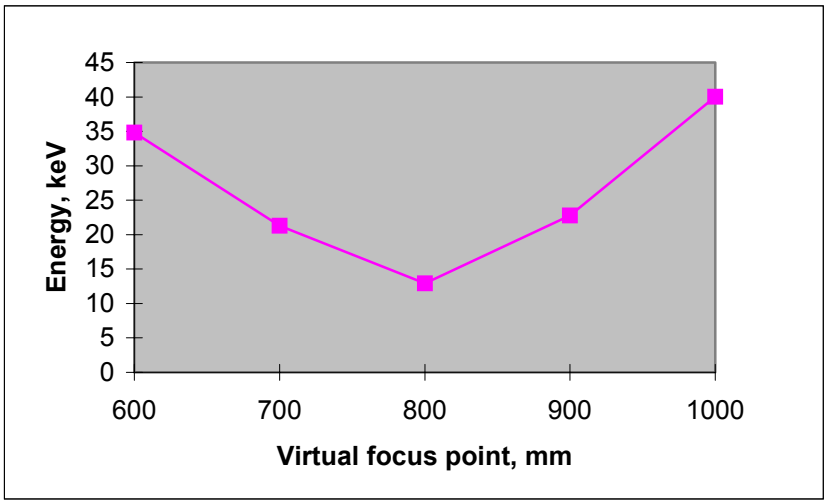

Figure 6-7. Iteration step 4: Radial energy as a function of the position of the virtual focus z_{foc} for r_{foc}= 4 mm.

Figure 6-8 shows ion trajectories calculated with SIMION for the best case found in the iteration process described above. The maximum radial energy pickup for this optimised beam injection and the corresponding loss of axial energy is about 13 keV (total energy). This is small compared to the +/- 100 keV spread of the injected beam.

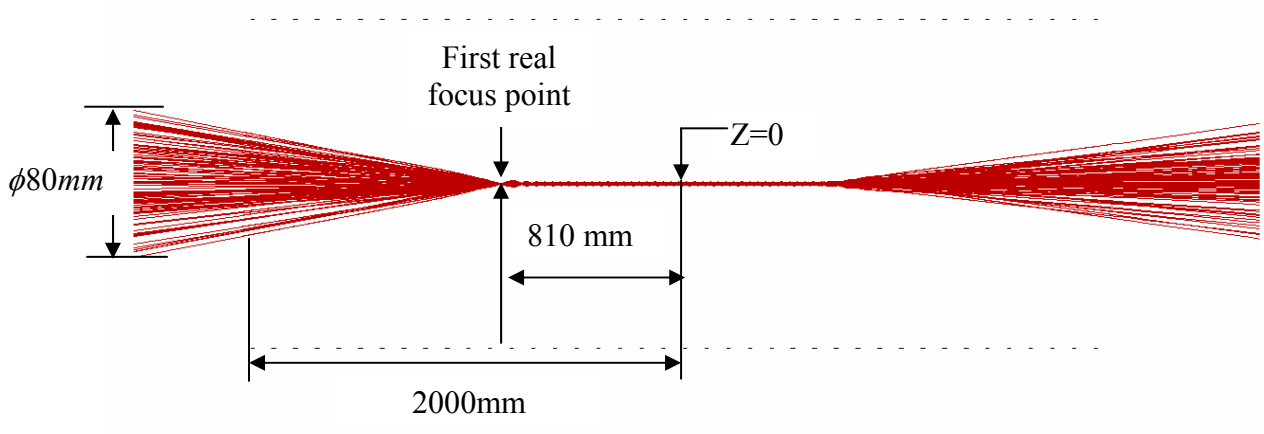

Figure 6-8. Injection of ions into the magnetic field of the cooler trap. Beam trajectories for a focus size of r_{foc}= 4 mm and a focus position of z_{foc}=800 mm. The beam diameter at the focal point is about 0.03 mm.

The initial ion bunch length of 1 μs at the exit of the RFQ decelerator is increased to about 1.2 μs at the entrance of the cooler trap due to the energy spread of the ion bunch. The cooler trap will be operated at a high voltage of about +8 kV in order to retard the incoming ion bunches. The resulting spatial length of the retarded ion bunches in the cooler trap is then about 0.8 m. A cooler trap length of only half the ion bunch length is required for capturing the ions because the incoming ions are reflected at the end of the cooler trap. Therefore, the total ion bunch can be captured in the 0.5 m long cooler trap (see Chapter 7).

The question of the optimum retardation voltage has been investigated as well. Taking the initial energy and time spread, it is easy to calculate the pulse length in the field center for different retardation voltages. For the case studied here, it is assumed that the initial bunch length is 1 μs and that the retardation takes place 1 m from the field center. Figure 6-9 shows the calculated spatial bunch length as a function of the beam energy after retardation. A broad minimum can be observed. Therefore, the value for the retardation voltage of the cooler trap is not a critical parameter.

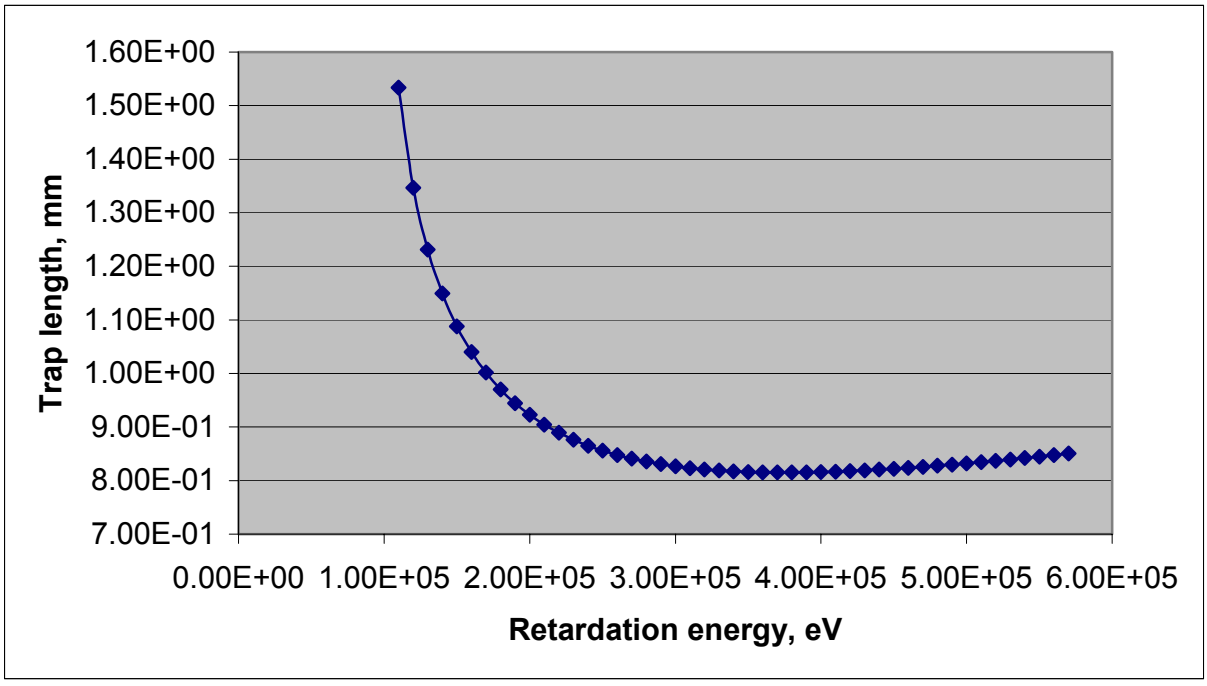

Figure 6-9. Spatial length of ion pulse at field centre as a function of the energy of the retarded beam.

6.2.3. Conclusions

- A beam with properties as specified in Table 6-1 can be injected *without losses* into a field as depicted in Figure 6-3.
- Good injection parameters are: focus size r_{foc}=4 mm and focus position z_{foc}=800 mm. With these parameters, the radial energy pickup is about 13 keV which is much smaller than the initial energy spread of the beam.
- Without changing the initial beam energy or further retardation, a pulse length of about 1.2 m is observed. The length is practically fully determined by the initial beam energy and time spread. If the beam is retarded inside the magnetic field, the pulse length can be reduced to about 0.8 m fitting well to the length of the cooler trap of 0.5 m (a trap length of only half the ion bunch length is required, because the ions are reflected at the end of the cooler trap).

In total, the proposed solution is well suited for the final injection of the beam into the cooler trap after deceleration in the IH and RFQ structures seams.

6.3. Summary of the Beam Transport sections

Here, a compilation of results of the different beam-transport chapters is presented with emphasis on emittances and transmission. The number of particles at the ejection energy of 4 MeV/u is an interpolation. With this assumption, the number of particles being trapped is more than 10^5 per operation cycle.

Table 6-2. Beam energies, velocities, magnetic rigidities and particle numbers for $^{238}U^{92+}$.

HITRAP Section	Chapter	Energy [MeV/u]	β	B ·ρ [Tm]	Trans-misson	tot. Trans.	No. of particles	Notes
ESR	2	5.0	0.1032	0.834			1×10^6	measured
		4.0	0.0924	0.746			(6×10^5) estimated	ejection energy
		3.0	0.0800	0.645			2×10^5	measured
Entrance Pre-buncher	2.6.1.3	4.0	0.0924	0.746	100 %	100 %	6×10^5	
Entrance IH	3	4.0	0.0924	0.746	28 %	28 %	1.7×10^5	loss by bunching
Exit IH / Entr. RFQ	3	0.5	0.0328	0.263	100 %	28 %	1.7×10^5	
Exit RFQ	4	0.006	0.0036	0.029	93 %	26 %	1.5×10^5	
LEBT, up to entrance of trap	6	0.006	0.0036	0.029	80 %	21 %	1.2×10^5	

Table 6-3. Emittances along the HITRAP decelerator

HITRAP Section	Chapter	Energy [MeV/u]	ΔT	$\varepsilon_{x,n}$ (=$\varepsilon_{y,n}$) [π mm mrad]	ε_x (=$\varepsilon_{y,}$) [π mm mrad]	Δφ	Notes
ESR	2	5.0	dp/p = 2.4×10^{-4}	0.093	0.9		measured
		3.0	dp/p = 1×10^{-4}	0.06	0.7		measured
Entrance IH	3	4.0	ΔT/T = 1.3×10^{-2}	0.2	2.2		[1])
Entrance RFQ	3 and 4	0.5	ΔT/T = 2×10^{-2}	0.24	7.3	± 9°	
Exit RFQ	4	0.006	ΔT/T = 8.3×10^{-2}	0.37	100		

[1]) A safety margin of a factor of 2 is considered in the calculation of the emittances, cf. Chapter 3.

7. Cooler Trap and connection to experiments

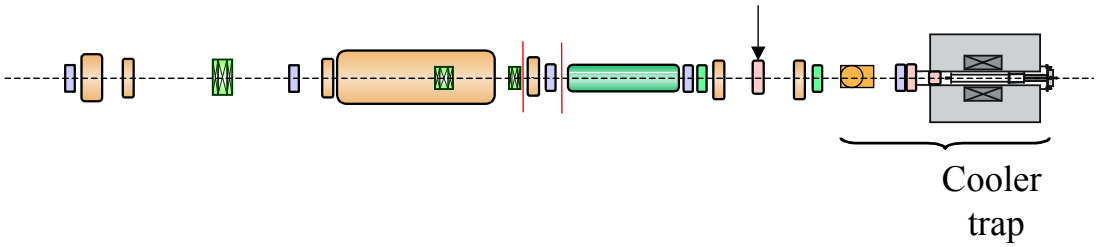

The cooler trap is designed to perform in-flight capture of a single bunch of ions and to store them for subsequent cooling. As cooling principle, sympathetic cooling by trapped electrons has been chosen. The electrons are produced and captured inside the trap prior to ion bunch capture. Synchrotron radiation due to the electrons' motion in the magnetic field of the Penning trap cools them to the ambient temperature of 4 K with a cooling-time constant of about 150 ms. The captured ions are then sympathetically cooled to roughly the same value due to Coulomb interaction with the electrons. Upon cooling and radial centring, the cold ion bunch is ejected from the trap with a high brilliance and is available for all subsequent experiments. The cooler trap is pre-evacuated to below 10^{-8} mbar when first taken into use. During normal operation, the vacuum is ensured by the cryogenic surrounding to be better than 10^{-14} mbar, allowing for completely loss-free storage during the typical cycle time. To protect this vacuum from gas flow along the beam line, a fast commercial valve will be installed before the cooler trap and outside the magnetic field of the superconducting magnet, which produces the magnetic trapping field B (cf. Fig. 1-5, 23). This valve will be opened only for loading of the cooler trap with a single ion bunch, i.e., it will have the same duty cycle as the cooler trap itself. Additionally, a diffusion barrier inside the 4 K region in close proximity to the trap will be installed to further reduce gas inlet to the trapping region.

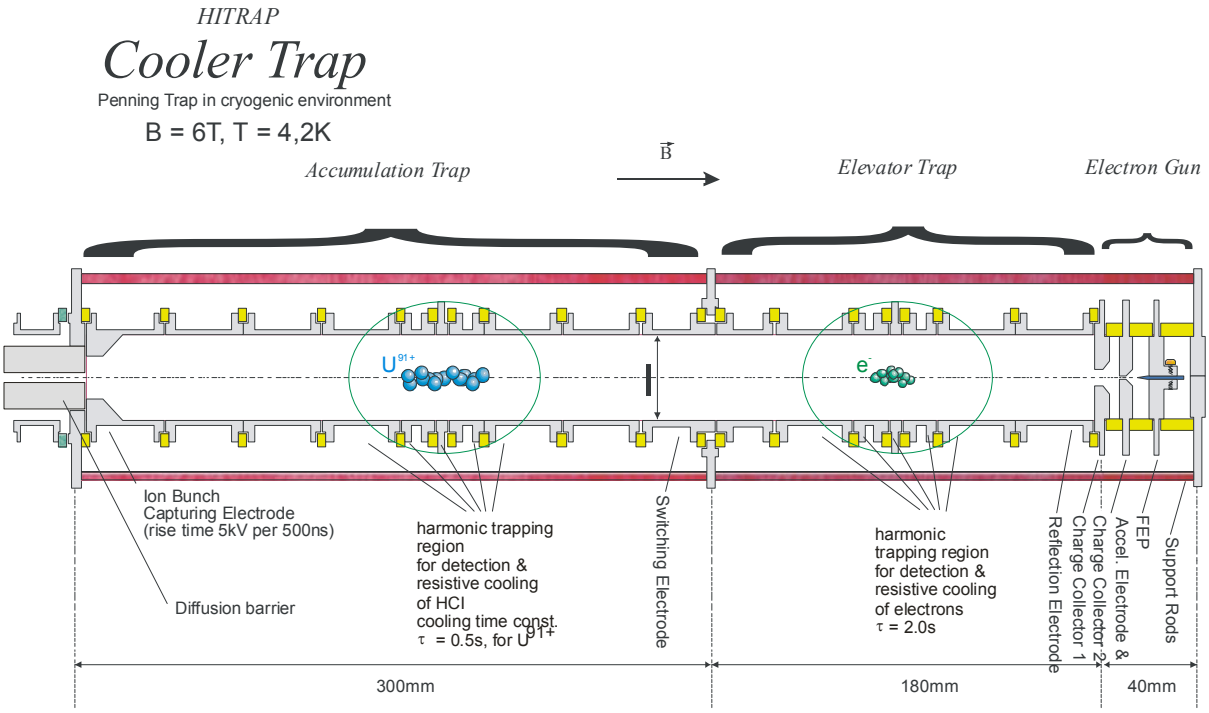

Figure 7-1. Detailed sketch of the cooler trap.

7.1. Layout

The cooler trap consists of a horizontal stack of 21 cylindrical electrodes and is divided into three sections:

- an electron gun, based on a field emission point (FEP) and designed to deliver 100 nA electron current at a low energy spread of about 0.1 eV,

- an 'elevator trap', used to collect and to transfer cold (ΔE = 0.1 eV) bunches of electrons (10^6 e^- per bunch) into the accumulation trap, and

- the 'accumulation trap', which fulfils the main tasks to store electrons, let them cool down to 4 K environment temperature by synchrotron radiation, merge them together with captured ions in a 'nested trap' configuration and proceed with resistive cooling in order to perform the final cooling of the HCI to 4 K.

Figure 7-1 shows the set-up of the cooler trap. Electrodes are manufactured from OFHC copper to avoid ferromagnetic impurities and magnetic field distortions. The electrodes are separated by sapphire elements for electric insulation. The stack of electrodes is mechanically stabilized by three rods spanning from the top of the electron gun to the bottom of the accumulation trap (see Fig. 7-1). The inner diameter (40 mm) is chosen to significantly exceed the expected diameter of the ion bunch (25 mm) to avoid ion loss due to contact with the electrodes. It is not chosen larger than 40 mm since resistive cooling by attached tank circuits will become less effective with increasing electrode diameter.

7.2. Functional Description

7.2.1. Electron Loading Cycle

Before cooling the highly charged ions with cold electrons, the latter have to be created and loaded into the trap. Therefore, an electron loading cycle is proposed which consists of the following steps (see also Fig. 7-2):

- *collect electrons (1.5 µs):* the current of the electron gun is switched on, the elevator trap is completely filled by a current of 100 nA within 1.5 µs with about 10^6 electrons in a flat (0.5 Volts) 'bath-tub' potential.

- *elevate (200 µs):* these electrons, having an energy width of roughly 0.1 eV (mainly due to the FEP) are elevated to the bottom voltage of the accumulation trap, elevation time is roughly 200 µs, which is quasi-adiabatic (giving little heating effect).

- *merge (200 µs):* the electrons are merged together in the trapping potential of the accumulation trap (having about 100 eV trap depth) by sweeping each electron bunch (~10^6 e^-) into the accumulation trap. This process is also (more or less) adiabatic, since axial oscillation (bouncing between in the trap) happens within typically < 1.5 µs, whereas the merging process is performed by more than two order of magnitude more slowly within ~200 µs.

The heating effect (energy increase) during the merging process (according to Liouville's theorem) can be roughly estimated as the electron number in the elevator trap, divided by the

electron number in accumulation trap, times energy spread in elevator trap. It therefore can be expected to result in a total increase of several eV after 2000 loading cycles, corresponding to 2×10^{10} loaded electrons after 1s. Due to fast collisional energy exchange on the millisecond time scale and radiative damping (with a cooling time constant of about 80 ms in a 6 T magnetic field) both axial and cyclotron energy of these 10^{10} electrons can be assumed to have the environmental temperature of 4 K (i.e. a thermal energy of less than 10^{-3} eV) within 5 s.

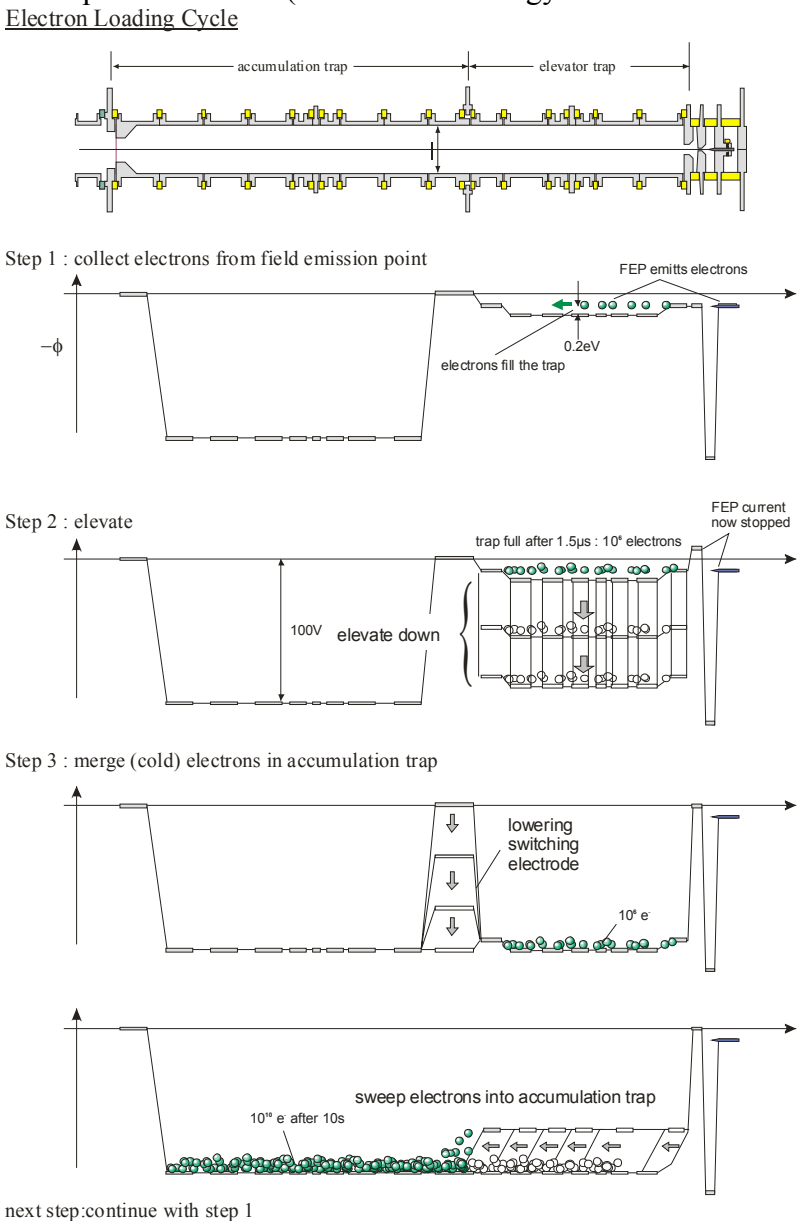

Figure 7-2. Electron-loading cycle in the cooler trap

7.2.2. Ion Loading Cycle

The decelerated ion bunches still consume a big phase-space volume. At an energy spread of several keV per charge they are supposed to enter the trap within about 2 µs. A capturing electrode which has to be switched by 5 kV at the trap entrance ensures the capture of a major part of the ion bunch. Subsequently they undergo collisions in the interaction sections with cooling electrons, resulting in a residual energy spread of rougly 10 eV. Appropriate choice of the trap potentials ensures spatial separation and thus avoids recombination. A following step merges the ions together into a harmonic trap region where final resistive cooling by means of

a superconducting tank circuit is performed, resulting in an extremely low energy spread in the meV region. The parameters of the harmonic trapping region are:

- trap depth 20V × q
- axial frequency f_z = 200 kHz
- resistive cooling time constant τ = 500 ms.

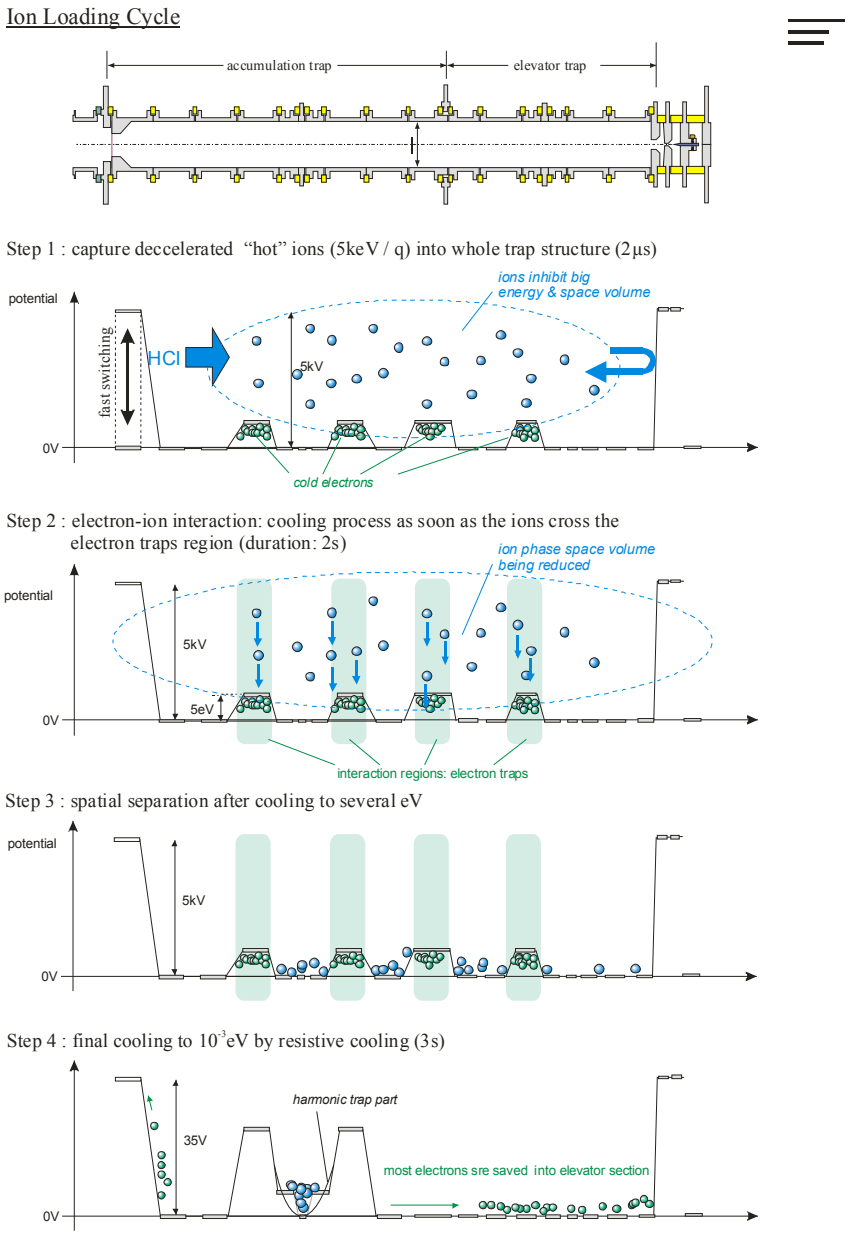

Figure 7-3. Ion-loading cycle in the cooler trap

7.3. Diagnostics inside the Cooler Trap

The cooler trap is designed to allow for diagnostics of all relevant processes. For a quick particle-number determination, a destructive method will be implemented. It incorporates three charge-collector plates on which positively and negatively charged particles can be swept. In conjunction with a cryogenic charge amplifier, they can be detected with a high sensitivity and a big particle-number range of more than five orders of magnitude. Due to unipolar signal processing this is applicable for electrons as well as for positively charged ions.

For the resisitive cooling, radio frequency LC-circuits will be implemented which will operate at the cryogenic environment of 4 K. These allow also for the non-destructive bolometric and FT-ICR detection. Based on proven experimental results of the GSI-Mainz g-factor experiment, these methods exhibit an even higher particle sensitivity in the order of less than five highly charged ions or ten electrons and allow also for monitoring energetic and spatial distribution of the particle clouds in the non-destructive way, i.e. keeping the particles at rest inside the trap. Table 7-1 gives an overview over the diagnostic methods inside the trap.

Table 7-1. Numbers of particles to be detected by different methods within the cooler trap.

Particle Type	Detection method	
	radio-frequency tank circuit - non-destructive -	charge-collector plates - destructive -
Electrons	10 …10^6	10^4…10^9
HCI, e.g. U^{92+}	5…20,000	10^2…10^7

In order to observe the resistive cooling process and bolometric/FT-ICR-detection, the cryogenic tank circuits and subsequent cryogenic amplifiers will operate at frequencies of 200 kHz and 29 MHz, correspoding to the axial ion motion (200 kHz) and ion cyclotron motion (29 MHz). The axial motion of stored electrons can delibarately also be tuned to 29 MHz in order to have a two-way use of the 29 MHz-circuit. GaAs-based amplifiers are foreseen for the cryogenic environment to provide low-noise amplification, the 200 kHz circuit will be implemented as a Type-II superconducting coil, made of niobium-titanium.

7.4. Cryogenic Surrounding and Superconducting Magnet

The cooler trap is positioned horizontally in the homogeneous field region of a commercial superconducting magnet that provides a field strength of 6 T. It is in close thermal contact to a liquid helium bath at 4 K temperature. Shielding of the cryogenic region is provided by a surrounding liquid nitrogen dewar at 77 K and further passive shielding. Exact numbers on liquid helium and nitrogen evaporation rates depend on details of the design, but can be given to a good approximation by 300 l of liquid helium and 2000 l of liquid nitrogen per month, as derived from similar existing set-ups.

Both the cooler trap and the diagnostic electronics are in thermal contact with the 4 K region cooled by liquid helium. The liquid helium tank is surrounded by a 20 K radiation shield inside the magnet bore which is cooled to liquid nitrogen temperature of 77 K. Access for liquid helium and liquid nitrogen refilling is possible from the top. The height of the setup in total is approximately 2 m, the diameter of the superconducting magnet is about 1.25m.

7.5. Infrastructural Requirements

The cooler-trap magnet is superconducting and thus needs no external power during normal operation. Liquid nitrogen and liquid helium consumption is expected as given above. Power consumption of the trap is small, since only DC voltages are being pulsed at low frequencies and power dissipation is low. Spatial requirements are according to the set-up drawings (cf. Figs. 1-3 and 1-4). The diameter of the trap (including cooling system and magnet) will not exceed 1.5 m, which allows for placement along the beam line. Integration into the

whole HITRAP system has to take into account the filling requirements (accessibility of the magnet with dewars). This is guaranteed if the HITRAP area is separated from the ESR in the access control system as if suggested in Section 12.3. Ferromagnetic materials in the direct surrounding to the magnet need to be avoided to the extent given by the map of the stray field of the magnet.

7.6. Instrumentation and costs for the trap

Prices are in Euro excluding VAT and excluding special discounts unless otherwise stated. Machine-shop hour prices are based on the prices to be calculated for the machine shop of the Mainz university (1.50€/hour for tools etc.). The rate $/€ is assumed to be 1:1.

Tab. 7-2. Detailed costs of the cooler trap

No.	Type of Instrument	Price each	Price total
	Mechanical Set-up:		
1	Superconducting magnet as specified incl. power supplies etc.		121.600 US$
1	Vacuum chamber for trap, insert for magnet bore		2.000€
24	Vacuum feed-throughs, non-magnetic	40€	960€
1	Vacuum feed-through HV for FEP, non-magnetic		200€
5	Field emission points	150€	750€
1	Manufacturing of electrodes, assembly with insulation elements, approx. 2000 man-hours work in machine shop		3.000€
80	Insulation elements between electrodes	25 €	2.000 €
	Cryogenics:		
1	He-Dewar for insertion into the magnet		7.500€
1	He level meter and controls		2.500€
1	N_2-Dewar for 77K shielding		9.000€
1	N_2 level meter and controls		2.500€
1	Passive 20K thermal shield		2.000€
	Control and Detection electronics:		
Pulsed vertical drift tube before trap entrance (energy matching):			
1	HV channel 10kV	960€	960€
1	Fast HV switch (e.g. Behlke HTS150 OT-10µ)	782€	782€
pulsed capture electrode at entrance of trap for ion capture:			
1	HV channel 10kV	960€	960€
1	Fast HV switch (e.g. Behlke HTS150 OT-10µ)	782€	782€
Cooler trap, right part 'elevator trap':			
2	HV channel 10kV	960€	1.920€
8	HV channels 500V, floating up to 8kV	840€	6.720€
Cooler trap, left part 'accumulation trap':			
8	Precise (0,001%) HV channels 500V	840€	6.720€
1	HV channel 10kV	960€	960€
Connection between left and right part (switching of connective electrode):			
1	HV switch (e.g. Behlke HTS 90-06)	695€	695€

	Electron gun inside cooler trap:		
2	HV channels 2,5kV, floating up to 8kV	840€	1.680€
	Timing-generation for drift tube and capture electrode:		
1	Pulse/Delay-generator (e.g. Stanford SRS DG535)	5.480€	5.480€
	Timing generation for control of electron gun, electron accumulation and connective electrode:		
1	Pulse/Delay-generator (e.g. Stanford SRS DG535)	5.480€	5.480€
	Destructive detection by charge collectors		
1	Cryogenic charge-sensitive amplifier, 3 channels, unipolar (suited for electrons and ions)	5.400€	5.400€
3	Low-noise post-amplifier at room temperature (e.g. SRS SIM911 BJT)	1.490€	4.470€
1	Rack for SIM-modules from SRS	1.520€	1.520€
1	Multi-channel oscilloscope for data acquisition (e.g. TDS 2014, 4 channels, incl. IEC-interface and software)	3.066€	3.066€
1	Power source for cryogenic amplifiers	3.500€	3.500€
	Non-destructive detection and resistive cooling:		
1	Superconducting LC-circuit, NbTi	8.500€	8.500€
1	RF-LC-circuit from OFHC, 25MHz, cryogenic	1.900€	1.900€
2	Cryogenic preamplifier	3.500€	7.000€
3	Cryogenic filter	2.500€	7.500€
2	Low-noise post-amplifier at room temperature (e.g. SRS SIM911 BJT)	1.490€	2.980€
2	Mixer-filter (down conversion)	2.500€	5.000€
2	RF-Signal generators as local oscillators (e.g. Rohde&Schwarz SML01)	4.920€	9.840€
1	FFT spectrum analyser (e.g. SRS SR780)	13.270€	13.270€
1	RF signal generator for ion excitation (e.g. Rohde&Schwarz SML01)	4.920€	4.920€
1	Noise generator for ion detection, e.g. SRS DS345)	2.900€	2.900€
	Radial ion centring:		
1	Function generator 30MHz (e.g. SRS DS345), for magnetron cooling in the harmonic region of the trap	2.900€	2.900€
1	Function generator 15MHz (e.g. SRS DS345), for application of the „rotating-wall“ technique	2.900€	2.900€
1	active multi-frequency phase shifter for „rotating-wall“ technique	4.500€	4.500€
	Total costs for the cooler trap:		**279.215€**

7.7. Vacuum instrumentation related to the Cooler Trap

7.7.1. Fast shutter

The planned duty cycle of the HITRAP decelerator is about 0.1 Hz, equivalent to one filling of the trap within 10 seconds. During the rest of the time, it is desirable to have the UHV section before the trap separated from the running cavity structures as much as possible. At the waist of the differential-pumping section after the RFQ, between both solenoids (cf. Section 6.1. and Figure 1-5, 18), a `diffusion valve' will be installed which does not seal the section from the cavities but reduces the cross section very much. A rapidly operating shutter is planned which will be closed immediately after each shot. Such a device will be manufactured by one of the machine tool shops involved in the project and therefore made fitting the requirements. The costs of such a device including electro-pneumatical equipment are estimated to not more than 5,000 Euro, if manufactured in the tool shop at the University of Mainz.

7.7.2. UHV valve

To be able to separate the trap completely from the rest of the beam line, an UHV gate valve will be installed in front of the trap. If this valve is placed immediately before the trap just outside the cryogenic beam line, the beam diameter is only about 40mm at max. (cf. Chapter 6) and a large cross section can be avoided. The cost for a good commercial valve is estimated to be 7,000 Euro.

7.7.3. Ball valve

It is planned to use the cooler trap also for storing of ions during times where the decelerator is not operated. The vacuum inside the trap should therefore be as good as possible, and the cryogenic section has to be completely shielded towards the beam line. It is planned to use a ball valve similar to the one in operation at the ATRAP experiment at CERN. There, a ball made from copper and equipped with coils is located inside the magnetic field of the trap. If a current is applied (typically 0.25 A) to these coils, the torque generated due to the presence of the strong magnetic field of the trap is sufficient to move the ball. Due to eddy currents present, the speed of movement can be controlled. A quarter-turn of the ball can be achieved within a minute or so.

A single bore inside the ball allows for particles to pass or not, depending on the orientation of the ball. The situation at ATRAP where the ball is located between two Penning traps is shown in Figure 7-4, where the coils are also given. The field emission point shown in that drawing is required as an electron source at ATRAP. In our case, it will not be required.

Care has to be taken to construct the whole ball valve with respect to its operation temperature. Figure 7-5 shows an exploded view of the ATRAP valve. All components will be manufactured in a tool shop (e.g., at Mainz) so that the total costs (including electrical equipment for the operation) will not exceed 2,000 Euro.

For further details of the ball-valve solution we refer to P. S. Yesley, PhD thesis, Harvard University, Cambridge, MA, Oct. 2001, from which all relevant information for this section was taken. We are grateful to the ATRAP collaboration for making the thesis available to us.

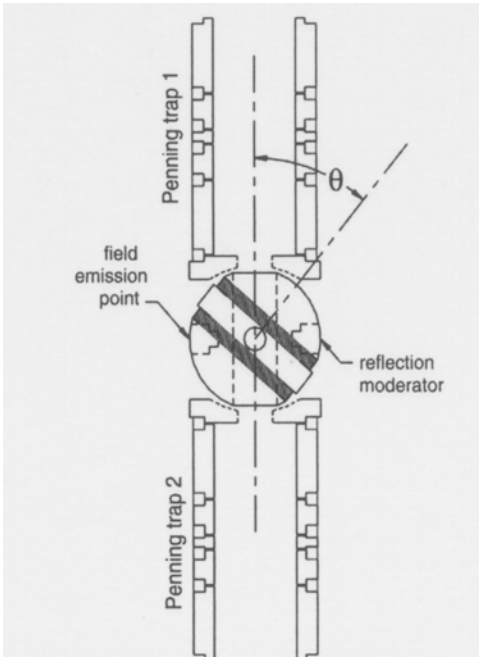

Figure 7-4. Scheme of the Ball valve at ATRAP. At 'open' position, the bore allows for transition of particles between the traps. A current applied to the coils and a counterbalancing by eddy currents makes the ball changing its orientation in the strong magnetic field of the trap. 'Field emission point' and 'reflection moderator' are not required in the HITRAP experiment. The picture is taken from P. S. Yesley, PhD thesis, Harvard University, Cambridge, MA, Oct. 2001.

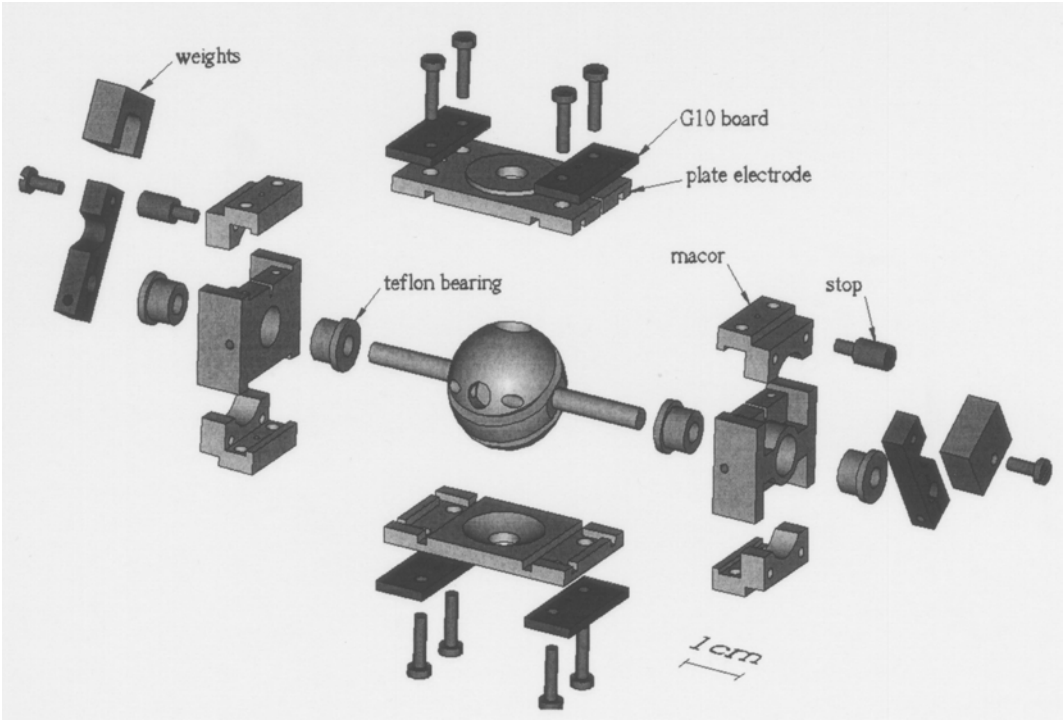

Figure 7-5. Exploded view of the ball valve at ATRAP. The picture is taken from P. S. Yesley, PhD thesis, Harvard University, Cambridge, MA, Oct. 2001.

7.7.4. Costs

Table 7-3. Costs for vacuum equipment around the trap. Values are in Euro.

7.7.1.	Diffusion valve (shutter) in the LEBT region	5,000
7.7.2.	UHV valve ahead of the trap	7,000
7.7.3.	Ball valve inside the trap	2,000
	Total:	**14,000**

7.8. Extraction to experiments: 10^5 ions/cycle at 4 Kelvin

7.8.1. Principle

In the trap, the ions are cooled to cryogenic temperatures (about 4 K). The cold ions will be extracted again and guided to experimental set-ups outside the cooler trap without increase of temperature. The ions are ejected into the beam line ahead of the trap and then upward through the ceiling of the re-injection channel on top of which the experiments will be located. The beam line towards the experiments is dealt with in Chapter 11. An extraction voltage of up to 20 kV will be used to extract the ions from the trap at cryogenic temperatures. Extraction can take place in any mode from emptying the trap by one pulse of a few micro-seconds up to a DC-like beam. From the experience gained at ISOLTRAP, no problems are to be expected. Both the extraction voltage and the extraction mode will be adjusted to the need of the running experiment by the experimentalists themselves. In general, the construction and setting-up of the components to transfer the beam of cold ions with extremely small emittance from the cooler trap to the individual experiments will largely be task of the experimental collaborations, in particular the EU-RTD network HITRAP.

7.8.2. Magnetic Bender

Most experiments will be located on top of the re-injection channel ceiling. This requires guiding the ions through a vertical beam line (cf. Fig. 1-4). In order to bring them into this beam line, an additional bender is required. At an extraction voltage of 20 kV, the magnetic rigidity of $^{238}U^{92+}$ is about 0.033 Tm. At a bending radius of 0.25 m, a magnetic field of approx. 0.13 T is required. Like in the LEBT beam line, solenoids with air-core coils will be employed. This allows for a fast switching between injection into the trap (LEBT solenoids 'on', bender 'off') and extraction from the trap (LEBT solenoids 'off', bender 'on').

Parts of the required coils and power supplies can be taken from stock. A suitable vacuum chamber will be manufactured in the tool shop in Mainz. The total costs of adjusting the magnets and installing the bender are estimated to be 12,000 Euro (cf. Table 7-4).

7.8.3. Costs

Table 7-4. Costs of the 90° bender, in Euro

Modification of existing coils	9,000
Vacuum chamber for junction	3,000
Total:	**12,000**

7.8.4. Alternative solution: Quadrupole deflector

Another option for the bender is an electrostatic quadrupole ion deflector as commercially available from ABB ('Quadrupole Deflector Energy Filter') or Colutron (Boulder, CO). Four hyperbolically shaped electrodes are mounted in a housing (Fig. 7-6), and by applying adequate voltages, bending of 90° or 270° is possible.

The commercially available deflectors cost about 10,000 Euro. Their slit size (cf. Fig. 7-7) of a few mm does not allow for a permanent location at any position before the ion trap, as the incoming ion beam from the RFQ has diameters up to 80 mm just after the second LEBT solenoid at the position of the bender. Any moving in and out of the beam does not seem feasible. A possibility would be to manufacture a bender based on the principles of the commercially available ones according to the needs of the HITRAP project, i.e., with large apertures and thus increased voltages on the rods. Such a device has already been manufactured at the NSCL at MSU, and the knowledge is available. Manufacturing it in one of the available tool shops within the collaboration would result in costs similar to those specified for the magnetic solution. As the quadrupole bender would necessarily imply the hyperbolic rods within the UHV vacuum and thus an additional possible source of vacuum problems, the magnetic solution is preferred.

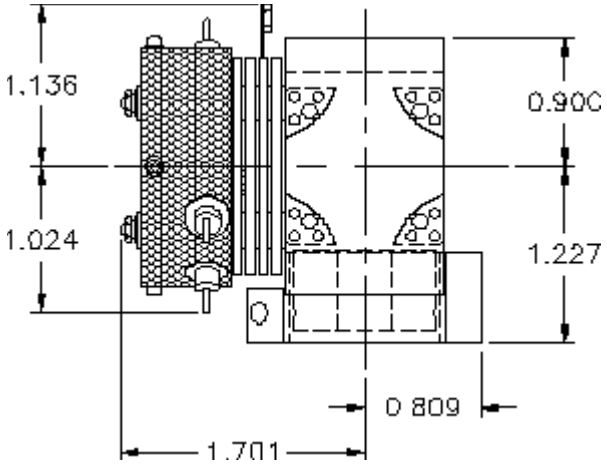

Figure 7-6. Sketch of the ABB Quadrupole bender. The four electrodes are visible in frontal view. Beams can pass the device in the four indicated directions perpendicular to the rods. The sizes are given in inches. The picture is taken from the WWW catalogue of ABB.

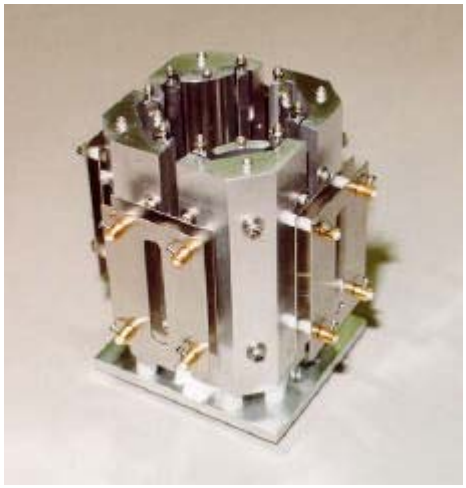

Figure 7-7. COLUTRON Model 900 Ion Deflector. The size of the bakeable device is 86mm × 86mm × 120mm. The picture shows the beam slits which are too small for any operation at HITRAP. The picture is taken from the COLUTRON web catalogue.

8. Magnets, Steerers, and their Power Supplies

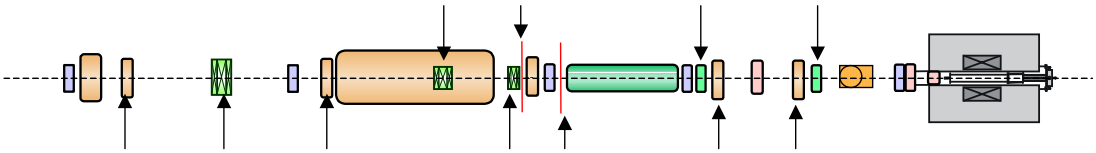

In this chapter, the magnets and steerers for the HITRAP decelerator are listed. This comprises all ion-optical elements relevant for the HITRAP decelerator inside the HITARP zone, i.e., after the wall that separates the re-injection tunnel from the ESR area. The ion-optical components ahead of this wall which are mentioned in Section 2.6.1., are part of the existing re-injection beam line and have to be neither purchased nor relocated.

The total costs for magnets and steerers do not comprise the inner-tank quadrupole triplet which is accounted for in the costs for Chapter 3. The total costs could be kept low do to considerable amounts of existing and available equipment at GSI. Magnets and steerers are presented in Table 8.1., their power supplies in Table 8.2.

Table 8.1. List of the parameters of magnets and steerers at HITRAP. Numbers in green specify the acquisition values of components available at GSI, which can be employed at HITRAP. The specified field gradients are those at design operation and not the maximal possible ones of the magnets.

Data				Costs (€)	Remarks
Magnetic Quadrupole Triplet ahead of the IH structure, DC operation					
	Lens 1	Lens 2	Lens 3	available, 35,000	Section 2.6.1.
Aperture	40 mm	40 mm	40 mm		
Effective Length	100 mm	100 mm	100 mm		
Magnetic induction at pole tip	0.6 T	0.6 T	0.6 T		
Field gradient	30 T/m	30 T/m	30 T/m		
Magnetic Quadrupole Triplet inside the IH cavity, pulsed operation					
	Lens 1	Lens 2	Lens 3	(60,000)	Chapter 3, costs considered in Chapter 3 together with the IH cavity
Aperture	16 mm	16 mm	16 mm		
Effective Length	70 mm	120 mm	70 mm		
Magnetic induction at pole tip	0.45 T	0.45 T	0.45 T		
Field gradient	53.3 T/m	52.0 T/m	53.3 T/m		
Magnetic Quadrupole Triplet in the inter-tank section, pulsed operation					
	Lens 1	Lens 2	Lens 3	60,000	Chapter 3
Aperture	30 mm	30 mm	30 mm		
Effective Length	40 mm	72 mm	40 mm		
Magnetic induction at pole tip	0.8 T	0.8 T	0.8 T		
Field gradient	53.1 T/m	52.0 T/m	53.1 T/m		
Solenoid magnets in the LEBT region					
	1st solenoid		2nd solenoid	available,	Section 6.1.

Aperture	60 mm	80 mm	2 × 8,000	
Effective Length	150 mm	150 mm		
Magnetic induction	0.35 T	0.17 T		
X/Y steering magnets ('steerers') ahead of the IH structure, bipolar, DC operation				
	1st pair of steerers	2nd pair of steerers	available, 2 × 6000	Section 2.6.1.
Aperture	100 mm	100 mm		
Effective Length	250 mm	250 mm		
Magn. induction	0.06 T	0.06 T		
Maximal deflection angle	20 mrad	20 mrad		
X/Y steering magnets in the inter-tank section, bipolar, DC operation				
	1st pair of steerers	2nd pair of steerers	20,000	Chapter 3, 10,000 Euro per pair of steerers
Aperture	30 mm	30 mm		
Effective Length	50 mm	50 mm		
Magn. induction	0.05 T	0.05 T		
Maximal deflection angle	10 mrad	10 mrad		
X/Y steering magnets in the LEBT section, bipolar, DC operation				
	1st pair of steerers	2nd pair of steerers	available, 2 × 6000	Section 6.1.
Aperture	100 mm	100 mm		
Effective Length	250 mm	250 mm		
Magn. induction	0.002 T	0.002 T		
Maximal deflection angle	15 mrad	15 mrad		
	Total costs:		**80,000**	
	Total savings:		**75,000**	

Table 8-2. List of power supplies for magnets and steerers which are available or have to be purchased. Where data are not specified, they are not relevant for the planned task. Figures in green indicate savings due to available material. HD refers to the ion-therapy linac currently under construction at the DKFZ in Heidelberg.

	1	2	3	4
Power-supply Type (PSU)	SVE2a-SF, in stock	SVEHD-M2, new, like HD	SVE1-HIT, simil. HD-L7	SVEHD-L5, new, like HD
Number of PSUs	3 (3 cabinets)	4 (1 cabinet)	4 (2 cabinets)	4 (2 cabinets)
Load	Unilac standard quadrupoles	2 pairs of steerers ahead of IH	IH quadrupole magnets (2 triplets)	2 pairs of steerers for inter-tank reg.
Direction of current	unipolar	bipolar	unipolar	bipolar
Min. current load I_{Lmin}	3 A	-13 A	0 A	-250 A
Max. current load I_{Lmax}	170 A	+13 A	1000 A	+250 A
Nominal direct current	170 A	±13 A	300 A	±80 A
Time of rise/fall into the tolerated region at jumps between I_{Lmin} and I_{Lmax}		1 s	15 ms rising 30 ms falling	15 ms rising 30 ms falling
Allowed over-/ undershot	arbitrary	arbitrary	arbitrary	arbitrary
Max. duration of flat top	3 ms	∞	3 ms	3 ms
Max. rate of repetition	0,1 Hz	1 Hz	0,1 Hz	0,1 Hz
Ohmic magneto resistance		5000 mΩ	38 mΩ (18...38 mΩ)	5 mΩ
Ohmic resistance of cables	57 mΩ	571 mΩ	28,6 mΩ	41 mΩ
Typ of cable/ length	4 x 25 mm^2/ 80 m	4 x 2,5 mm^2 / 80 m	4 x 50 mm^2 / 80 m	4 x 35 mm^2/ 80 m
Inductivity at load		19 mH	0,28 mH (0,12...0,28 mH)	8,6 µH
Mean inductive voltage at load $L_L \times di_L/dt$		±0,5 V	+23,3 V	±0,15 V
Output voltage at Nominal direct current Nominal power	40 V 170 A 6,8 kW	±72,4 V ±13 A 941 W	20 V 300 A 6 kW	±3,7 V ±80 A 300 W
Controlled variable	Current load	Current load	Current load	Current load
Stability and allowed ripple of current at constant current		±50 mA	±200 mA	±250 mA
Stability and allowed ripple of current during ramping	arbitrary	arbitrary	arbitrary	arbitrary
Costs per PSU cabinet	avail., ~ 18 k€	78 k€	60 k€	51 k€

Table 8-2. (continued)

	5	6		
Power-supply type (SVE)	SVEHD-L4 new, like HD	SVE2a-SF, in stock		
Number of PSUs	4 (1 cabinet)	2 (2 cabinet)		
Load	2 pairs of steerers for LEBT	Solenoid magnets (ex. EPOS)		
Direction of current	bipolar	unipolar		
Min. current load I_{Lmin}	-10 A	3 A		
Max. current load I_{Lmax}	+10 A	300 A		
Nominal direct current	±10 A	300 A		
Time of rise/fall into the tolerated region at jumps between I_{Lmin} und I_{Lmax}	1 s			
Allowed over-/ undershot	arbitrary	arbitrary		
Max. duration of flat top	∞	3 ms		
Max. rate of repetition	1 Hz	0,1 Hz		
Ohmic magneto resistance	538 mΩ			
Ohmic resistance of cables	571 mΩ	57 mΩ		
Typ of cable/ length	4 x 2,5 mm^2/ 80 m	4 x 25 mm^2/ 80 m		
Inductivity at load	12,8 mH			
Mean inductive voltage at load $L_L \times di_L/dt$	±0,26 V			
Output voltage at Nominal direct current Nominal power	±11,5 V ±10 A 115 W	40 V 170 A 6,8 kW		
Controlled variable	Current at load	Current at load		
Stability and allowed ripple of current at constant current	± 10 mA			
Stability and allowed ripple of current during ramping	arbitrary	arbitrary		
Costs per PSU cabinet	39 k€	avail, ~ 22 k€		

The total costs of required power supplies for magnets and steerers are compiled in Table 8-3.

Table 8-3. Total costs for power supplies of magnets and steeres. Green indicates savings due to existing material which can be employed for HITRAP.

No.	Type	supplies	Number	Cabinets	Costs/ cabinet	Costs/ Total
1	SVE2a-SF	QP ahead of IH	3	3	18 k€	54 k€
2	SVEHD-M2	steerers ahead of IH	4	1	78 k€	78 k€
3	SVE1-HIT	QPs in and after IH	4	2	60 k€	120 k€
4	SVEHD-L5	inter-tank section steerers	4	2	51 k€	102 k€
5	SVEHD-L4	LEBT steerers	4	1	39 k€	39 k€
6	SVE2a-SF	LEBT Solenoids		2	22 k€	44 k€
	Total:					**319 k€**
	Savings:					**98 k€**

9. Beam Diagnostics

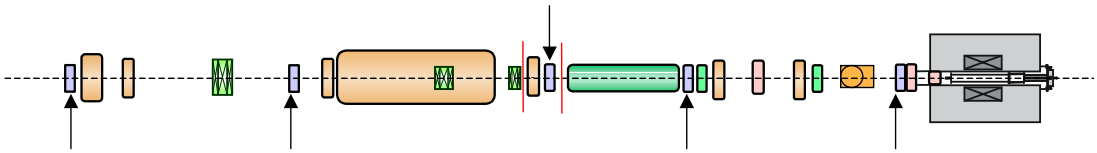

For the commissioning and operation of the HITRAP facility, beam-diagnostic devices are mandatory. A precise alignment of the beam requires the determination of the beam parameters at several locations.

9.1. Extracted beam from ESR

The *bunch structure* of the extracted beam from the ESR has to be determined with a pick-up. The band width of this pick-up can be restricted to 100 MHz to monitor the relatively long bunches delivered by the ESR. This serves also as a control of the right extraction parameters inside the ESR.

9.2. Pointing stability

For an *online control of the transverse beam stability,* halo counters can be used. They are to be mounted at aperture-limited locations, e.g. at the IH input. Fast particle detectors, like CVD diamonds or glass scintillators, are foreseen. Fixed transverse positions are sufficient for them, saving the cost of the expensive remote-controlled movable feed throughs.

9.3. Current measurement with Faraday cups

The *current* in front and behind each deceleration section should be determined to yield the transmission under various module-parameter settings. Only a destructive measurement by Faraday cups is suited for this low current. They will be installed with a pneumatic vacuum feed-through on a Ø 100 mm flange in special diagnostic vacuum chambers. This kind of detector uses a standard technology, having a permanent magnet system for the secondary electron suppression and a low-noise current amplifier.

9.4. Transverse beam profile

The *transverse beam profile*, including the beam's centre-of-mass, can be determined by standard SEM grids, having wires with a diameter of 0.1 mm and a spacing of about 1 mm. 16 wires are sufficient for each plane due to the small emittances. Several SEM grids can be used consecutively, each with a transmission of about 80%, due to the ratio of wire diameter to spacing. Each wire is connected to a standard current amplifier and the signal is multiplexed for digitalisation. As a cost-efficient alternative, scintillation screens can be observed with a CCD camera. However, tests have to be performed to match the generation of light to the beam parameters. Like for the cups, these systems are mounted with pneumatic vacuum feed-throughs on a Ø 100 mm flange at the diagnostic chambers.

9.5. Bunch structure

The forming of the *bunches* has to be monitored with pick-ups. Three ring shaped pick-ups are foreseen in front and behind the IH structure and behind the RFQ. They serve as a control of the right setting of the buncher amplitude and the two tank rf-amplitudes and rf-phases. The required band width is about 1 GHz. Low-noise equipment developed at GSI can be used.
Having a non-relativistic beam, the *bunch structure* of the bunched and decelerated beam can only be estimated from the pick-up signal. For the commissioning of the buncher and decelerator a more precise measurement of this critical parameter might be necessary. Such a monitor is available at GSI and could be installed temporarily during the commissioning time. Minor modifications are required to adopt this system to the given beam parameters.

9.6. Measurement of beam energy

The *mean energy* of the decelerated beam in the IH structure can be controlled by the two pick-ups behind this module and behind the RFQ using the well established time-of-flight method.

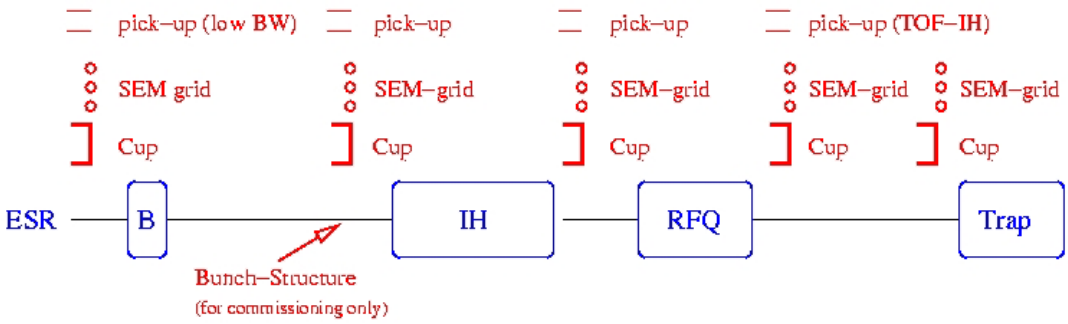

Figure 9.1. Schematic layout of the beam-diagnostics devices at the HITRAP facility. `TOF-IH' refers to the use for time-of-flight measurements in order to determine the energy after the IH structure. The location of the diagnose boxes with respect to the other HITRAP components can be inferred from Figure 1-5 and from the sketch at the beginning of this chapter.

9.7. Compilation of devices for beam diagnostics

The diagnostic devices are summarized in Figure 9-1 and Table 9-1. Most of the diagnostics can be built according to the long-standing experience at the UNILAC. Only minor changes have to be performed to adopt the use of the diagnostic elements to the relatively

short pulse length of about 3 µs given by the revolution period inside the ESR. The space is very limited between the IH and RFQ tanks due to the matching requirements. A special mechanical construction has to be worked out to fit adequate diagnostics into this limited space.

The described devices are designed for typically 10^5 bare uranium ions. The signal strength will be large enough to evaluate the required beam parameters on a pulse-by-pulse scale, i.e. no time-consuming averages are needed. If a much lower number of ions per pulse has to be monitored, special particle detectors have to be developed.

Table 9-1. Beam diagnostic devices at HITRAP facility.

Location	Device	Meas. beam quantity	Remarks
before 4-gap buncher	cup SEM-grid pick-up	charge transverse profile bunch length	 long bunch (BW < 100 MHz)
before IH	cup SEM-grid pick-up halo-counter	charge transverse profile approx. bunch length transverse. stability	 short bunch (BW ~ 1 GHz)
before RFQ	cup SEM-grid pick-up	charge transverse profile approx. bunch length	limited space short bunch (BW ~ 1 GHz)
behind RFQ	cup SEM-grid pick-up	charge transverse profile energy after IH	 short bunch (BW ~ 1 GHz)
behind 90º bender	cup SEM-grid	charge transverse profile	

9.8. Costs for diagnostics

Table 9-2. Cost estimation of the beam diagnostic devices at HITRAP facility. The last column shows the reduced costs, if the devices from the GSI-pool (i.e. device previously mounted at the UNILAC) can be used.

Device	Quantity	Mechanics	Electronics	Cost (subsum)	Cost (pool)
Cup	5	8 k€	2 k€	50 k€	30 k€
SEM grid	5	12 k€	15 k€	135 k€	85 k€
Pick-up (low BW)	1	4 k€	3 k€	7 k€	7 k€
Pick-up (wide BW)	3	4 k€	5 k€	27 k€	15 k€
Fast digital oscilloscope	1		15 k€	15 k€	15 k€
Halo counter	1	15 k€	15 k€	30 k€	30 k€
Cabling		3 k€		3 k€	3 k€
Diagnose boxes	5	4 k€		20 k€	0 k€
Total sum				287 k€	**185 k€**

The expected costs of all diagnostic installations are summarized in Table 9.2. Pick-ups and cups have only a single-channel output, making the subsequent electronics relatively cheap. The multi-channel SEM-grid electronics requires a low-noise current amplifier for each channel, which gives rise to a large fraction of the cost. A large **cost reduction** of **102 k€** is possible by reusing of standard devices previously mounted at the UNILAC. In particular the mechanics and some parts of the electronics for the SEM-grids should be available.

As stated above, scintillation screens might be an alternative, reducing the costs to about 10 k€ per location but requires some technical development for the adoption to the short macro-pulse length of about 3 µs.

All required front-end electronic will be place outside of the radiation area on the foreseen HITRAP-platform in the ESR hall within two 19'' racks. The data evaluation and visualisation will be embedded into the general control system, as for the existing GSI-facility.

9.9. Appendix: Non-standard instrumentation

In the preceding sections, a completely sufficient system for beam diagnostics has been presented. Below, possible alterations and extensions are mentioned which were not taken into consideration due to either a large amount of development required or due to the considerable additional costs for each unit. These possible extensions can be kept in mind for the case of an operation of the HITRAP set-up at the GSI Future Facility (cf. Chapter 16).

- *Profile measurement with scintillation screens:*
  Screen is viewed by CCD camera → considerably cheaper than profile grid.
  Disadvantage: Needs some development.
- *Bunch shape measurement for longitudinal matching into IH structure:*
  Secondary electrons emitted by a wire and rf detector (time-to-space converter).
  Costs: about 50 - 100 k€.
- *Medium current and profile measurement:*
  Secondary electrons emitted by a foil and detected with MCP-phosphor.
  Costs: about 30 k€ per location.
- *Low current and profile measurement:*
  Single-particle detection using position-sensitive, segmented counters.
  Costs: about 30 k€ per location.

10. Controls

10.1. Outline of the HITRAP Control System

- The decelerator will be controlled from the HKR (main control room of the GSI accelerators).
- The present computer capacity of the ESR console is sufficient for handling the additional HITRAP control software.
- The required consoles will be provided from the experiment-control consoles where input/output operation takes place via present X-terminals.
- The required software for device control and user interfaces exists to a good deal: Reverts can be made to the existing HLI programs.
- For device control, standard components of the control system will be employed.

10.2. Timing system

The operation of the HITRAP decelerator is planned as follows:

- A 5 – 10 Hz pulser is employed to keep the RF transmitters at operation temperature (cf. Section 5.3.5). The pulser is synchronized with the 50 Hz mains.
- About one second before an extraction from the ESR, the ESR standard-system time ('ESR Pulszentrale') sends an 'inhibit' signal to this pulser.
- The extraction and the operation of the decelerators get the 'sync' from the 'ESR-Pulszentrale'.

10.3. Costs

Table 10-1. Costs for embedding HITRAP into the GSI control system.

Item	Details	est. costs [k€]
1. Console	No costs for standard elements	0
	Cables, switches, trivia	1
	2 Oscilloscopes for analogue display	5
2. Connections and computers for device control		
	VME crates with GμP, TIF, and 8 SEs	15
	40 Device interfaces (incl. wiring)	60
3. Timing components (trigger, pulser)		5
4. Adaptations of software		20
5. Wiring		5
Total costs for controls		**111**

These costs are just an estimate. However, the major part (device connection and control) is fairly safe and therefore the total sum should be rather reliable.

After disassembly of the existing ESR in the framework of the GSI Future Facility, all hardware components can be used otherwise within the GSI accelerator control system.

11. Vacuum system

11.1. General remarks:

As the ESR UHV-system is running at a base pressure in the low 10^{-9} Pa region (10^{-11} mbar), a differential pumping section has to be integrated into the beam transport line between the ESR and the HITRAP installation. This differential pumping section has to guarantee a minimized gas flow from the 4-gap buncher and the IH-structure into the ESR.

The ion traps behind the decelerator operate at liquid helium temperature and so, with extremely high vacuum. A second differential pumping system has to guarantee a minimized gas flow from the RFQ structure into the beam line of the ion traps and into the ion traps themselves. The vacuum system of the decelerator (4-gap buncher, IH structure, RFQ, and beam focussing elements) is planned to deliver a base pressure within the low 10^{-5} Pa region (10^{-7} mbar) by the use of turbo-molecular pumps (TP) and ion-getter pumps (IP). The ion-trap beam line has to be designed bakeable, prepumped by a turbopump system (used during bake-out, separable after bake-out) and finally pumped by IP and titanium-sublimation pumps (TSP) to reach a pressure level of 10^{-9} Pa (10^{-11} mbar).

The following sections indicate the detailed scheme of the HITRAP vacuum conception including all required components. All components are considered to be purchased. The total price of all listed vacuum systems amounts to a total of appr. 480 k€. Included in this estimated sum are all vacuum pumps, diagnostics, beam pipes, valves, vessels (without IH / RFQ vessels), bake-out equipment, mounting frames, cables and controls.

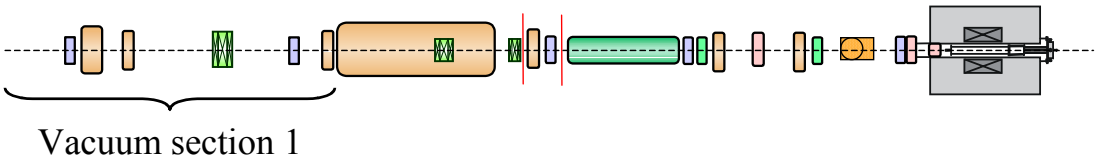

11.2. Differential-pumping stage between ESR and IH cavity

11.2.1. Schematic view of the section

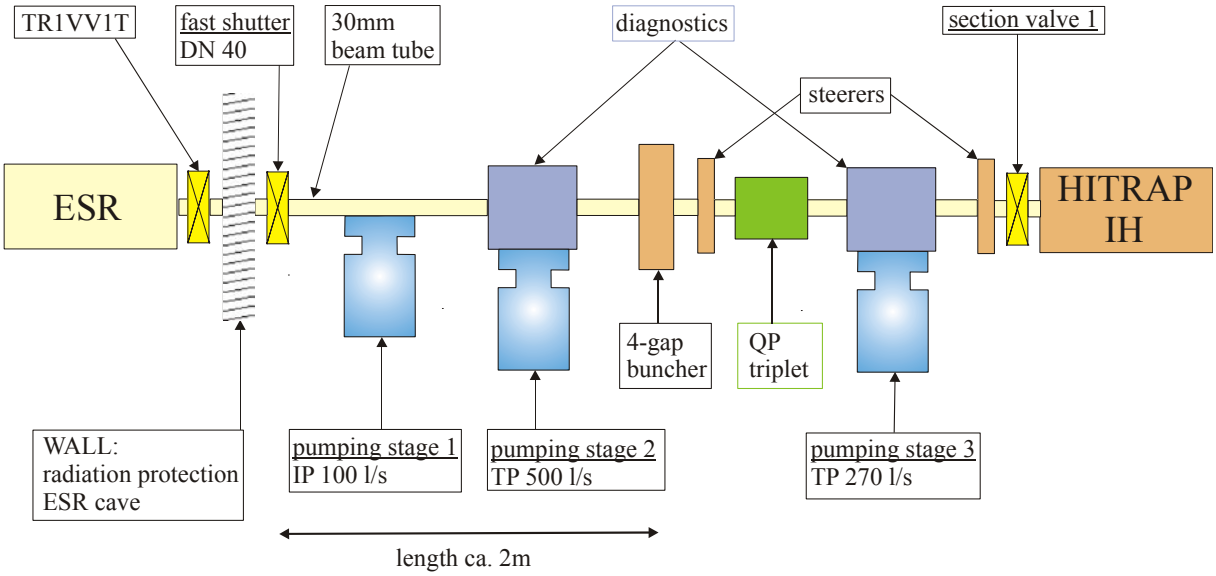

Figure 11-1. Vacuum scheme between the ESR section (left) and the IH cavity (right). Underlined items refer to major entries in Table 11-1. The pumping stages allow for the installation of beam-diagnostic tools in the pumping chambers. Left of the valve TR1VV1T, the current re-injection beam line is employed. The drawing is not to scale.

11.2.2. System components

Table 11-1. Detailed list of required vacuum and beam-line components for the section between the ESR and the IH cavity.

Item	characteristics	amount	est. price [k€]	notes
Fast shutter	system DN40	1	12	UHV safety ESR
Pumping stage 1	IP 100 l/s	1	6	pump
	p[Pa] measurement	1	2	diagnostics
	four-way cross DN100	1	3	vacuum vessel
	straight tubes DN40	2	1	beam pipe
Pumping stage 2	TP 500 l/s PP 10 m^3/h Valve DN100 local controls	1	25	turbo-pump station
	p[Pa] measurement	1	2	diagnostics
	four-way cross DN100	1	3	vacuum vessel
	straight tubes DN40	2	1	beam pipe
Pumping stage 3	TP 270 l/s PP 5 m^3/h Valve DN100 local controls	1	20	turbo-pump station
	p[Pa] measurement	1	2	diagnostics
	four-way cross DN100	1	3	vacuum vessel
	straight tubes DN40	4	2	beam pipe
Section valve 1	DN40	1	3	entrance IH
Cables	HITRAP to control electronics location	~10	5	remote control of pumps, diagnostics and valves
Controls	interface to GSI control system	2 crates	6	remote control of pumps, diagnostics and valves
Frames	mounting of vessels and beam pipes	~ 4	5	
Total costs			**101**	

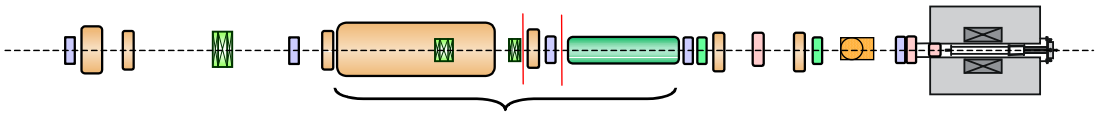

11.3. Vacuum system of the decelerator IH / RFQ structure

11.3.1. Schematic view of the section

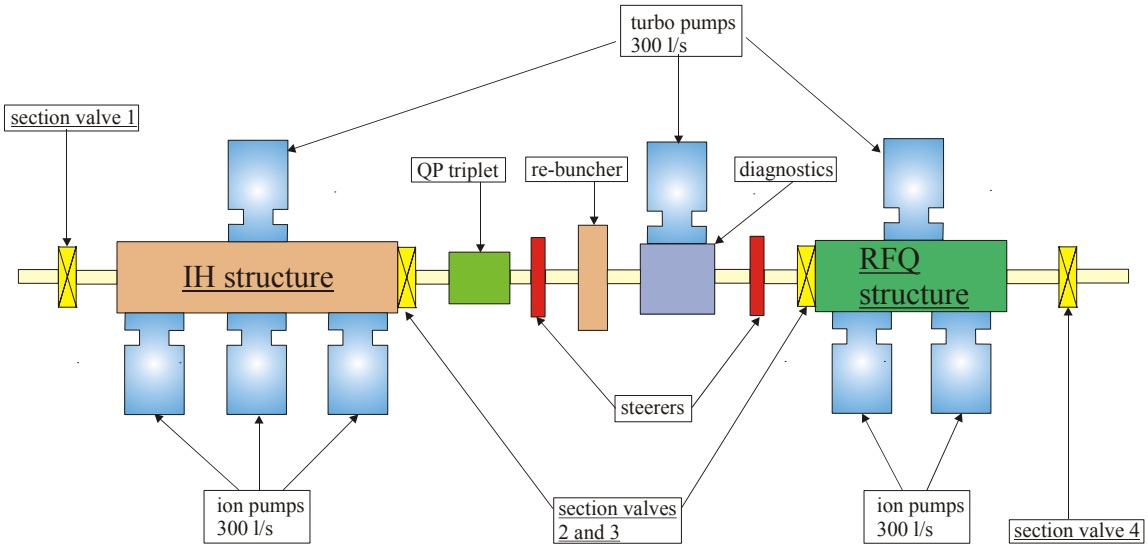

Figure 11-2. Vacuum scheme of the section comprising IH tank and RFQ tank. Underlined items refer to major entries in Table 11-2. Beam diagnostics will be housed in the inter-tank pumping chamber. The drawing is not to scale.

The planned vacuum system of the IH / RFQ structures is comparable to the existing GSI-HLI (High-charge injector) installation.

11.3.2. System components

(The vacuum vessels and frames for the IH structure and the RFQ structure are not included in this list. Cf. Chapters 3 and 4.)

Table 11-2. Detailed list of required vacuum and beam-line components for the IH tank, the RFQ tank, and the section between them. The vacuum vessels for the tanks are not included in this list.

Item	characteristics	number	est. price [k€]	notes
IH structure	IP 300 l/s	3	30	Ion pump
	TP 300 l/s PP 10 m^3/h Valve DN100 local controls	1	25	turbo-pump station
	p[Pa] measurement	1	2	diagnostics
Section valve 2	valve DN100	1	5	exit IH
	p[Pa] measurement	1	2	diagnostics
IH/RFQ 4-pole section	TP 300 l/s PP 10 m^3/h Valve DN100 local controls	1	25	turbo-pump station
	p[Pa] measurement	1	2	diagnostics
	four-way cross DN100 + 4-pole chamber	1	5	vacuum vessel
Section valve 3	valve DN100	1	5	entrance RFQ
RFQ structure	IP 300 l/s	2	20	Ion pump
	TP 300 l/s PP 10 m^3/h Valve DN100 local controls	1	25	turbo-pump station
	p[Pa] measurement	1	2	diagnostics
Section valve 4	valve DN100	1	5	exit RFQ
cables	HITRAP to control electronics location	~20	10	remote control of pumps, diagnostics and valves
controls	interface to GSI control system	3 crates	9	remote control of pumps, diagnostics and valves
frames	mounting of vessels and beam pipes	2	3	
Total costs			**175**	

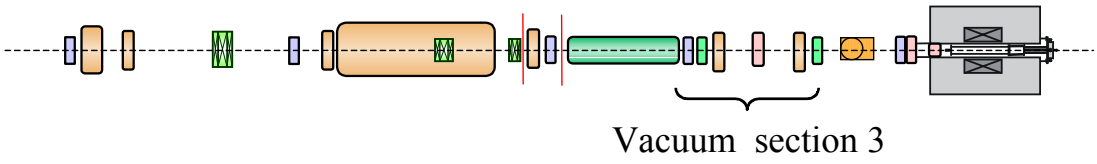

11.4. Differential pumping stage between RFQ and the ion-trap beam line

11.4.1. Schematic view of the section

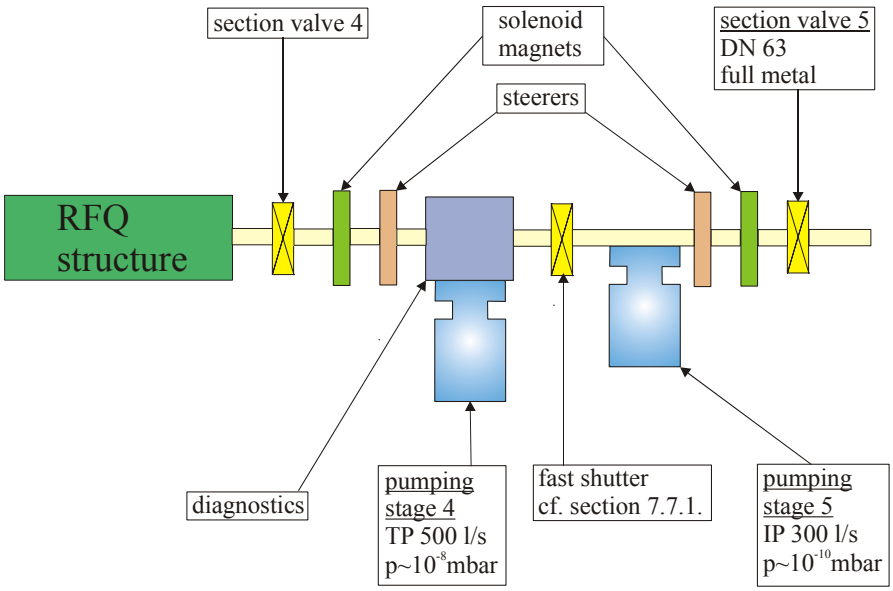

Figure 11-3. Vacuum scheme of the differential pumping stage behind the RFQ. Underlined entries refer to major items in Table 11-3. Beam-daignostics tools will be housed in one of the pumping chambers. The drawing is not to scale. The fast shutter (cf. Section 7.7.1.) is not part of the vacuum considerations here.

11.4.2. System components

Table 11-3. Detailed list of required vacuum and beam-line components for the differential pumping stage after the RFQ.

Item	characteristics	amount	est. price [k€]	notes
Pumping stage 4	TP 500 l/s PP 10 m^3/h Valve DN100 local controls	1	25	turbo-pump station
	p[Pa] measurement	1	2	diagnostics
	four-way cross DN100	1	3	vacuum vessel
	straight tubes DN100	2	2	beam pipe
Pumping stage 5	IP 300 l/s	1	10	ion-pump station
	p[Pa] measurement	1	2	diagnostics
	four-way cross DN100	1	3	vacuum vessel
	straight tubes DN100	4	4	beam pipe
Section valve 5	DN100	1	10	exit diff.pumping , **full metal valve**
Cables	HITRAP to control electronics location	~10	5	remote control of pumps, diagnostics and valves
Controls	interface to GSI control system	1 crate	3	remote control of pumps, diagnostics and valves
Frames	mounting of vessels and beam pipes	~ 2	2	
Total costs			**71**	

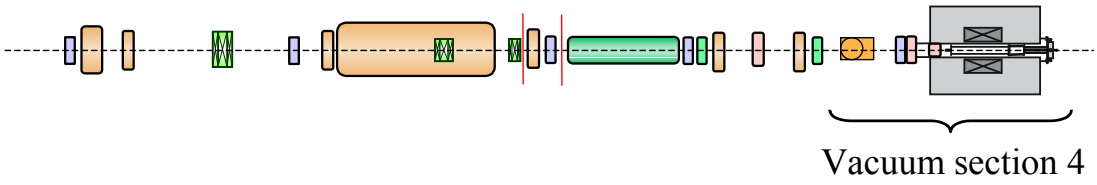

11.5. Ion-trap beam line

11.5.1. Schematic view of the section

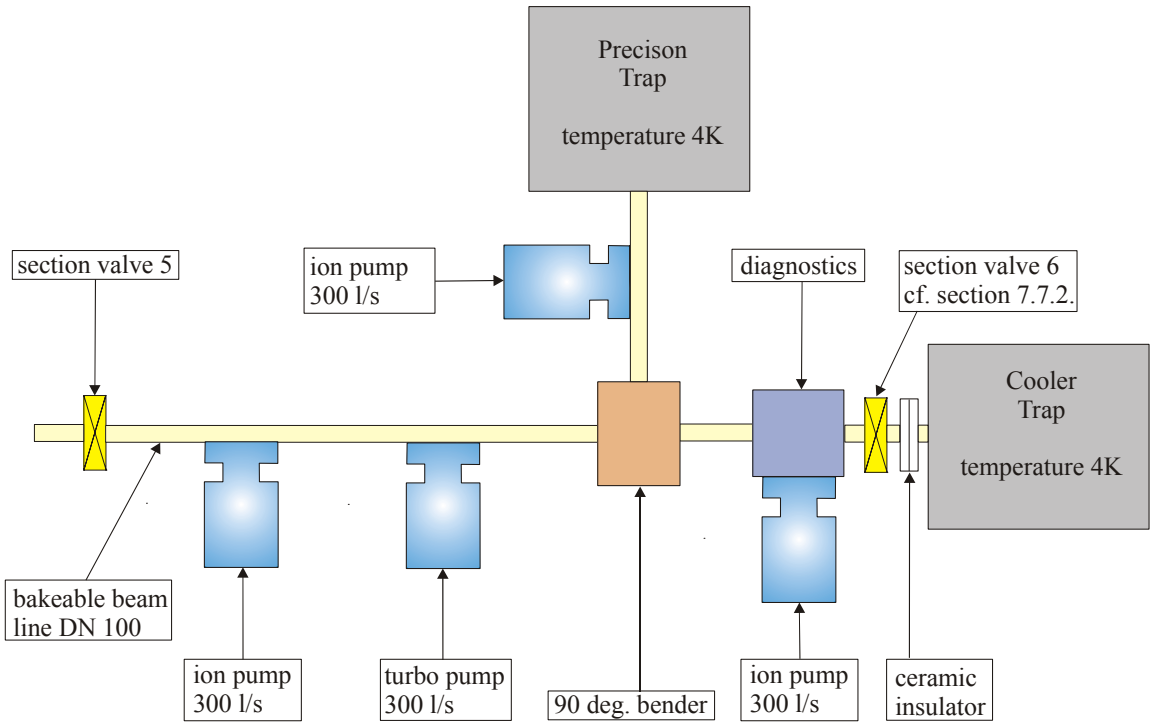

Figure 11-4. Vacuum scheme for the beam lines close to the ion traps. In addition to the precision trap, also other experiments (with similar requirements) can be attached to the set-up. The ceramic insulator allows to put the Cooler Trap on high voltage potential. The drawing is not to scale. The section valve 6 (cf. Section 7.7.2.) is not part of the vacuum considerations here.

The vacuum system of the ion-trap beam line is planned to be bakeable at 300°C. UHV conditions are reached by a combination of turbo-pump pre-pumping and ion-pump final pumping. The turbo-pump system at this location will be used only during bake-out and has to be separated after bake-out by a full metal DN100 UHV valve. With a NEG-coating (optional) of the vacuum tubes, the minimum pressure of the beam line could be improved further. The presentation here is not affected by additional valves and a diffusion barrier as planned for the operation of the Cooler Trap (cf. Chapter 7). These components do not form

part of the general vacuum layout as presented here and are also not part of the cost estimate here.

11.5.2. Technical remarks

With a total length of the beam line of about 8m after the differential pumping stage, and a DN100-beam pipe diameter, the inner surface is app. 2.5×10^4 cm^2. Typical outgassing rates after bake-out are 10^{-10} Pa l/(s cm^2) [10^{-12} mbar l/(s cm^2)]. With an installed final pumping speed of 900 l/s (IP), the pressure will reach a level of 10^{-9} Pa (10^{-11} mbar).

The conductance of an orifice (entrance ion trap) of 30mm diameter can be calculated to be ~70 l/s for N_2 and ~300 l/s for H_2. At an average pressure of 5×10^{-9} Pa (5×10^{-11} mbar; beam tubes pumped by IP) at the entrance of the ion traps, the gas load into the vacuum system of the ion traps will be at the order of 3.5×10^{-7} Pa l/s (3.5×10^{-9} mbar l/s; ~8.4×10^{10} N_2 /s) for N_2 and of 1.5×10^{-6} Pa l/s (1.5×10^{-8} mbar l/s; ~ 3.6×10^{11} H_2 /s) for H_2.

NEG coating of the inner surface of the vacuum tubes is a recommended option and would increase the pumping speed for reactive gas species (e.g. CO, H_2, …) by about two orders of magnitude.

11.5.3. System components

Table 11-4. Detailed list of required vacuum and beam-line components for the beam lines close to the ion traps. The total costs include the recommended option of NEG coating for the beam lines.

Item	characteristics	amount	est. price [k€]	notes
Pumping stage 6	TP 300 l/s PP 10 m^3/h Valve DN100 (full metal) local controls	1	30	turbo-pump station for bake-out, full metal valve for separation
	p[Pa] measurement	1	5	UHV diagnostics
	four-way cross DN100	1	3	vacuum vessel
	straight tubes DN100	4	4	beam pipe
Beam line	IP 300 l/s	3	30	Ion-pumps
	p[Pa] measurement	2	10	UHV diagnostics
	bake-out equipment		10	heating jackets+control
	bending-magnet chamber	1	5	
	ceramic isolation	1	5	electric isolation for cooler trap
Cables	HITRAP to electronics control location	~10	5	remote control of pumps, diagnostics and valves
Controls	interface to GSI control system	1 crate	3	remote control of pumps, diagnostics and valves
Frames	mounting of vessels and beam pipes	~ 2	2	
NEG coating	straight tubes DN100	4	20	option
Total costs			**132**	

11.6. Required manpower and total costs

11.6.1. Required manpower for the installation of the HITRAP set-up

The manpower estimation for the installation of the vacuum system is given under the following conditions:

- No additional mechanical work is required on delivered components like IH-tank, RFQ-tank, magnets, vacuum chambers, frames, etc.
- No installation of infrastructure (electric, water, controls) is included here.
- Adjustment (standard telescope adjustment, no transfer) is included in all work packages.

Table 11-5 Required manpower for installation of the HITRAP setup.

Work package	time [days]	capacity [man equivalents]
Dismounting existing beam line	20	4
11.2: Beam line ESR (TR1VV1T) to ICH	10	4
11.3 IH and RFQ tanks, inter-tank section	30	4
11.4 Beam line RFQ to Cooler Trap	10	4
11.5 Cooler trap, beam line to the experiments	30	4
sum	100	4
Total:	**400 person days**	

11.6.2. Vacuum-system project management

The estimation for the project management of the vacuum system is given on condition that :
– The following work packages are included:
- Vacuum technical design,
- Construction work of vacuum components,
- Call for tenders, supervision of production,
- Conceptional work for assembling, mounting and adjustment.

– The following work packages are not included:
- Construction work of accelerator structures (IH, RFQ, buncher, beam diagnostics),
- Technical-design aspects of the ion traps.

Table 11-6. Required full-time equivalents [FTE] for the vacuum-system project management.

Work package	Vacuum physicist [FTE]	Vacuum engineer [FTE]	Construction engineer [FTE]
Vacuum-technical design	5 % × 1 month	5 % × 1 month	
Construction work of vacuum components			100 % × 2 months
Conceptional work for assembling, mounting and adjustment	5 % × 1 month	5 % × 1 month	
Call for tenders, supervision of production	5 % × 6 months	5 % × 6 months	
Total:	3.3 % FTE	3.3 % FTE	16.6 % FTE

11.6.3. Total costs

The presented solution for the vacuum at the HITRAP decelerator allows for safe operation of both the decelerator and also the ESR. As an advantage, the pumping chambers of the various pumping stations can house tools for beam diagnostics. To reach the best possible vacuum close to the ion traps, beam lines both bakeable and also NEG coated are planned in this region. The total costs for vacuum equipment (including beam lines and vacuum supply for the decelerator tanks but not the tanks themselves) are given in Table 11-7.

Table 11-7. Total cost estimate for the HITRAP vacuum system.

Section	Details in	Costs [k€]
Section before the IH-tank	Table 11-1	101
IH/RFQ tanks	Table 11-2	175
Differential pumping section after the RFQ tank	Table 11-3	71
Beam lines at the ion traps	Table 11-4	132
Total costs		**479**

12. General Infrastructure and Supplies

12.1. Civil engineering

12.1.1. Mechanical support of the decelerator

All components of the decelerator will be mounted on conventional steel frames. Costs for these components are already considered in the relevant sections (cf. in particular Tables 15-1 to 15-3). Adjustable supports for alignment ('Justierfüße') are available in sufficient number in GSI stock.

12.1.2. Alignment

As described in Section 11.6., a standard telescope alignment of the decelerator will take place. In the rare case of transition to re-injection operation and back, this alignment has to be partially repeated. The duration of the co-existence of HITRAP decelerator and the re-injection beam line at the same location is limited so that any cost-intensive solutions for a more advanced method of alignment are not considered for the present location.

12.1.3. Procedure to change from HITRAP to re-injection and vice versa

The apertures of many components of the HITRAP decelerator do not allow for passage of a high-energetic beam form the ESR back to the SIS even in case the beam is cooled. Therefore, the HITRAP decelerator has to be dismounted in case re-injection takes place. The original re-injection beam line has to be re-installed.

Any mechanical set-up, which would have allowed for an easy shifting between both beam lines, turned out to be too costly with respect to the up-to-now rare re-injection events and the limited time of co-existence of both set-ups (cf. also 12.1.2). The current solution with a standard mechanical support and alignment will require about four persons working for two weeks (320 man-hours) in order to change from HITRAP operation to re-injection and about four persons working three and a half weeks (520 man hours) to re-install HITAP at the re-injection beam line. These changes do not require a major shut-down, i.e., they can be performed while the other accelerators at GSI are working and the work load of the accelerator-construction team is lower than in major shut-down periods.

In order to allow for an easy handling of the heavy components within the tunnel, a movable gibbet-like crane with a payload of 500 kg will be stationed there. This crane has to be purchased.

12.1.4. Procedure to change from HITRAP to PHELIX operation and vice versa

As a second experiment within the re-injection tunnel, within the PHELIX project a laser experiment is planned where a part of the PHELIX laser beam is guided down into the tunnel (cf. Figs. 1-3 and 1-6), compressed, and brought to interaction with the incoming high-energy ion beam from the ESR. This requires an interaction zone (of about 2m length) and a beam dump. The experiment will be located at the ESR side of the re-injection channel beam-up of the HITRAP-IH tank. In this case it is sufficient to disassemble only the differential pumping section, the four-gap buncher, and the adjacent drift section to the IH tank. Compared to the transition to re-injection operation, the mechanical work is considerably less and does therefore not seriously hinder any of the two projects.

12.1.5. Civil-engineering works in the re-injection tunnel

The re-injection-tunnel shielding consists of concrete with a thickness of 1.6 m. A hole of 250 mm diameter has to be drilled through the top shielding in order allow for the passing of the beam line from the cooler trap to the experiments (cf. Fig. 1-4). In addition, the planned separation of the control-access areas 'ESR' and 're-injection tunnel' (cf. Section 12.3.) requires a proper strengthening (of 1m) of the present wall between the ESR and the re-injection tunnel and also an additional wall behind the cooler trap, towards the section of the re-injection channel located closer to the SIS. These requirements are represented in the cost estimate given below.

12.1.6. Platform

In the north-western corner of the ESR hall where the section re-injection channel housing HITRAP is located, at present there is hardly space to place experiments or their supplies on the existing supports. Therefore, the experiments, consisting of a precision trap for g-factor measurements, an UHV chamber for surface-interaction studies, a reaction microscope and set-ups for laser spectroscopy and x-ray spectroscopy, will be located on the existing concrete roof of the re-injection channel (cf. Figs. 1-2 and 1-7). To house the RF-power supplies, the racks for the electronics for controls and beam diagnosis and all equipment for control of the experiments as well as two containers as measurement rooms, a triangular-shaped platform is planned in the area surrounded by the outer wall of the ESR hall (taking into account all supply lines on the inner side), the roof of the re-injection channel, and the existing stairs which lead to the ceiling of the ESR itself (cf. Fig. 1-7). This platform will be made from a steel frame and with a grid floor covered by chequer plate from aluminium. To the outer-wall side, it will be mounted on supports, on the re-injection-channel side it will be supported by the existing walls of the re-injection channel which are sufficient to carry an extra load. The platform will overbuild the existing magnet-power supplies located in this corner of the ESR hall. The concept has the advantage that it requires only slight reconstruction of the existing shielding. Furthermore, a double bottom for cable laying is not required since all wiring can be performed under this platform.

The stairs in the south are already present. Only short stairs have to be constructed to give access to the platform from these stairs, and in addition, another short stair is required to give access to the ceiling of the re-injection channel.

On the platform, the containers as well as all required supply-units will be installed. The presented layout takes into account the free path for the big crane of the hall as well as future installations in connection with the PHELIX experiment. The floor of the platform is calculated to be 4.23 m above floor level whereas the beam-line centre of PHELIX runs at a height of 7.5 m. Even a beam line diameter of 1 m therefore allows for a placement of 2.6 m high RF-transmitter components under that beam line. The platform is planned for a load of one metric ton/m^2.

12.1.7. Containers

To house smaller equipment and give room for experiment control, two containers will be installed on the platform. Considering the limited lifetime of the experiment at the location, refurbished containers will be purchased which are considerably cheaper than new ones (up to a factor of 3). The planned sizes of the two containers are 3 m × 5 m and 6 m × 5 m, respectively (cf. Fig. 1-7).

12.1.8. Costs for Construction

Table 12-1. Costs for construction work in the ESR hall related to HITRAP. Prices are excl. VAT.

12.1.	Construction	price/unit	subtotal
12.1.3.	**INSTALLATION TOOLS**		
1	Crane, gibbet-like, pay load 500 kg	€ 5,000	
			€ 5,000
12.1.5.	**SHIELDING**		
2.	Ceiling: Core drilling of diameter = 250mm	€ 1,500	
3.	Shielding wall between the re-injection channel and the ESR: Enlarge thickness to 1m	€ 4,500	
4.	Second shielding wall in direction SIS (4m x 4m).	€ 14,100	
			€ 20,100
12.1.6.	**PLATFORM, steel-made, load 1 t/m², floor height at + 4.26m // bottom line of construction at + 4.00m.**		
5.	Supports per 4m x I 200: 15 pcs. x 26.2kg/m x 3.50€/kg x 4m height + trivia	€ 6,200	
6.	Frame I 200: 141m x 26.2 kg/m x 3.50 €/kg + trivia.	€ 14,000	
7.	Trapezoidal profile E 50 (50mm height): ca. 158 m² x 45.-.€/m²	€ 8,500	
8.	Al-chequer plate, 1 mm: approx. 158 m² x 110.- €/m² (1kg per 3.50€)	€ 18,000	
9.	Railing, tripartite + base board: approx. 93 m x 180.- €/m	€ 17,000	
10.	Stairs south to the existing staircase (0.75m height), 1 m wide, railings on both sides.	€ 2,000	
11.	Stairs north on the ceiling of the re-injection channel (1.35m height), 1 m wide, railings on both sides.	€ 1,900	
			€ 67,600
12.1.7.	**CONTAINER, incl. illumination, wall plugs etc., windows, w/o blinds.**		
12.	Container, refurbished, 2 halves per 2.5m W /6m L/ 2.75m H = 30m² x 650.- €.	€ 7,000	
13.	Container, refurbished, per 3m W / 5m L / 3.0m H = 15m² x 700.- €.	€ 3,500	
			€ 10,500
	Total:		**€ 103,200**

12.2. Media

12.2.1. Electricity

For the required electrical energy of the RF transmitters, an allocation station will be placed on the platform which will be supplied by from the main allocation line =IN (Fragment separator). Because of the considerable switch-on peaks of the existing amplifiers, the fuses and feed-ins will have to be modified. The required power for the magnetic power supplies is available from the installations of the re-injection channel magnets.

Cables without PVC insulation will be used (fire protection).

Besides the high-power network, the measurement-and-control network is available for total powers of < 5 kW. For equipment that has to operate even in case of power failure, a stand-alone UPS (uninterruptible power supply) will provide a power up to 1.5 kW. This supply is suitable for in-rack housing. Illumination will be provided by a separate network. It will be restricted to the containers and the area below the platform. No installations for fire alarm are planned since this will be covered by the main installation in the ESR hall.

12.2.2. Cooling water

Table 12-2 displays the requirements with respect to cooling water of each of the HITRAP components to be cooled. The magnets are not included in this list. They will be cooled by the existing magnet-cooling-water network present also in the re-injection channel and do not require further consideration.

Table 12-2. Cooling-water requirements for the components of the HITRAP set-up.

Unit	Power to be dissipated	Flow Temperature and pressure	Return Temperature and pressure	Quality of cooling water
Electronics for control and measurement	approx. 6 kW	16-18°C / 4 bar	30°C / 3 bar	no requirements
RF transmitters	approx. 11 kW	27°C / 6.5 bar	33°C / 2 bar	conductance < 1μS/cm
Tank cavities	approx. 2 kW	27°C / 4.5 bar	29°C / 2 bar	ferritic circuit ('black water')

All media provided by GSI are available in the region of the experimental zone, above the platform. This includes cooling water, cold water, pressurized air, nitrogen, and exhaust air from vacuum pumps. From this line, the platform can be supplied with all media. The cooling water is made fitting the requirements by conversion circuits.

To cool the electronics for control and measurement, the switchboards contain special cooling elements, which are supplied with cooling water by a mixer station. By admixing a component of water at a temperature of 6° C from the existing cold-water network into the warmer return (Fig. 12-1), in the flow a temperature of 16° C – 18° C is generated.

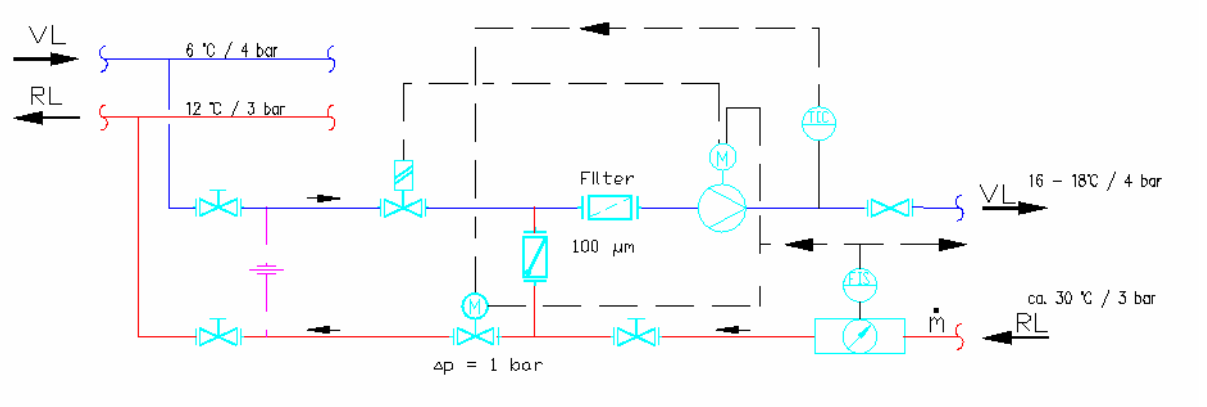

Figure 12-1. Mixing scheme for cooling of electronics. 'VL' = flow, 'RL' = return.

The RF transmitters require cooling water with a conductance of less than 1 μS/cm. To generate the required quality of water, a second circuit with a blending-bed-filter ion exchanger (Fig. 12-2) is operated via a separation-heat exchanger in parallel current. By a connection with the return of the main line, the system is filled and water losses are automatically accounted for.

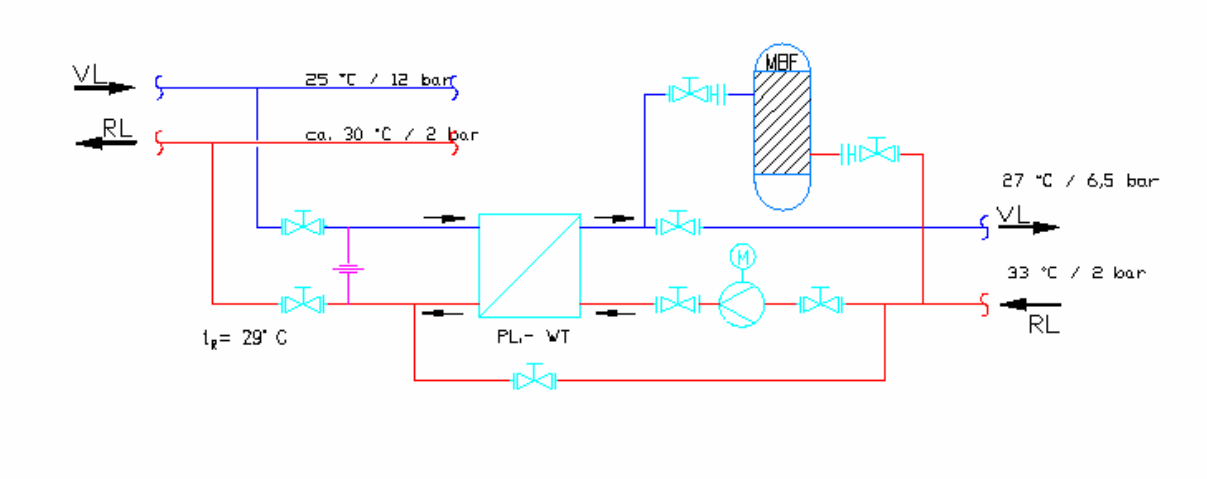

Figure 12-2. Blending-bed-filter ion exchange set-up for the cooling of the RF transmitters. 'VL' = flow, 'RL' = return, 'WT' = heat exchanger, 'MBT' = blending-bed-filter ion exchanger.

To cool the cavity tanks, a power dissipation of only 2 kW is considered. The ferritic water is not available at the experimental site, and therefore a system similar to the one depicted in Figure 12-2 would be required. To reduce the total costs, the department GA from GSI suggests fulfilling this cooling task by a separate cooling unit. Standard commercial units can be cooled by the cold-water network and are available for less than 10.000 Euro.

12.2.3. Air conditioning

Air-cooling devices will be operated for cooling the RF transmitters and the electronics located inside the containers. In the containers, distributed devices mounted at walls or under the ceiling will be installed with a maximal cooling power of 7 kW/unit. The absorbed heat will be carried away by the GSI-cold-water network. One unit is planned per 15 m^2 of area inside the containers. Altogether three of these devices are required.

Figure 12-3. Air-conditioning devices, to be mounted either on a wall or under the ceiling.

The existing RF transmitters tolerate higher temperatures than the electronics, up to max. 60° C. To keep costs low, the RF components will be cooled only by air from the surrounding ESR hall. Approx. 2500m^3/h of air from the hall will be sucked into a central unit (Fig. 12-4), filtered, and made available at the RF via a pipeline system and manually operated damper flaps. The heated exhaust air subsequently will be blown into the hall freely. The central unit has an option for mounting an additional cooler. If, contrary to expectations, problems with

temperature arise during operation, provision with the additional cooling mechanism is possible.

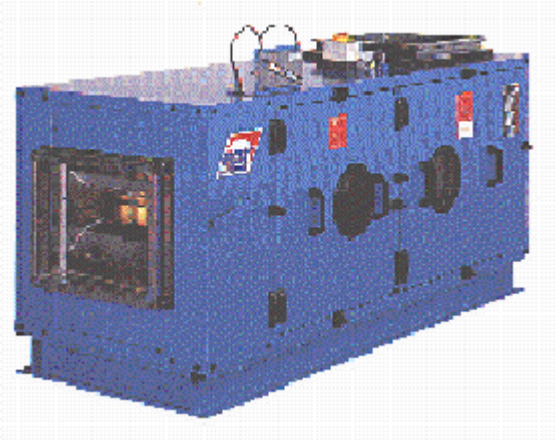

Figure 12-4. Central unit for ventilation with an option for cooling

12.2.4. Pressurized Air, Nitrogen and Vacuum-Exhaust Air

These media are available at the site of the experimental area above the platform. All media can be supplied on the platform by pipelines. These pipelines will be equipped with the corresponding fittings for connecting to the final set-ups.

12.2.5. Costs related to media supply

Table 12-3. Costs for media supply in the ESR hall related to HITRAP. Prices are excl. VAT.

12.2.	**Media** (incl. measurement and control of supplies)	**price/unit**	**subtotal**
12.2.1.	**ELECTRICITY**		
1.	RF Power supply 200 kW, from =IN	€ 10,000	
2.	Power supply for electronics and light in the containers	€ 10,000	
3.	Illumination under the platform	€ 8,000	
4.	Installation of telephone, emergency lighting, etc.; trivia	€ 5,000	
			€ 33,000
12.2.2.	**WATER COOLING**		
5.	Cooling of electronics for control and measurement	€ 20,000	
6.	Cooling of RF transmitters (2 × 15 l/min, < 1 μS/cm)	€ 20,000	
7.	Cooling of tank cavity, with standard commercial unit	€ 10,000	
			€ 50,000
12.2.3.	**AIR CONDITIONING**		
8.	Air cooling within the containers (3 units per 7 kW)	€ 15,000	
9.	Air cooling of RF components	€ 5,000	
			€ 20,000
12.2.4.	**Pressurized Air, Nitrogen, Vacuum-exhaust air**		€ 5,000
	Total:		**€ 108,000**

12.2.6. Expenses of manpower and time from start of the project

The following compilation assumes a detailed experimental planning and clearly specified requirements. It comprises both civil engineering and media supply.

Table 12-4. Manpower and time required for civil engineering and media supply. The costs for external personal are included in Tables 12-1 and 12-3.

	Time slot (duration)	**Person hours (GSI)**	**Person hours (external)**
Internal planning of media supply	approx. 4 weeks	400 h	
Ordering and delivery times	approx. 8 weeks	70 h	
Realisation by ext. personnel	approx. 6 weeks		1120 h
Supervision by GSI personnel		110 h	
Comissioning and approval	approx. 3 weeks	70 h	60 h
Total		**650 h**	**1180 h**

12.3. Safety

12.3.1. Radiation Protection and Industrial Safety at HITRAP

During deceleration at HITRAP in the tunnel of re-injection channel, the generation of ionising radiation has to be regarded because of the

1. X-ray production by the RF fields in the cavities and
2. Production of neutrons due to the unavoidable heavy-ion-beam losses in the decelerator structure.

Whereas the x-ray production can cause a substantial radiation exposure of personnel, the generation of neutron radiation can usually be neglected because of the low number of low energetic ions slowed down in the cavities (cf. the estimations in the following).

Access Control System

Access to areas, where the primary beam is transported or where cavities or septa are active, is not possible at GSI. The access to radiation-controlled areas at GSI is supervised by the ZKS. The access to the HITRAP area also has to be controlled. Up to now, the HITRAP area is used for the re-injection of completely stripped ions from the ESR back into the SIS. Therefore, the re-injection tunnel is only used in combination with the ESR and represents one access unit (see Fig. 12-5a). The existing coupling of these two areas may hamper the work of personnel in the HITRAP area while in the ESR the accelerator components are in operation and the radiation levels are above the limit.

The separation of these two areas may provide advantages for the operation, the maintenance of the components and for the preparation of the experiments (see Fig. 12-5b). Prerequisite for the separation is the construction of a proper shielding wall between the ESR and the HITRAP tunnel, which does not exist at present. The access-control system has to be adjusted to the introduction of a new radiation-controlled area. Although the HITRAP tunnel has its own personal gate, major modifications in the control system are necessary which implies the installation of new cable connections to the main-control computer system and the adjustment of the control program. The total cost for these installations is estimated to be about 58.000 Euro (cf. Table 12-5).

Expected Radiation Levels at HITRAP

The expected major component of ionising radiation in HITRAP will be the x-rays produced by the cavities operated for the deceleration of ions coming from the ESR. The x-ray radiation levels were estimated by U. Ratzinger. The dose-rate levels are estimated to about 100 µSv/h near the cavity structure. This level implicates the installation of a radiation-controlled area due to the German Radiation Protection Ordinance (§ 36 StrlSchV), because the level of 3 µSv/h is exceeded. Due to the safety rules at GSI, no stay of personnel is accepted for a dose rate of 100 µSv/h or higher. Therefore access to the HITRAP tunnel will only be possible if the cavities are switched off. The access control system (ZKS) will direct the admission to the HITRAP tunnel. The dose rates outside the tunnel and on the roof of the tunnel will be negligible during the operation. The maximum voltage of the cavities will be 650 kV. The shielding of the produced x- rays, which have a tenth-value thickness of about 10 cm for normal concrete (see Fig. 12-6), is ensured by a total concrete thickness from 80 to 160 cm. Therefore the expected dose rates caused by the x-rays outside the shielding are 8 to 16 orders of magnitude lower than the dose rates in the vicinity of the cavities.

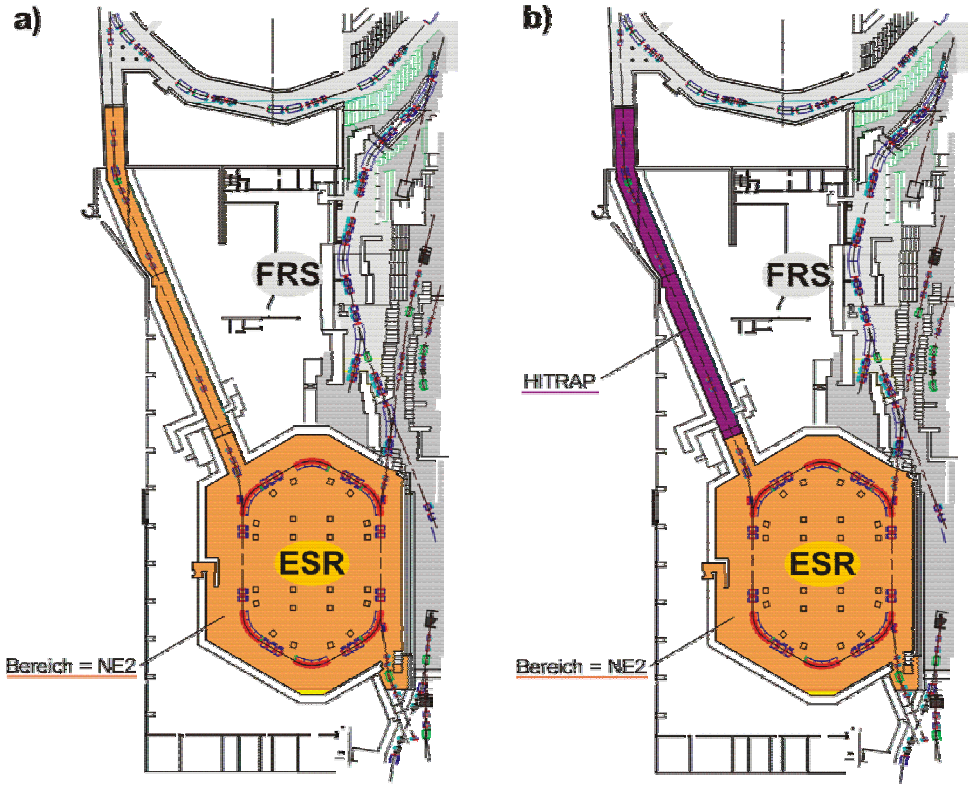

Figure 12-5. Possibilities of the organisation of the access to the areas of the ESR and the HITRAP tunnel. a): One radiation-control area (existing state). b): Two independent radiation-control areas (recommended).

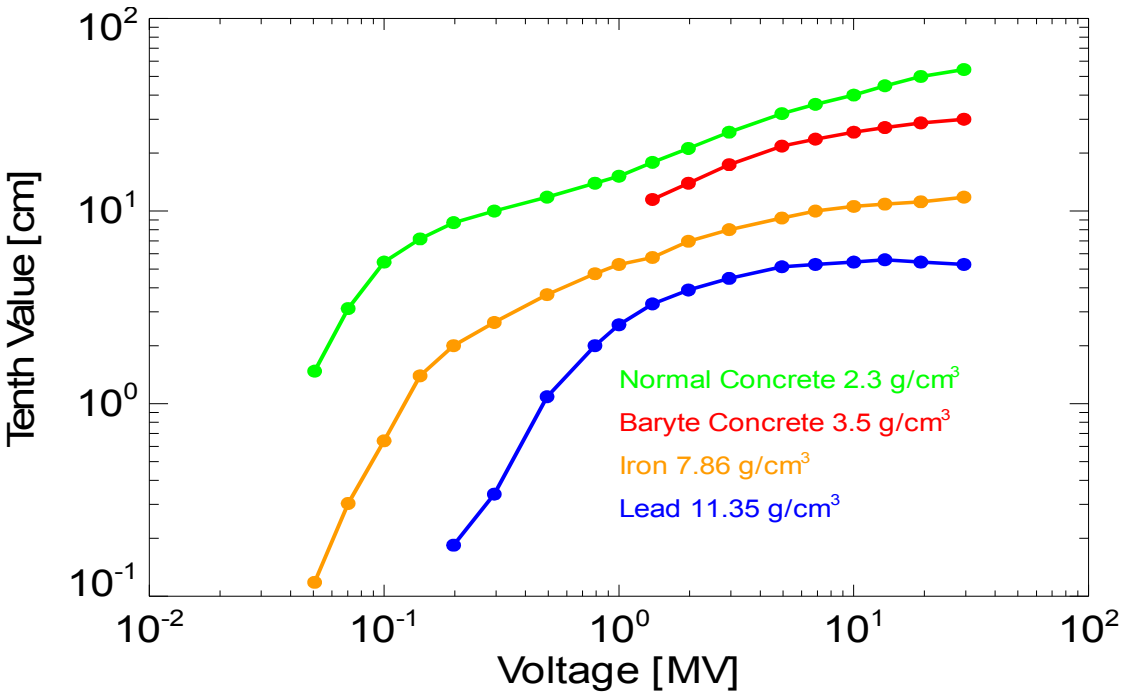

Figure 12-6. Attenuation of x rays as a function of the accelerating voltage. The attenuation is represented as the tenth value thickness of the dose rate for the materials normal concrete, barite concrete, iron and lead. The maximum high voltage for the cavities is about 650 kV. Therefore the tenth value thickness is expected to be 10 cm for normal concrete. The data are taken from Vogt/Schultz, Grundzüge des praktischen Strahlenschutzes, Carl Hanser Verlag, 1992.

If heavy ions have energies high enough to exceed the Coulomb threshold in collisions with nuclei of the target, neutrons can be evaporated from the created compound nuclei. For this report an example is calculated for a uranium beam slowing down in an iron target. The neutron production is calculated for the energy range from 5 MeV/nucleon to 20 MeV/nucleon. The dose rate is related to one particle nA (see Fig. 12-7). Because of the low number of ions which are estimated to 10^6 with a duty cycle of 30 sec, the neutron dose rate can be neglected even for lighter ions with a similar average ion current.

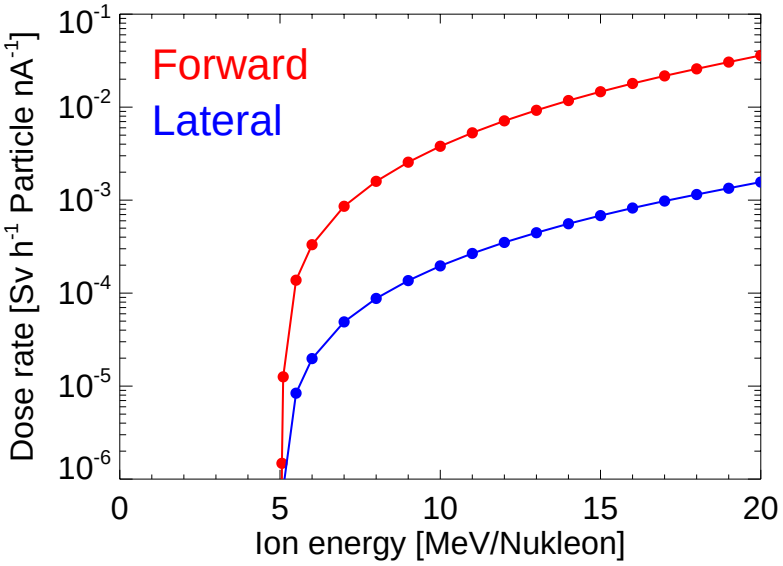

Figure 12-7. Neutron-dose rate caused by ^{238}U ions slowed down in iron. The dose rate is related to one particle nA. The dose rate in forward direction exceeds the lateral dose rate by one order of magnitude. The threshold of the compound formation and the neutron production is near 5 MeV per nucleon.

Summary of radiation safety measures for the operation of HITRAP

The radiation safety of the HITRAP area must be controlled by the installation of active dose-rate monitors that are sensitive to photon and neutron radiation. If the monitors indicate a dose rate higher than 3 µSv/h, the accelerator will be switched off. The control link from the monitors to the accelerator control will be given by the ZKS. In addition the operation of the RF of the HITRAP cavities must be controlled by the ZKS, because during the operation persons must not stay in the HITRAP decelerator area.

If one intends to separate the radiation controlled areas of the ESR and the HITRAP area it is necessary to modify the ZKS (see comments above). A new client computer system together with new cable installations for the connections to the main computer system must be installed. Furthermore the enhancement of the hitherto incomplete concrete shielding between the HITRAP area and the ESR must be carried out.

The HITRAP area will be close to the SIS tunnel. Consequently the dose rate levels within the re-injection tunnel are highly influenced by the synchrotron operation. Therefore it is recommended either to enhance the shielding to the SIS tunnel or to install an additional fence in the tunnel to avoid access from the HITRAP area to the area near the SIS-tunnel.

12.3.2. Electrical protection

The RF generators with the power supplies have to be installed in an "enclosed electrical workshop" (abgeschlossene elektrische Betriebsstätte). The railing specified in Section 12.1 fulfils the requirements and coincides with the usual GSI standards.
The maximum permissible limits for 108.408 MHz inside this room are for the power 10 W/m², for the magnetic field-strength 0.163 A/m and for the electrical field strength 61.4 V/m. Outside the mentioned room the limits are 2 W/m²; .073 A/m and 27.5 V/m. These are the normal limits and there should be no difficulties to observe them.
The observance of VDE or EU regulations is self-evident. Maintenance and trouble shooting should only be done by skilled and well-trained personnel.

12.3.3. Cryogenics

There has to be a safe special sling (ropes and webbings are not sufficient) for the transport of the containers for liquid helium and nitrogen.

The platform on which the filling of liquid helium and nitrogen will be done has to be constructed in such a way that the liquids cannot flow into beneath lying rooms.
Measuring devices for the oxygen content have to be installed at the place of the normal stay during the filling operation and in the beneath lying room; these devices has to warn the people in case of an oxygen deficit.

12.3.4. Platform

The platform has to be constructed with the required railings and stairs. There has to be installed a normal staircase (no stopgap). Because of safety reasons it is not recommended to install containers on the roof of the experimental area of HITRAP, i.e., the re-injection tunnel itself. The above given design of the platform, stairs, and railings (cf. Section 12.1.) fulfils all requirements.

12.3.5. Fire Prevention

For the fire prevention it is recommended to use flame resistant materials, especially the cables should be flame resistant and should not contain any PVC.

12.3.6. List of the Cost Estimate for Safety Measures

A summary of all costs is given in Table 12-5. The measures are distinguished between desired and necessary measures. The costs include installation of the equipment. Costs for the fortification of the wall to the ESR and for the erection of a new separation wall towards the SIS are included in the cost estimate of Section 12.1. and are not considered here.

Table 12-5. Cost estimate for safety measures in the HITRAP area. Not all measures are prerequisites for the safe operation of the HITRAP experiment, but the feasibility for the preparation of experiments and the operation of HITRAP in combination with the ESR is significantly improved. The numbers for the costs are given in Euro.

Measure			**Costs**
Desired	Necessary		
Separation into 2 radiation control areas		VME Crate Input/Output Reg. Data processing unit/Cabling Block d'Arret Ionisation Chamber	3,000 20,000 15,000 10,000 10,000
	Dose-Rate Meter		20,000
	Oxygen-level measurement		2,600
Total	Minimum: **22,600** / Maximum: **80,600**		

Due to the desirable accessibility of the re-injection tunnel during ESR operation, in the general cost estimates the sum of **80,600 Euro** is considered.

13. Time schedule

Table 13-1 specifies the planned time schedule in setting up the HITRAP decelerator in the re-injection channel. The facility is planned to be ready for operation within 30 months after start of the project.

Table 13-1. Time schedule (in months) and manpower (in person years) for the HITRAP Project. The commissioning of the HITRAP Facility will take place in the beginning of the third year.

Tasks	1-12				13-24				25-30	
IH-Linac and RFQ, **10 PY**										
Radio-frequency supply, 2 **PY**										
Low Energy Beam Transport from the RFQ to the Cooler Trap, 1**.75 PY**										
Cooler Trap and junction to experiments, **2.5 PY**										
Magnets, steerers, and their power supplies, **0.75 PY**										
Beam diagnostics, **2 PY**										
Controls, **0.4 PY**										
Vacuum system, **2.25 PY**										
General infrastructure and supplies, **0.75 PY**										
Commissioning without beam, **0.5 PY**										
Commissioning with beam and first experiments, **0.5 PY**										

14. Manpower

Table 14-1. Required manpower for the HITRAP Project. More than 40% of the required manpower will be provided by the groups of U. Ratzinger and A. Schempp (IAP Frankfurt), and the group of G. Werth (Univ. Mainz). The manpower required for experimental set-ups to be connected to HITRAP is provided by the collaborators of the EU-RTD network HITRAP and not included in this table.

Tasks	**Manpower** (person years)	**provided by**	
		GSI	**IAP Frankfurt*, Univ. Mainz****
IH Linac and RFQ	**10 PY**	**2.5 PY**	**7.5 PY***
Radio-frequency supply	**2 PY**	**2 PY**	**0**
Low Energy Beam Transport from the RFQ to the Cooler Trap	**1.75 PY**	**1.75 PY**	**0**
Cooler Trap and junction to experiments	**2.5 PY**	**0**	**2.5 PY****
Magnets, steerers, and their power supplies	**0.75 PY**	**0.75 PY**	**0**
Beam diagnostics	**2 PY**	**2 PY**	**0**
Controls	**0.4 PY**	**0.4 PY**	**0**
Vacuum system	**2.25 PY**	**2.25 PY**	**0**
General infrastructure and supplies	**0.75 PY**	**0.75 PY**	**0**
Commissioning without beam	**0.5 PY**	**0.3 PY**	**0.2 PY***
Commissioning with beam and first experiments	**0.5 PY**	**0.3 PY**	**0.2 PY***
Total manpower	**23.4 PY**	**13.0 PY**	**10.4 PY*,****

15. Total costs and spending profile

The total costs for the HITRAP facility will amount to a sum of 2,860,000 Euro. Table 15-1 summarizes the costs for each component and shows the planned spending profile corresponding to the time schedule specified in Chapter 13.

Table 15-1: Costs and spending profile of the HITRAP project. A part of the costs in the first year will be spent for advance payment of equipment.

Investment, equipment, construction (cf. chapter/section)	**Costs [k€]**			
	first year	**second year**	**third year**	**sum of three years**
IH structure and bunchers (Chapter 3, Tables 3-5 –3-7)	200	200	86	486
RFQ cavity (Chapter 4, Table 4-2)	80	80	37	197
RF supplies (Chapter 5, Table 5-1)	0	280	125	405
Cooler trap, including 90° bender and valves (Chapter 7, Tables 7-2 – 7-4)	0	306	0	306
Magnets and steerers (Section 8.1., Table 8-1)	0	80	0	80
Power supplies for magnets and steerers (Section 8.2., Tables 8-2 and 8-3)	0	319	0	319
Beam diagnostics (Chapter 9, Table 9-2)	36	113	36	185
Controls (Chapter 10, Table 10-1)	0	111	0	111
Vacuum (Chapter 11, Tables 11-1 – 11-4 and 11-7)	90	230	159	479
Civil engineering (Section 12.1., Table 12-1)	30	73	0	103
Media supply (Section 12.2., Table 12-3)	30	78	0	108
Safety (Section 12.3., Table 12-5)	0	56	25	81
Sum for individual years and **total sum:**	**466**	**1926**	**468**	**2860**

16. Outlook: HITRAP @ NESR

The HITRAP set-up will be an integral part of the GSI Future Facility (cf. the Conceptual Design Report of the GSI Future Facility, http://www.gsi.de/GSI-Future/cdr). There, HITRAP will serve as a tool for investigations with particles at rest after the so-called New Experimental Storage Ring (NESR). The major areas of investigations with HITRAP (g-factor and mass measurements, laser spectroscopy, x-ray spectroscopy, collision studies, and ion-surface interaction studies with slow heavy highly charged ions) will be extended to antiprotons and radioactive ions. The experience gained at the planned set-up of the current facility should allow for a successful operation of the experiment without too many transition losses.

Essential for the presented facility is the compatibility with the future facility in all major components (decelerator, traps, adjacent experiments). After successful operation at the ESR and the final shut-down of this storage ring, the HITRAP components can be dismounted and mounted again at their new location. Further work for development will not be required, except adjusting controls, beam diagnostic tools etc. to the then new standard for GSI, which at present does not yet exist. It is expected that these relatively minor modifications will allow for a successful continuation of the experimental work almost immediately after start of operation of the NESR and thus contribute to the scientific output of the new facility right from the beginning.

The HITRAP facility as presented in this TDR is designed to decelerate heavy ions and to make them available for experiments, which require them at rest or at very slow velocities, compared to what a storage ring could provide. Besides heavy ions, the decelerator and the trap can be equally well used for antiprotons to bring them down to sub-thermal energies as all components have been carefully designed to be operable in a q/A range of > 1/3. This will be of considerable interest since using antiprotons will be a pronounced feature of the GSI Future Facility. Besides the existing AD at CERN, HITRAP will be the only facility where antiprotons at rest are available. The existing community (ASACUSA, ATHENA, ATRAP), presently located at CERN, has expressed their utter interest to use HITRAP located at NESR for future experiments. While this TDR has been in its final stage in September 2003, a workshop took place at GSI where spokesmen from all collaborations and also from the MPI-K in Heidelberg and the IAP in Frankfurt presented elaborate ideas about experiments to be carried out at the new GSI Future Facility, employing ultra-cold antiprotons delivered by HITRAP. The HITRAP set-up will therefore serve in a two-fold way at the new 'Facility for Low-energy Antiproton and Ion Research at the future GSI facility' (FLAIR). More information on HITRAP at the GSI Future Facility will be available in the Letter-of-Intent of the Flair collaboration which will be available in short time (http://www-linux.gsi.de/~flair). The FLAIR facility might be in operation in a decade from now. It would be highly desirable to investigate the properties of a world-unique decelerator for heavy ions until then.

17. Acknowledgements

We would like to thank both our friends from the experimental highly-charged ion community, i.e., the groups of J.-P. Grandin, R. Morgenstern, R. Schuch, R. Thompson, J. Ullrich, A. Warczak, and all GSI-colleagues, as well as our collaborators from the theoretical side, J. Burgdörfer, L. N. Labzowsky, I. Lindgren, P. J. Mohr, K. Pachucki, V. M. Shabaev, and G. Soff, who eagerly look forward to receiving numbers generated by HITRAP in order to check their existing and future calculations with a precision not yet provided by experiments. In addition, all existing low-energy antiproton collaborations (ASACUSA, ATHENA, ATRAP) expressed their wish not only to see HITRAP put into operation but also to employ it for their own purposes, thus even enlarging the originally envisaged range of the experiment. Their great enthusiasm was a big motivation in performing this report. A special thank you goes to O. Kester, who volunteered to peer-review it before it was cast into its final form.

The creation of a report like this with many institutions and departments involved implies a considerable effort also from the point of view of communication. All secretaries, office neighbors, and people present just by chance were extremely helpful in getting the 'person in charge' to the telephone or handing over the desired information otherwise. It would have been impossible to list them all without forgetting somebody. Still, we would like to thank everyone of them here.

The editors also want to thank all of the authors for delivering their contributions on time, and in a way that it was a pleasure to include them into this report. Next to the IAP of the University of Frankfurt, this particularly includes the Accelerator department at GSI where we met undivided eagerness to help us, and the civil engineering department. All the support and expertise we met during the creation of this report was very reassuring and convincing in demonstrating that GSI is the right place to carry out projects like this.

The creation of this report was supported by the EU (HPRI-CT-2001-50036).